Expression of the Progesterone Receptor, Bcl-2 and Bax in Clomiphene Citrate Treated Rat Uteri

Thérèse Dix-Peek

A dissertation submitted to the Faculty of Science, University of the Witwatersrand, in fulfillment of the requirements for the degree of Master of Science

Johannesburg, 2011

DECLARATION

I declare that this dissertation is my own, unaided work. It is being submitted for the degree of Master of Science in the University of the Witwatersrand, Johannesburg. It has not been submitted before for any degree or examination in any other University.

_____

_____day of _____2011

ABSTRACT

Clomiphene citrate (CC) is a synthetic oestrogen receptor modulator that may act to promote or inhibit oestrogenic responses depending on the type of tissue or organism. CC acts as a superovulator and has been widely prescribed in the treatment of female infertility. However, pregnancy rates after CC treatment are low, possibly due to the CC causing morphological and other unidentified changes to the uterus.

This study investigated the changes caused by CC on the progesterone receptor (PR), the anti-apoptotic protein, Bcl-2, and the pro-apoptotic protein, Bax.
PR with its ligand, progesterone, is important for the maintenance of a pregnancy. Bcl-2 is a cell survival molecule and acts in opposition to Bax, which promotes apoptosis, which is important in allowing an attaching blastocyst to infiltrate the maternal endometrium.

A high physiological dose of CC (1.25 mg) was administered to ovariectomised rats, either as a single treatment, or prior to a hormonal treatment regime characteristic of pre-implantation animals. The single CC treated animals were compared with single 5 mg progesterone (P_4) treated animals and vehicle controls. The animals treated with CC in conjunction with the ovarian hormone milieu (CCPPPE treatment) were compared to PPPE treated animals or to the vehicle controls.
The effects of CC, P_4, PPPE and SPPPE on the morphology of the uteri were investigated by light microscopy. Expression of the PR, Bcl-2 and Bax were investigated using immunohistochemistry and enzyme linked immunosorbent (ELISA) techniques.

The present study showed that CC treatment affects the microanatomy of the uterine compartments, particularly the shape of the lumen and the luminal epithelial height. The expressions of PR, Bcl-2 and Bax in the entire uterus were

not significantly affected by the various treatments applied to the ovariectomised rats, as measured using ELISA. However, expression of the proteins in the various uterine compartments was altered by CC treatment. The single CC and CCPPPE treatments had an oestrogenic effect with regards to PR expression in the uteri as seen in the immunolocalisation, whereas the single P_4 treatment decreased the PR expression, as expected. CC treatment caused patchiness in both Bcl-2 and Bax expression surrounding the endometrial lumen. Moreover, treatment with CC maintained expression of Bcl-2 in the luminal epithelium, whereas the expression of Bax shifted away from the luminal epithelium. This suggests that CC treatment promotes cell survival of the luminal epithelium, which may diminish the ability of the blastocyst to infiltrate the maternal tissue.

CC action is both dose sensitive and has a cumulative effect with multiple treatments. Future studies would aim to separate the various uterine compartments in order to quantitatively assess the actions of CC on expression in the PR, Bcl-2 and Bax. In addition, it would be interesting to investigate how the accumulation of subsequent CC doses affects the expression of apoptotic markers, as this would be a more realistic model for human infertility treatment.

ACKNOWLEDGEMENTS

I would like to gratefully thank my supervisor, Prof. M. Hosie for her continual encouragement, support, suggestions, assistance, friendship and infinite patience during the course of this Masters.

I would like to thank Prof. B. Kramer, Prof. J. Maina and Prof. J. Daly, who as heads of School, have supported me enormously over the years.

The technical staff at the school of Anatomical Sciences, Mrs G. Veale, Mrs A. Mortimer, Mrs S. Rogers, Mrs H. Ali, Mrs L. York and Mr R. Tseki, have been very generous with their time and knowledge.

Many thanks to the team at the Central Animal Services who have been willing to assist with the rats and explain the procedures used. My grateful thanks as well to Ms. M. Badenhorst at Physiology for use of the ELISA plate reader, and to Dr T. F. Chirwa for all his help with the statistics.

I would like to thank the members of staff, and the postgraduate students at the school of Anatomical Sciences for their continued support and encouragement, particularly Mrs K. Theron, Miss K. Thomson, Dr M. Štrkalj, Mr T. Khoza, Mr T. Tikolo, Dr C. Penny, Dr E. Hurter, Prof. J. Daly. Thank you for your friendship.

I would like to particularly thank my parents, Hilary and Douglas, for unreserved support, and my siblings Dominique, Michele, Andrew and Stewart for encouragement and for showing the light at the end of the tunnel. A special thanks to my aunt, Marie Brand for long distance talks at any time of the day. Thanks also go to Miss Caroline Dickens for her understanding and empathy and many cups of coffee.

I would like to extend my gratitude to the National Research Foundation (NRF) and the University of the Witwatersrand for financial assistance over the course of this project.

TABLE OF CONTENTS

LIST OF FIGURES

LIST OF TABLES

LIST OF GRAPHS

ABBREVIATIONS

α	Alpha
AIF	Apoptosis inducing factor
AM	Anti-mesometrial pole
APAF1	Apoptosis protease-activating factor 1
ApC	Apoptotic cell
APES	3-aminopropyltriehoxysilane
ART	Assisted reproductive techniques
ATP	Adenosine triphosphate
Bax	Bcl-2 – associated X protein
Bcl-2	B cell lymphoma/leukemia-2
β	Beta
BH	Bcl-2 homology domain
bm	Basement membrane
BSA	Bovine serum albumin
χ^2	Chi-squared
c	Cytoplasm
Calpains	Calcium activated neutral proteases
CC	Clomiphene citrate
°C	Degrees celsius
Da	Dalton
DAB	3,3' Diaminobenzidine tetrahydrochloride
dATP	Deoxy adenosine triphosphate
DBD	DNA binding domain
ddH_2O	Distilled, deionised water
dH_20	Distilled water
DL	Dark layer
DNA	Deoxyribonucleic acid
E_2	17-β-Estradiol
EDTA	Ethylene diamine tetraacetic acid
ELISA	Enzyme linked immunosorbent assay
ER	Oestrogen receptor
Fig.	Figure
FSH	Follicle stimulating hormone
GIFT	Gamete intrafallopian transfer
γ	Gamma
GE	Glandular epithelium
gl	Glands
GnRH	Gonadatropin releasing hormone

H	Hinge
H&E	Haemotoxylin and Eosin
HRP	Horse radish peroxidase
ICSI	Intracytoplasmic sperm injection
IgG	Immunoglobulin G
IHC	Immunohistochemistry
IP	Intraperitoneal
IVF	In vitro fertilisation
kg	Kilograms
LE	Luminal epithelium
LBD	Ligand binding domain
LH	Luteinising hormone
M	Mesometrial pole
M	Molar
µg	Micrograms
µl	Microlitres
µm	Micrometres
mg	Milligrams
ml	Millilitres
mm	Millimetres
mM	Milli molar
mins	Minutes
n	nucleus
nm	Nanometres
nmb	Nuclear membrane
P_4	Progesterone
PBS	Phosphate buffered saline
PCD	Programmed cell death
PPPE	Treatment regime: 5 mg progesterone on days 1 and 2, followed by 5 mg progesterone and 0.5 µg 17β oestradiol on day 3
PR	Progesterone receptor
mRNA	Messenger ribonucleic acid
S	Stroma
SC	Subcutaneous
SEM	Standard error of the mean
SOOO	Treatment regime: saline on day 1, followed by oil treatment for 3 days
TNFα	Tumour necrosis factor alpha
TNFR-1	Tumour necrosis factor receptor 1
TBS	Tris buffered saline, pH 7.6
TBST	TBS-Tween 20
WHO	World Health Organisation

W	Watts
w/v	Weight by volume
x	Times
ZIFT	Zygote intrafallopian transfer

CHAPTER 1. INTRODUCTION

1.1. Infertility

Childlessness has enormous social, cultural, spiritual and financial implications in all human societies, particularly amongst African societies. Little research has been done to assess infertility rates in Sub-Saharan Africa, due to the perception of high fertility rates in the region (Hollos, 2003, Motseki, 2004). However, there is a significant problem regarding infertility in various African societies, with regional effects from 10-20% up to as high as 30-40% (Dyer *et al.*, 2002b, Motseki, 2004). Infertility is regarded as the inability to conceive after one year of unprotected intercourse (Collins *et al.*, 1983, Larson, 2005).

It is estimated that 40% of infertility causes are due to male infertility, 40% are due to female infertility, and 20% of cases have unknown etiology (Bernstein, 1999). Unfortunately, within most traditional and patriarchal societies, blame tends to fall most often upon women (Juries, 2005). Studies in South Africa show that childless women often feel guilt and are desperate for babies. A childless woman may suffer from the threat of marital dissolution or infidelity, verbal or physical abuse, loss of social status, loss of economic income, isolation and stigmatization from the community and enormous social pressure to get pregnant (Dyer *et al.*, 2002a, b, Dyer *et al.*, 2004, Dyer *et al.*, 2005).

The problems with infertility are further compounded by the fact that South Africans appear to have a poor understanding of involuntary childlessness, with theories such as “dirty wombs”, “God’s will”, “witchcraft”, “weak sperm”, “abnormal menstruation”, and “punishment for pre-marital sex” being proposed for infertility (Dyer *et al.*, 2002a, Juries, 2005). A lack of education, and low economic income diminishes women’s ability to access facilities that treat infertility, and diminish their ability to pay for treatments (Juries, 2005).

Specific causes of infertility include tubal factors, ovulatory dysfunction, endometriosis, diminished ovarian reserves, anovulation, luteal phase defect, cervical factors, uterine factors, male factors and unexplained infertility (Sharara and McClamrock, 2000, Motseki, 2004, Wright *et al.*, 2007).

Various methods are used to treat infertility. Drugs, such as clomiphene citrate, may be used to stimulate egg production and an infertile couple may try to conceive "naturally", or the eggs may be harvested for assisted reproductive techniques (ART).

ART involves retrieving eggs from a woman, combining the harvested eggs with sperm in a laboratory, fertilising, and transferring the fertilised eggs into a uterus. ART is often combined with *in vitro* fertilisation (IVF), where the implanted embryo is generally older than 2 days. Other ART procedures include gamete intrafallopian transfer (GIFT), which involves transferring gametes (an unfertilized egg and sperm) directly into the uterine tubes, or zygote intrafallopian transfer (ZIFT), which involves transferring the single-cell zygote into the fallopian tubes. Another ART method used is intracytoplasmic sperm injection (ICSI), where a single sperm is injected directly into the egg. ICSI is used most commonly to treat male infertility (Wright *et al.*, 2007, Zegers-Hochschild *et al.*, 2009).

1.2. The human female reproductive system

The female reproductive system is characterised by ovulation, followed by menstruation if conception does not occur. The ovarian and menstrual cycles run for about 28 days in length in the average human (Stevens and Louw, 1992, Carlson, 1998, Brosens and Gellersen, 2006).

The Ovarian Cycle

There are three phases of the ovarian cycle: the follicular phase, the ovulatory phase and the luteal phase. The follicular phase consists of the development of the primordial follicle to the Graafian or tertiary follicle, which is ready for ovulation. The ovulatory phase is characterised by the oocyte being released into the uterine tube. The luteal phase refers to the period between ovulation and the onset of either menses or implantation. The corpus luteum, the remains of the follicle, secretes hormones in preparation for implantation (Stevens and Louw, 1992, Carlson, 1998). The phases of the ovarian cycle can be seen in Fig. 1.1.

The menstrual cycle

The uterus is lined by the endometrium which contains a simple cuboidal to columnar epithelium and stromal tissue, and is surrounded by three thick muscle layers, the myometrium. The menstrual cycle can be divided into three phases; the menstrual phase, the proliferative phase and the secretory phase, which correspond to the three phases of the ovarian cycle.

Menstruation occurs in the absence of a fertilised ovum, which results in the cessation of progesterone and oestrogen secretion by the corpus luteum. Menstruation is characterised by sloughing of the endometrium and consequent bleeding. The proliferative phase is characterised by the proliferation of the endometrial stroma, which becomes thicker and more vascularised, and largely under the influence of oestrogen. The simple tubular glands proliferate and become secretory at the onset of ovulation. The secretory phase under the influence of progesterone occurs subsequent to ovulation and the endometrial glands produce a glycogen-rich secretion (Stevens and Louw, 1992, Carlson, 1998, Young and Heath, 2002).

The phases of the menstrual cycle are shown in Fig. 1.1.

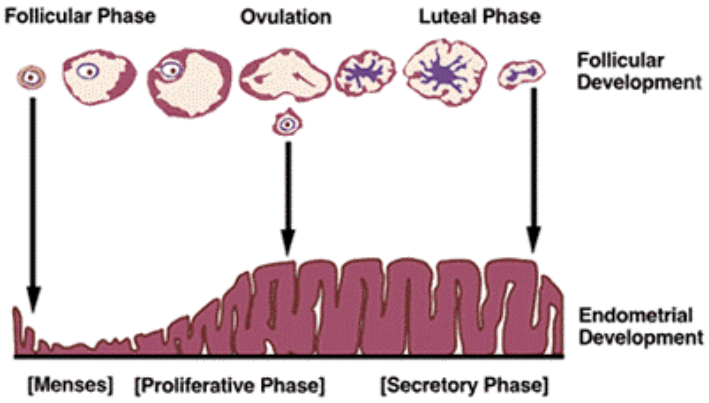

Figure 1.1. The menstrual and ovarian cycles
A new follicle begins to develop around the onset of menses and matures until it has developed into the tertiary follicle. The uterus undergoes proliferation at this time. The mature oocyte is released from the ovaries at ovulation. During the luteal phase, the corpus luteum produces progesterone to maintain a possible pregnancy and the endometrium is concurrently in the secretory phase. If the oocyte does not implant, the menstrual and ovarian cycles will be repeated. http://www.sw.org/web/patientsAndVisitors/iwcontent/public/womens_inst/en_us/html/womensinst_endoInfertility_reproSystems.html (Accessed August 2010)

Effect of hormones on the reproductive cycle

There are four main hormones directly associated with the female reproductive cycle: luteinising hormone (LH) and follicle stimulating hormone (FSH) which are produced by the pituitary, and oestrodial 17-β (E_2) and progesterone (P_4) which are produced by the ovaries (Stevens and Louw, 1992, Kierszenbaum, 2002).

The day immediately preceding menstruation usually has extremely low concentrations of the ovarian sex steroids. Menses is followed by the follicular phase. Gonadatropin-releasing hormone (GnRH) from the hypothalamus causes the release of LH and FSH from the anterior pituitary. Follicles are produced and the theca interna cells surrounding the developing oocytes produce androgens, which are converted to E_2 by the granulosa cells. Follicle stimulating hormone is necessary for the conversion of androgen into oestrogens. The oestrogens cause the endometrium to proliferate. In the pre-ovulatory phase, an LH surge leads to an increase in oestrogen levels which spike immediately preceding ovulation. During ovulation, the dominant follicle ruptures to release the mature egg, and the remains of the follicle that has been ruptured becomes the corpus luteum. During the luteal phase, the corpus luteum produces P_4, which is necessary to maintain

the endometrium for implantation. (The endometrium has now entered its secretory phase.) If the corpus luteum is not supported by human chorionic gonadatropin (hCG), which is produced by the fertilized embryo, it will involute. This involution leads to low levels of ovarian hormones, which leads to the menstrual cycle being repeated (Stevens and Louw, 1992, Carlson, 1998, Kierszenbaum, 2002).
The expression of ovarian and pituitary hormones during the menstrual cycle are shown in Fig. 1.2.

1.3. The rodent female reproductive system

The rodent model has been extensively used to measure uterine tissue responsiveness to ovarian steroid stimulation (Baranda-Avila *et al.*, 2009). Like humans, rats have a haemo-chorial placentation. The placenta invades deep into the maternal decidua, to allow direct contact with maternal blood. This allows for an intimate association between the developing embryo, and the nutritional source from its mother (Loke and King, 1995).

Rats and mice have an oestrous cycle, rather than a menstrual cycle, which lasts about 4 – 7 days. The oestrous cycle is characterised by 4 phases; proestrus, oestrus, metestrus (also referred to as diestrus 1) and diestrus (also referred to as diestrus 2) (Mandl, 1951, Marcondes *et al.*, 2002).

The ovarian follicles start to grow during proestrus, which lasts between 12-14 hours in rats. During oestrus, the female is sexually receptive to the male and ovulation occurs during this phase. This phase lasts about 25-27 hours in rats. Metestrus lasts about 6-8 hours and diestrous lasts for about 55-57 hours (Long and Evans, 1922, Mandl, 1951, Goldman *et al.*, 2007, Westwood, 2008).

During the oestrous cycle, prolactin, LH and FSH levels remain low and increase in the afternoon of the proestrus phase. Estradiol levels begin to increase during

metestrus and reach peak levels in the morning of proestrus (Baranda-Avila *et al.*, 2009), returning to baseline at oestrus. Progesterone secretion increases during metestrus and diestrous with a decrease afterwards. Progesterone peaks a second time toward the end of proestrus (Smith *et al.*, 1974, Marcondes *et al.*, 2002, Baranda-Avila *et al.*, 2009). Wood *et al.* (2007) found that higher E_2 levels in mice correlated with an increase in uterine width, proliferation of stromal cells and had a lower proliferation of glandular epithelia. In contrast, higher P_4 levels correlated with a decrease in uterine width and less proliferation in the luminal epithelium. Wood *et al*. (2007) and Baranda-Avila *et al*. (2009) found that the epithelial cells underwent proliferation at the start of metestrus, approximately 40 hours after E_2 levels had peaked. By contrast, ovariectomised rodents had proliferation of epithelial cells about 24-48 hours after E_2 administration.
The expression of hormones in a rodent female is shown in Figure 1.2.

1.4. Implantation window

Pregnancy is a unique condition in which the tolerance of a genetically dissimilar tissue, the foetus, is established *in utero* (Vigano *et al.*, 2002). A successful pregnancy depends on the interaction between a viable embryo in tandem with a receptive endometrium (Develioglu *et al.*, 1999, Reese *et al.*, 2001).

Molecular communications between the uterus and a functional blastocyst are necessary for successful implantations (Reese *et al.*, 2001, Achache and Revel, 2006). The window of implantation is defined as the period when the uterus is primed to attach to the developing blastocyst under the influence of ovarian steroid hormones (Psychoyos, 1973, Develioglu *et al.*, 1999, Reese *et al.*, 2001). The process of implantation has been classified into three stages: apposition, adhesion and invasion. Apposition involves the trophoblast cells of the blastocyst coming into contact with the uterine luminal epithelium; adhesion is defined as the period when the blastocyst anchors onto the endometrium and cannot be washed off from the endometrium; and invasion is when the blastocyst penetrates

through the endometrial luminal epithelium (Enders and Schlafke, 1967, Achache and Revel, 2006).

In humans, the window of receptivity is estimated to occur about 7 – 10 days after ovulation (Wilcox *et al.*, 1999, Wang and Dey, 2006) and embryos that implant beyond 10 days after conception are at a significantly greater risk of early pregnancy loss (Wilcox *et al.*, 1999). The oestrous cycle in rodents is less regular than the human menstrual cycle and is therefore more difficult to determine when the window of implantation occurs (Wang and Dey, 2006), although there is evidence that it usually occurs on day 4 of pregnancy in mice (Abrahamsohn and Zorn, 1993, Song *et al.*, 2007) and lasts for about 24 hours (Ma *et al.*, 2003). However, Ma *et al.* (2003) found that lower E_2 levels extended the window of receptivity, whereas high levels of E_2 contracted the window of receptivity.

At implantation, microvilli on the uterine luminal epithelial cells tend to become flattened and less dense, whereas they are usually long and regular during estrus, suggesting that the uterine epithelium and trophoblast cells have a flattened area of contact. It has been suggested that flattened microvilli are necessary for pregnancy (Murphy and Shaw, 1994, Murphy, 2004). Other documented changes include deeper lateral tight junctions between luminal epithelial cells and progesterone affecting the disassembly of some focal adhesion molecules (Murphy, 2004, Kaneko *et al.*, 2009).
Figure 1.2. shows the receptive period for both humans and mice.

Both humans and rodents undergo decidualisation during the reproductive cycle, which involves remodeling of the stromal compartment. It occurs especially in animals where the implanting embryo invades the maternal tissue (Brosens *et al.*, 2002). Decidualisation is due to maternal factors in humans, whereas it is driven by signals from the implanting blastocyst in rats (Shaw and Murphy, 1996, Dey *et al.*, 2004, Brosens and Gellersen, 2006).

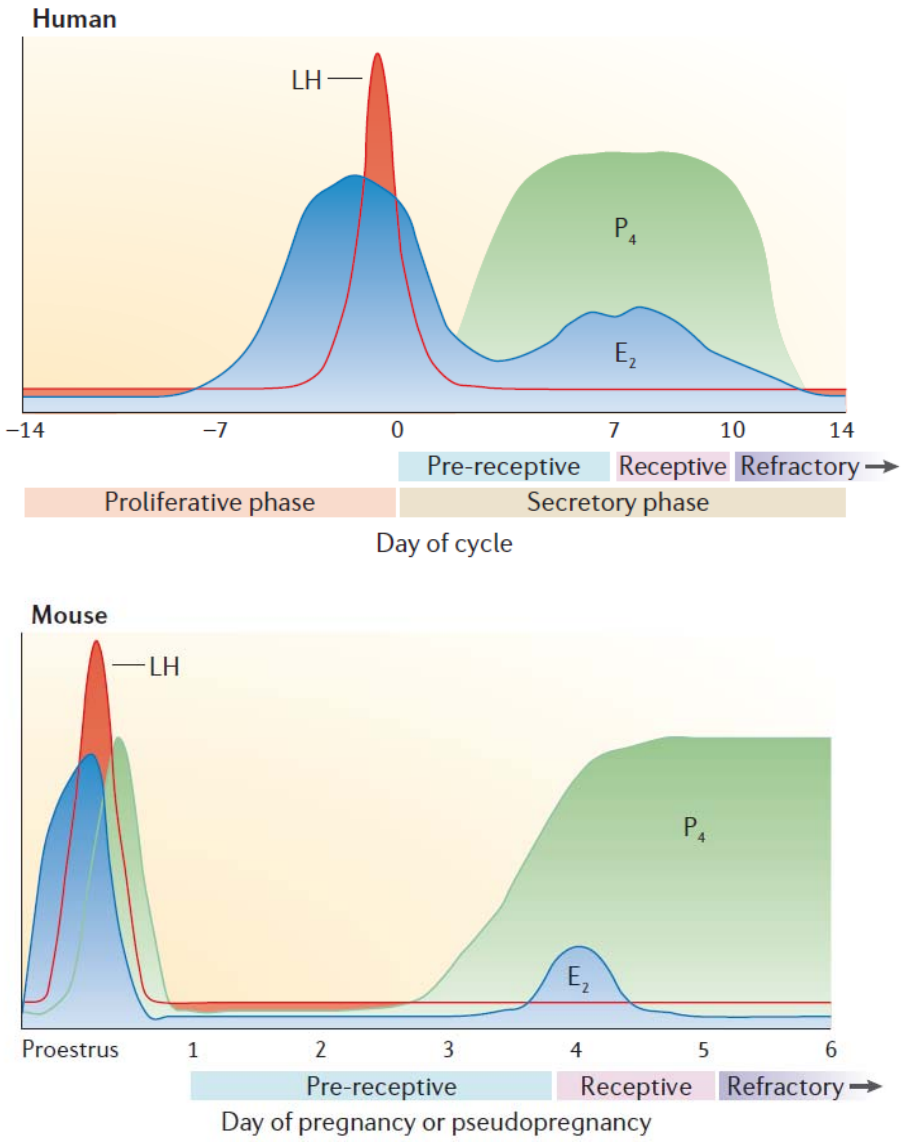

Figure 1.2. Implantation period and expression of P_4, E_2 and LH during the menstrual cycle in humans and oestrous cycle in mice

In humans there are low concentrations of the ovarian hormones immediately preceding menstruation (day -14). During the proliferative phase (or follicular phase), follicles promote the production of oestrogens which promote the proliferation of the endometrium. Immediately before ovulation (day 0), there is a surge of LH which causes a spike in E_2 levels and the mature egg is released. The corpus luteum produces P_4 during the secretory phase (days 0-14).

In the mouse, E_2 spikes in the morning of proestrus and there is a surge of LH and P_4 in the afternoon of proestrus and these hormones return to baseline during oestrus. Metestrus and diestrus are characterised by high P_4 levels.

The uterus may be divided into a pre-receptive, receptive and refractory (non-receptive) phase during implantation. The pre-receptive phase is characterised by the uterus being unable to initiate implantation of the blastocyst. During the refractory period, the uterine environment is hostile to blastocyst survival. In humans, the receptive period is about 7-10 days after ovulation, and the mice are receptive about 4-5 days after proestrus.

Reprinted by permission from Macmillan Publishers Ltd:, Wang and Dey, 2006, NATURE REVIEWS GENETICS, 7: 185-99

1.5. Clomiphene citrate

Clomiphene citrate (CC) is a triphenylethylene compound, belonging to a family of synthetic non-steroidal oestrogens/antioestrogens and selective oestrogen receptor modulators (SERMS). These compounds, when compared to the natural oestrogens, have both agonistic and antagonistic properties and have a chemical similarity to oestrogen, seen in Fig. 1.3. (Jordan, 1984, Fritz *et al.*, 1991, Pike *et al.*, 1999, Jordan *et al.*, 2001, Shelly *et al.*, 2008).

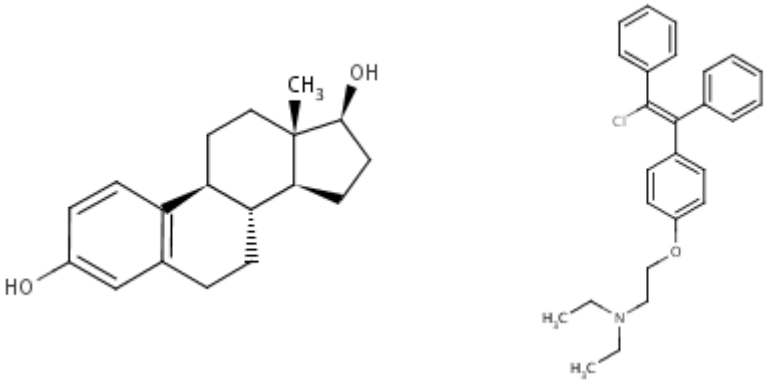

A. Oestradiol 17 β B. Clomiphene citrate

Figure 1.3. Chemical structure of E_2 and CC
The triphenylethylene, clomiphene citrate (B) has a similar structure to Estradiol 17 β (A) and can therefore bind as a ligand to the oestrogen receptor. This can result in CC causing oestrogenic effects in some tissues, and inhibiting the effects of oestrogen in other tissues.
Accessed from open software files, Drugbank, www.drugbank.ca, (A) Oestradiol 17 β filed as DB00783, and (B) Clomiphene citrate filed as DB00882

The oestrogen ligand-binding domain of the oestrogen receptors is quite large and therefore will bind a wide variety of oestrogen compounds and SERMS (Hubbard *et al.*, 2000, Pike *et al.*, 2000, Haskell, 2003). Depending on the conformation of the receptor after binding to the SERMS, the receptor-ligand complex will elicit an agonistic or antagonistic response (Hubbard *et al.*, 2000, Pike *et al.*, 2000, Sexton and Gherman, 2001, Haskell, 2003).

The triphenylethylene derivatives bind to the cytoplasmic oestrogen receptors, alpha and beta, and are translocated to the nucleus in a similar manner to that of the oestrogen receptor bound to oestrogen (Sasson and Notides, 1982, Grese *et al.*, 1997). Clomiphene binds with a high affinity to oestrogen-receptor systems of

target cells, and to anti-oestrogen specific binding sites that have been identified in the cytosols of oestrogen-receptor positive tissues, for example, the mammary gland and uterus (Gazit *et al.*, 1986). In the reproductive system, this includes sites in the hypothalamus, pituitary, ovary, endocervix, and endometrium (Fritz *et al.*, 1991). Anti-oestrogens also inhibit the natural binding of estradiol-17β to the oestrogen receptor and thereby block oestrogen-regulated processes (Tran *et al.*, 1997). However, these antagonists fail to fully induce and inhibit the oestrogen–promoted growth of the target tissues (Sasson and Notides, 1982) and may act as both oestrogen agonists as well as antogonists, depending on the species, tissue, dose level, and time of administration (Clark and Markaverich, 1982, Hosie, 1997). Clomiphene may also interact with other hormones, such as progesterone (Hosie, 1997).

Clomiphene citrate was introduced into clinical trials in 1960 as a cis/trans isomer mixture (6:4) (Greenblatt *et al.*, 1961, Gazit *et al.*, 1986). In 1967 it was introduced into clinical practice to treat infertility (Adashi, 1986). Clomiphene will induce ovulation in 55% to 90% of women (Aksel *et al.*, 1986), is economical, safe, easy to administer and has short-lived side effects (Derman and Adashi, 1994, Edwards, 1996). For these reasons, it is commonly prescribed to treat infertility.

The problem with CC use is that it results in relatively low pregnancy rates of 2.7% per cycle (Aksel *et al.*, 1986, Boostanfar *et al.*, 2001). This may be due to CC causing a detrimental change in uterine histology and carbohydrate expression (Hosie and Murphy, 1992, 1995, Hosie *et al.*, 1999, Hosie *et al.*, 2000) as well as causing endometrial abnormalities in terms of development and thickness (Cummings *et al.*, 1991, Rogers *et al.*, 1991). These changes in uterine structure may affect the ability of CC treated women to have successful implantations, which may possibly be related to apoptosis.

1.6. Sex steroids and steroid receptors

Sex steroid hormones control cell proliferation and cell differentiation in many organs, and the uterus is affected by sex steroid action (Critchley and Saunders, 2009). Oestrogen (Fig. 1.3.) and progesterone (Fig. 1.4.), acting via steroid receptors, oestrogen receptor α (ERα) or β (ERβ) and progesterone receptor (PR) A or B cause the adult human female endometrium to undergo cyclic growth and development (Gregory *et al.*, 2002). Oestrogen and progesterone are necessary for implantation to occur in normal and ovariectomised females (Logeat *et al.*, 1980).

In the follicular phase, ovarian follicles secrete E_2 which induces proliferative changes and increases endometrial sensitivity to oestrogen and progesterone by increasing the levels of ERα and PR (Garcia *et al.*, 2001, Gregory *et al.*, 2002). During ovulation, the corpus luteum secretes progesterone which induces secretory changes and dampens the response to oestrogen and progesterone (Garcia *et al.*, 2001, Gregory *et al.*, 2002).

The ER and PR have been found in the nuclei of uterine epithelial, stromal and myometrial cells (Coppens *et al.*, 1993). Coppens *et al.* (1993) investigated the topographical distribution of oestrogen and progesterone receptors in the uterus and uterine tubes in women. They found that there were higher concentrations in the fundal part of the endometrium and the ampullar region of the uterine tube. This gradient persisted through menstruation and after menopause (Coppens *et al.*, 1993). The highest concentrations of ER and PR occur in the epithelial and stromal cells during the late proliferative phase of the menstrual cycle (Nisolle *et al.*, 1994) and are significantly lower in the endometrium in the late secretory phase (Garcia *et al.*, 2001).

Rats were found to have double the concentration of progesterone and oestrogen receptors in the nuclei at implantation sites, when compared to non-implantation sites, suggesting that the blastocyst assisted in the delivery of the steroids to the endometrium (Logeat *et al.*, 1980).

Embryos can remain dormant for prolonged periods in the uteri of ovariectomised rats maintained on progesterone alone (in a process known as diapause) and E_2 provides the nidatory impetus (Develioglu *et al.*, 1999).

1.6.1. Progesterone receptors

The progesterone receptor (PR) is a ligand-activated nuclear transcription factor that mediates the action of progesterone in target cells (Murata and Higuchi, 2003, Gellersen *et al.*, 2009) and is highly conserved among a number of species, including humans, chickens, rats, rabbits and mice (Pinter *et al.*, 1996).

It is expressed predominantly in breast tissue, the basal layer of the epithelium, stromal cells of the endometrium and smooth muscle cells of the myometrium, as well as brain tissue (Graham and Clarke, 1997). Immunostaining shows the receptor to be predominantly nuclear (Ohta *et al.*, 1993).

These receptors contain well defined functional domains: the N-terminal transactivation domain, which codes for the two known isoforms of the PR, PRA and PRB. This is known as the A/B region. A third isoform of PR that lacks the AB domain, PRC, has been described. However, the natural occurrence of the PRC isoform is debatable (Gellersen *et al.*, 2009). The central region consists of a DNA-binding domain, followed by the hinge region and the C-terminal region which binds hormones (Pinter *et al.*, 1996, Murata and Higuchi, 2003, Critchley and Saunders, 2009). Fig.1.4. shows the structure of the PR isoforms.

Progesterone binds to the receptor, causing a conformational change in the receptor from an inactive, non-DNA binding form to a form that binds DNA. This is associated with the dimerisation of the receptor. The PR dimer can then bind DNA sequences within the promoter region of progesterone responsive genes, which are referred to as progesterone response elements (Aksel *et al.*, 1986, Chabbert-Buffet *et al.*, 2005).

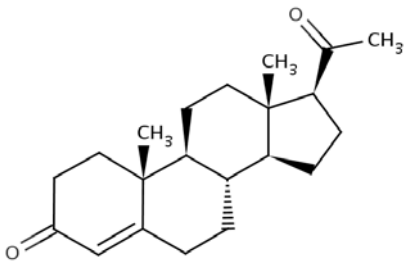

A. Chemical structure of Progesterone

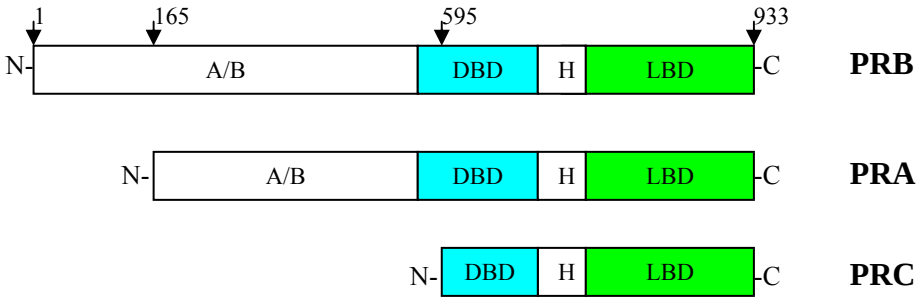

B. Functional domains of PR isoforms

Figure 1.4. Chemical structure of progesterone and the functional domains of the PR isoforms

A. Chemical structure of progesterone (accessed from openware Drugbank, www.drugbank.ca, file DB30096)

B. Isoforms of PR modified from Gellersen *et al.*, 2009. The functional domains of PRA, PRB and PRC are shown. This includes the A/B region at the N-terminal end, the DNA binding domain (DBD), the hinge region (H) and the ligand binding domain (LBD) which binds progesterone, at the C-terminal end. PRB has 933 amino acids. PRA was translated from residue 165 and PRC was translated from residue 595.

Weak DNA-dependent dimerisation of receptors is mediated by the DNA-binding domain (region C), whereas strong ligand-dependent dimerisation is mediated by the hormone-binding domain (region E) (Aksel *et al.*, 1986). Even in the absence of ligand, PRs seem to have a dynamic movement between the nucleus and the cytoplasm, with the receptor diffusing into the cytoplasm and being actively transported back into the nucleus (Pinter *et al.*, 1996).

The isoforms PRA and PRB have similar ligand and DNA binding activities, but have different functions depending on the cell type and context of the target gene promoter (Chabbert-Buffet *et al.*, 2005), where PRB is generally a stronger transcription activator than PRA. Under some conditions, PRA is inactive as a

transcription activator, but in response to binding to progesterone agonists or antagonists can repress the activities of other steroid receptors, including PRB, ER and the androgen receptor (Chabbert-Buffet *et al.*, 2005, Brosens and Gellersen, 2006). Therefore, PRA may decrease the responsiveness of the tissue to progesterone (Graham and Clarke, 1997). PRA can repress ER-mediated transcription without heterodimerising with the ER, without interfering with the ability of the ERs to interact with DNA and without changing the biochemistry of the ERs. PRA may therefore regulate other steroid receptors by competing with them for a common binding site for transcription, or for an individual binding site of a common factor (Pinter *et al.*, 1996).

Gene expression of PR in the uterus seems to be primarily controlled by oestrogen, as expression is greatest during the oestrogen dominated proliferative phase (Critchley and Saunders, 2009). Oestrogen induces PR mRNA and protein in the uterus *in vivo* (Pinter *et al.*, 1996). In humans, this regulation appears to be at the transcriptional level and may be indirect. Oestrogen is important in the synthesis of LH receptors, and so is important for preparing granulosa cells for gonadatropin induction of PR synthesis (Pinter *et al.*, 1996, Graham and Clarke, 1997). Murata and Higuchi (2003) found no significant difference in mRNA levels of PR during the oestrous cycle of rat uteri. However, these results did not distinguish between the different isoforms of PR (A, B or C), and did not indicate translational expression of PRs during the oestrous cycle. In contrast, immunohistochemical studies in the rat showed high expression of PRs in the epithelial cells nuclei at diestrus, and the stromal cell nuclei at metestrus. The PR levels seemed to decrease when oestrogen levels were low (Ohta *et al.*, 1993).

1.6.2. Effect of clomiphene citrate on sex-steroids and steroid receptors

Clomiphene citrate competes with oestradiol for binding to the endometrial cytosol oestradiol receptor (Aksel *et al.*, 1986, Homburg, 2008). Oestradiol is only available for a few hours. By comparison, CC may be found circulating six weeks post administration (Aksel *et al.*, 1986). The extended half life of CC may cause

the reduction of ER and PR concentrations in the endometrium (Sasson and Notides, 1982, Aksel *et al.*, 1986). Inadequate oestrogen or progesterone receptor or abnormal receptor function could result in delayed, inadequate or asynchronous endometrial development (Fritz *et al.*, 1991).

However, some studies seem to deny that clomiphene has an adverse effect on the endometrium. Hecht *et al.* (in Fritz *et al*., 1991) suggested that nuclear oestrogen and progesterone receptor levels and binding affinity in normal ovulatory women were no different after both low dose (50mg) and high dose (150mg) clomiphene treatment compared to spontaneous cycles (Fritz *et al.*, 1991). In contrast to this, recent work by Palomino *et al*. (2005) found that 40% of women treated with CC did not have a down regulation of endometrial PR during the window of implantation. The down regulation of PR may be important in endometrial receptivity which may account for low implantation rates in CC treated individuals (Palomino *et al.*, 2005). In addition, production of P_4 is higher in clomiphene-induced cycles when compared to spontaneous cycles (Fritz *et al.*, 1991, Palomino *et al.*, 2005).

In the brain, CC seems to interfere with the process of oestrogen receptor replenishment at the hypothalamic level, which causes a misinterpretation of circulating oestrogen concentrations. This in turn leads to a hypogonadal state. It also stimulates the increase of pituitary gonadatropin release and enhanced follicular development by changing the availability of gonadotropin-releasing hormone (Fritz *et al.*, 1991).

1.7. Programmed cell death

Programmed cell death (PCD) is important in development, tissue homeostasis and elimination of damaged cells. It has been classified into three main morphologies: type I, apoptosis; type II, autophagy and type III, programmed necrosis (Bras *et al.*, 2005, Sun and Peng, 2009), and Galluzzi *et al.* (2007) also classified mitotic catastrophe as a form of PCD.

Apoptotic cell death (type I) has been well characterised both genetically and biochemically and acts by eliminating damaged, senescent or unwanted (in terms of development) cells (Sun and Peng, 2009). Apoptosis will be detailed below (section 1.8.).

Autophagy (type II PCD) is Greek for "self eating". It is a catabolic process that is characterised by dilation of the mitochondria, intracellular membrane remodeling and the formation of double membrane autophagosomes, which are organelles that enclose various cellular constituents. The autophagosomes fuse with lysosomes to become autolysosomes where the cellular components are digested (Bras *et al.*, 2005, Sun and Peng, 2009).

Programmed necrosis, or oncosis, (type III PCD) is a passive process that usually affects a number of cells, rather than an individual cell. It is distinguished from type I and type II forms of PCD by the lack of lysosomal and caspase involvement. There are two subtypes of Type III PCD, III A and III B. Both subtypes are characterised by early swelling of cellular organelles (e.g. mitochondria, endoplasmic reticulum, Golgi bodies,) followed by loss of plasma membrane integrity. In type III B, less cytoplasmic damage occurs than type III A. The organelles are spilled into the surrounding tissue and so this type of cell death is associated with an inflammatory response (Bras *et al.*, 2005, Galluzzi *et al.*, 2007, Sun and Peng, 2009).

Mitotic catastrophe is the cell death that occurs during or shortly after a failed mitotic event (Broker *et al.*, 2005, Galluzzi *et al.*, 2007). It is caused by DNA damage and microtubule stabilising or destabilising agents. It is characterised by micronucleation and multinucleation (Broker *et al.*, 2005, Galluzzi *et al.*, 2007).

1.8. Apoptosis

The term “apoptosis” was first used by Kerr *et al*. (1972) and is used to describe an energy dependant, genetically controlled process that removes damaged or unwanted cells without an inflammatory response (Williams and Smith, 1993, Thatte and Dahanukar, 1997, Harada *et al.*, 2004). It is a naturally occurring process of physiological cell death that is important in normal development and homeostasis of a number of tissues, including the uterus (Vaux and Strasser, 1996, Tao *et al.*, 1997).

Under specific physiological or pathological conditions, the apoptotic process begins. The dying cell separates from its neighbours, usually with the loss of specialised membrane structures such as desmosomes and microvilli. It undergoes a period of blebbing and contortion. The blebs are membranous extensions of the cytosol that are usually devoid of organelles, and that can be reversibly extruded and resorbed. The cytoskeleton collapses. This is followed by an irreversible condensation of the cytoplasm, concurrent with an increase in cell density. Mitochondria swell and become porous. The nuclear chromatin condenses to form dense granular caps underlying the nuclear membrane. Nuclear pores disappear from the membrane and the nuclear centre separates from its transcription factors. The endoplasmic reticulum dilates and forms vesicles that fuse with the plasma membranes, leading to the expulsion of the endoplasmic reticulum contents out of the cell. The cytoplasm shrinks and the cell becomes highly convoluted. It loses contact with neighbouring cells. The cell splices into a number of membrane-bound bodies that contain a variety of organelles. Phosphatidylserines on the cell membranes translocate from the cytoplasmic to the extracellular side of the cells and act as a target for phagocytes. Apoptotic cells are phagocytosed by viable neighbouring cells or by phagocytes, where they are rapidly digested without an accompanying inflammatory response (Thatte and Dahanukar, 1997, Wyllie, 1997, Inbal *et al.*, 2002, Harada *et al.*, 2004).

Apoptosis is activated by a variety of external signals which may trigger the two major apoptotic pathways; the extrinsic pathway (death receptor pathway) or the intrinsic pathway (mitochondrial pathway) (Jin and El-Deiry, 2005). The extrinsic pathway is activated by the binding of death inducing ligands to a specific receptor on the cell membrane, for example the Fas / Fas ligand or Tumour necrosis factor α (TNFα) / Tumour necrosis factor receptor 1 (TNFR1). The intrinsic pathway is activated by intrinsic signals, such as DNA damage, growth factor deprivation or oxidative stress. It often involves the mitochondria or the endoplasmic reticulum, discussed below (Van Cruchten and Van Den Broeck, 2002, Jin and El-Deiry, 2005).

Mitochondria

During apoptosis, the mitochondria become porous and induce cell death by releasing pro-apoptotic proteins into the cytosol. Cytochrome c is released from the mitochondrion and complexes with apoptosis protease-activating factor 1 (Apaf-1), dATP and procaspase 9 to form the apoptosome. The apoptosome then activates caspases -3 and -7, which then activate further procaspases, and cause the apoptotic response (Bras *et al.*, 2005).

Proteins such as apoptosis inducing factor (AIF) and endonuclease G are also released from the mitochondria, and promote non-caspase associated DNA degradation. AIF translocates from the mitochondria to the nucleus where it is involved in large scale DNA fragmentation and chromatin condensation without nuclease activity. Endonuclease G seems to work in conjunction with both AIF and the caspase activated DNases in chromatin condensation and nuclear degradation (Bras *et al.*, 2005).

Permeabilisation of the mitochondrial membrane is considered to be a marker of cell death as cells are not expected to survive after the membrane becomes porous (Galluzzi *et al.*, 2007). The Bcl-2 and Bax proteins are intimately involved in regulating apoptosis in the mitochondria (see section 1.9.).

DNA

DNA fragments during apoptosis and Ca^{2+}- and Mg^{2+}- dependent endonucleases are activated (Thatte and Dahanukar, 1997), leading to internucleososomal DNA cleavage, which results in DNA fragments of 180 to 200 base pairs and multiples. This allows for the "ladder" pattern seen on agarose gel electrophoresis and is considered important as a marker for apoptosis (Thatte and Dahanukar, 1997). DNA may also be fragmented into 50 to 300 kilobase pair lengths and single-stranded DNA during apoptosis (Thatte and Dahanukar, 1997). The chromatin becomes pyknotic and packs along the nuclear membrane (Majno and Joris, 1995).

Lysosomes

Permeabilisation of the lysosomes cause proteolytic enzymes to be released into the cytosol. If selective permeabilisation occurs, apoptosis-like cell death will occur, whereas an extensive breakdown of the lysosomes results in necrosis. The cysteine proteases, cathepsin B and D, which are abundant lysosomal proteins, seem to have the greatest effect on programmed cell death. Members of the Bcl-2 family may be translocated to the lysosomes and induce the formation of pores (reviewed in Broker *et al*., 2005). Alternatively, lysosomal proteases may trigger the permeabilisation of the mitochondrial membrane through the Bcl-2 family protein Bid, and so cause the release of mitochondrial proteins (Broker *et al.*, 2005).

Endoplasmic reticulum

The endoplasmic reticulum can initiate PCD in response to unfolded proteins or by releasing calcium into the cytosol which activates caspase 12. Endoplasmic reticulum stress can also cause the permeabilisatiom of the mitochondrial membrane. The Bcl-2 family members and cytoplasmic calcium influx caused by oxidative stress seem to mediate interactions between the mitochondria and endoplasmic reticulum (reviewed in Broker *et al*., 2005).

Cytosolic calcium can activate the calpains (calcium activated neutral proteases) which can act downstream of caspase activation. Bax appears to be involved in the cross talk between the calpains and caspases (reviewed in Broker *et al*., 2005).

1.8.1. Apoptosis in the human endometrium

Apoptosis seems to maintain homeostasis of the uterine epithelium by eliminating senescent cells during the late secretory phase and the menstrual phase (Harada *et al.*, 2004).The apoptotic cells in the endometria have characteristic morphological features when stained with haematoxylin and eosin. These include cell shrinkage, chromatin margination or chromatin condensation with the formation of apoptotic bodies (Mereseman *et al.*, 2000, Mereseman *et al.*, 2002).

Havelka *et al.* (2005) found that the apoptotic index (i.e. apoptotic cells seen) increased on the second day after menstruation, mainly in the epithelial cells, while the stromal cells had far fewer apoptotic cells. This suggested that apoptosis was under the influence of hormones during the menstrual cycle, which was independent of menstrual bleeding (Havelka *et al.*, 2005). Stromal cells underwent apoptosis subsequent to uterine epithelial apoptosis, with an increased proliferation rate and PR expression as well as decreased Bcl-2 levels (Brosens and Gellersen, 2006).

Havelka *et al.* (2005) also found that the number of apoptotic cells increased as menstruation approached. They found that there was a relative independence of programmed cell death from the levels of steroid hormones as menstruation approached, whereas other studies had found that higher estradiol levels had a protective effect against apoptosis.
Apoptosis in the glandular epithelia seems greatest in the late secretory and menstrual phase (Harada *et al.*, 2004).

1.8.2. Apoptosis in the rodent endometrium

In the rat endometrium, apoptosis is found to be greatest in uterine luminal cells during metestrus and lower at oestrus, which corresponds to the reduction of oestrogen at metestrus and oestrus. The glandular epithelial cells have the highest apoptotic index at oestrus, which diminishes during metestrus. Neither tissue showed apoptosic activity during proestrus or diestrus (Sato *et al.*, 1997). There is a constant low level of apoptosis in the stromal cells during all phases of the oestrous cycle (Sato *et al.*, 1997).

Wood and co-workers (2007) found that circulating P_4 had an inverse relationship to apoptosis in the stromal cells of the mouse uterus. They also found that E_2 levels were inversely related to apoptosis in the lumen, glands and stroma. Interestingly, this data suggests that apoptosis may be regulated in the different uterine compartments by both ovarian hormones.

1.9. The Bcl-2 family

Bcl-2 was first identified through its involvement in B-cell lymphomas (Brown, 1996). This association gave it its name; the B Cell Lymphoma/leukemia-2. The Bcl-2 gene codes for a 25-26 kDa protein. It has four highly conserved domains, BH 1, 2, 3 and 4. (BH refers to the Bcl-2 homology domains). The C-terminal 21 amino acids are hydrophobic and are required for insertion into membranes (Chen-Leavy and Cleary, 1990, Brown, 1996). It has been shown that the ability of Bcl-2 to insert into membranes is associated with its ability to regulate apoptosis (Hockenbery *et al.*, 1990, Brown, 1996).

Bcl-2 has been found to immunoprecipitate with a number of structurally similar proteins that are collectively known as the Bcl-2 family. These proteins are defined by having at least one of the BH domains. The Bcl-2 family of genes have

been widely conserved both structurally and functionally throughout evolution (Tao *et al.*, 1997). One of these proteins is Bax.

Bax stands for the Bcl-2 – Associated X protein. It is a 21 kDa protein. Bax has about 45% amino acid homology with Bcl-2. This includes the BH1, BH2 and BH3 binding domains, as well as the C-terminal transmembrane domain (Brown, 1996). A common feature of the proapoptotic Bcl-2 subfamily is that they have the BH1, BH2 and BH3 binding domains, but lack the BH4 domain (Viegas *et al.*, 2008).

Bax may form homodimers, or it may form heterodimers with Bcl-2 (Oltvai *et al.*, 1993, Williams and Smith, 1993, Yang *et al.*, 1995, Brown, 1996).
The Bax protein moves from the cytosol to the mitochondria, where it forms selective channels in the outer mitochondrial membrane and facilitates the release of cytochrome c into the cytosol. The cytochrome c forms a complex with procaspase 9 and Apaf-1 (this complex is called an apoptosome). This leads to an ATP-dependent cleavage and activation of pro-caspase 9, which is the initiator caspase in mitochondrial apoptosis (Obrero *et al.*, 2002).

Bcl-2 is present on the mitochondrial outer membrane, the nuclear membrane, with localization around the nuclear pore complexes and the endoplasmic reticulum (Brown, 1996). Bcl-2 is orientated so that most of the protein is on the cytosolic face of the ER (Hockenbery *et al.*, 1990, Brown, 1996).

1.9.1. Bcl-2, Bax and apoptosis

Bcl-2 is a proto-oncogene that blocks apoptosis induced by different stimuli (Oltvai *et al.*, 1993, Tao *et al.*, 1997, Mereseman *et al.*, 2002). It can protect cells against some forms of apoptosis, but does not induce cell proliferation (Oltvai and Korsmeyer, 1994).

Bcl-2 inserts into the outer membranes of the mitochondria and the nuclear envelope, and the endoplasmic reticulum membranes. This insertion helps its cytoprotective action (Wyllie, 1997, Viegas *et al.*, 2008). Mitochondrial transmembrane potential is known to discharge during apoptosis. Bcl-2 may regulate the probability of this (Wyllie, 1997, De Falco *et al.*, 2001).

Overexpression of Bcl-2 has been shown to prevent apoptosis induced by physiological, pathological and experimental stimuli in a number of cell types (Hockenbery *et al.*, 1990, Bissonnette *et al.*, 1992, Tao *et al.*, 1997). However, Bcl-2 cannot prevent apoptosis in all instances, which indicates the existence of a Bcl-2 independent pathway to regulate cell death (Tao *et al.*, 1997). A number of Bcl-2 related genes that share a significant amino acid homology with Bcl-2 have been shown to interfere with the action of Bcl-2 (Yang and Korsmeyer, 1996, Tao *et al.*, 1997).

Bax occurs as a monomer in viable cells. Bax acts in opposition to Bcl-2, and co-expression of Bax with Bcl-2 allows apoptosis to proceed (Williams and Smith, 1993, Viegas *et al.*, 2008). Bax translocates to the mitochondria during apoptosis and oligomerises, which may contribute to the permeabilisation of the outer mitochondrial membrane (Assuncao Guimaraes and Linden, 2004, Viegas *et al.*, 2008). Bcl-2 forms heterodimers with the Bax protein, and the relation of the Bcl-2/Bax determines the cell's susceptibility to an apoptotic stimulant (Oltvai *et al.*, 1993, Antonsson *et al.*, 1997, Tao *et al.*, 1997, Mereseman *et al.*, 2002). Bax can also actively induce apoptosis in transfected cells (Hsu and Hsueh, 1998).
The Bax gene is ubiquitously expressed and represents a protective factor, whose expression is activated by different stimuli such as radiation (De Falco *et al.*, 2001). Bax is a downstream mediator of p53, following sublethal damage of DNA.

Mutagenesis studies of the BH1 and BH2 domains in Bcl-2 showed single amino acid substitutions disrupted Bcl-2/Bax heterodimers, but not Bcl-2/Bcl-2 heterodimers. The Bcl-2 mutants that did not bind Bax could not inhibit apoptosis

(Yin *et al.*, 1994, Yang *et al.*, 1995). This suggests that the family functions by protein-protein interactions.

Pecci *et al.* (1997) found that when progesterone was removed from rat endometrial cell culture, or when antiprogestins were added, apoptosis increased. They found that this increase did not affect the mRNA levels of Bcl-2 or Bax, but affected the levels of other Bcl-2 family members.

1.9.2. Bcl-2, Bax and the menstrual cycle

The Bcl-2 protein may be regulated by ovarian hormones. Otsuki *et al*. (1994) found that the cyclic proliferation of Bcl-2 was similar to the expression of both the progesterone and the oestrogen receptors during the menstrual cycle in human females. All three biochemicals had higher concentrations during the proliferative or early secretory phase, but the concentrations dropped during the late secretory phase. Circulating oestrogens increase the expression of Bcl-2, and progestins decrease Bcl-2 expression (Harada *et al.*, 2004). The expression of Bcl-2 was greatest in the glandular and stromal tissue during the proliferative phase and peaked during the late proliferative phase, but decreased during the late secretory and menstrual phases (Medh and Thompson, 2000, Harada *et al.*, 2004).

Havelka *et al*. (2005) found that uterine myomas had an inverse relationship to non malignant uteri; Bcl-2 expression increased in the secretory phase (P_4 regulated) and decreased after progesterone therapy had ceased (Havelka *et al.*, 2005). Concurrent with the decrease of Bcl-2 was the increase of apoptotic bodies. Bax increases in the stroma at the end of the menstrual cycle and the Bcl-2/Bax ratio mRNA level decreases (Otsuki *et al.*, 1994, Castro *et al.*, 2002). Tao *et al.* (1997) found Bcl-2 to be confined topographically to the basilis layer during the proliferative phase, and the Bax was localized to the epithelial cells of the functionalis layer during the secretory phase.

Bcl-2 deficient mice were found to have extensive apoptosis in the uterine glands and myometrium and therefore Bcl-2 may be important for the survival of endometrial and myometrial cells (Daikoku *et al.*, 1998, Harada *et al.*, 2004).

1.10. Summary

Infertility has important social, cultural, spiritual and financial implications for women. Clomiphene citrate has been used to treat infertility since the 1960s. It is a selective oestrogen receptor modulator, and as such causes both oestrogen-agonist as well as antagonist responses in cells and tissues. In the reproductive tissues, clomiphene binds to the oestrogen receptors in the hypothalamus, thus blocking their oestrogenic effects. This causes increased levels of the follicle stimulating hormone, which causes an increase in the ova released by the ovaries. Despite the ovarian hyperstimulation, women treated with CC have relatively low pregnancy rates (2.7% per cycle).

The human reproductive cycle is characterised by events in the ovaries (ovarian cycle) and uterus (menstrual cycle). The ovarian cycle is characterised by the follicular phase, which involves the development of the primordial follicle to the tertiary follicle and the production of oestrogen; the ovulatory phase in which the oocyte is released into the uterine tube; and the luteal phase, which is the period between ovulation and either menses or implantation. During the luteal phase, progesterone is produced by the corpus luteum. The menstrual cycle runs concurrently with the ovarian cycle. The proliferative phase (follicular) involves the endometrium becoming thicker and vascularised and is under oestrogen control. The secretory phase (luteal) is under progesterone control and produces a glycogen rich secretion. In the absence of an ovum being fertilised, menstruation will occur, which is characterised by sloughing of the endometrium and low levels of oestrogen and progesterone.

Rodents have an oestrous cycle. Proestus is the period when the follicles develop and has a peak in the progesterone and oestrogen hormone levels. These levels drop during oestrus, when ovulation occurs. During metestrus and diestrus, oestrogen peaks a second time, at a lower level, and progesterone levels increase and spike again during proestrus.

Both humans and rats have a "window of implantation", which is the period where the endometrium must be receptive to a viable blastocyst in order for implantation to occur. This period is characterised by apposition of the blastocyst against the endometrium; adhesion, where the blastocyst cannot be washed off the endometrium; and invasion, where the blastocyst invades into the maternal tissue. Both humans and rats undergo decidualisation in response to implantation and both species have haemochorial placentation. Rats have therefore been extensively used as models for infertility studies.

Changes in the concentrations of the progesterone receptor, Bcl-2 or Bax may contribute to the low pregnancy rates of CC treated individuals.

Progesterone is important in the maintenance of the endometrium for implantation and subsequently for pregnancy. Its effects are induced by binding to the progesterone receptor. The progesterone receptor levels are increased by oestrogen. Therefore, the SERM, CC, may decrease the levels of PR in the endometrium and thus cause the inadequate development of the endometrium. Alternatively, CC may inhibit the down regulation of PR during the window of implantation. This lack of down regulation may result in the endometrium being less receptive to the implanting blastocyst.

Apoptosis is important in tissue homeostasis and has a profound effect on the remodeling of the endometrium during the menstrual cycle, implantation and pregnancy. The intrinsic (mitochondrial) apoptotic pathway has been well characterised in terms of the events and molecules involved. Two important biochemicals that regulate the intrinsic apoptotic pathway are Bcl-2 and Bax. The

interactions between the pro-survival protein Bcl-2 and pro-apoptotic protein Bax regulate cell survival or death. In the endometrium, Bcl-2 predominates during the proliferative phase and decreases during the secretory phase and during menstruation. Oestrogens increase the levels of Bcl-2 while progestins decrease Bcl-2 concentrations. Bax levels increase during the secretory and menstrual phases and may be affected by progesterone levels.

1.11. Aim and objectives

The aim of this study was to investigate the expression of the progesterone receptor, Bcl-2 and Bax in clomiphene citrate treated rat uteri. Changes in the expression of these proteins may suggest an apoptotic cause for the low implantation rates in clomiphene citrate treated individuals.

Specific aims:

- To compare the effects of a single CC dose, a single P_4 dose, a treatment regime that reflects the hormonal actions during pregnancy or CC in conjunction with the treatment regime on the general morphology and morphometry of ovariectomised rat uteri.
- To compare the changes in localisation of PR, Bcl-2 and Bax using immunohistochemistry caused by a single CC dose, a single P_4 dose, a hormonal treatment regime or CC in conjunction with the treatment regime on ovariectomised rat uteri.
- To compare the changes in protein expression of PR, Bcl-2 and Bax using enzyme linked immunosorbent assays caused by a single CC dose, a single P_4 dose, a hormonal treatment regime or CC in conjunction with the treatment regime on ovariectomised rat uteri.

CHAPTER 2. MATERIALS AND METHODS

2.1. Animal model

A total of 48 sexually mature female in-bred Hooded Wistar Rats (12 to 14 weeks old) were obtained from the Central Animal Unit at the University of the Witwatersrand. The animals weighed, on average, 219.1 g (±10.4 g) prior to ovariectomy. Two to three animals were housed per cage, at a constant temperature of 23 °C, and fed *ad libitum* on mouse cubes (Epol, Rainbow Farms Pty Ltd, South Africa) and water. Animal ethics clearance was obtained from the Animal Ethics committee of the University of the Witwatersrand (AEC No: 2002/80/04).

2.1.1. Ovariectomy

The rats were bilaterally ovariectomised under Xylazine: Ketamine (1:4) anaesthesia (0.1 ml per 100 g) (Bayer Pty Ltd, Isando, South Africa). Surgery was performed by the resident veterinary surgeon at the Animal Unit at the University of the Witwatersrand. The animals were left to recover for four to six weeks following surgery, to ensure that no residual ovarian hormones remained in the system before experimentation. Ljungkvist (1971a) found no residual effects of the ovarian hormones after 10 days.

The animals were randomly divided into eight groups of 6 animals per group. The animals weighed, on average, 289.2 g (±33.1 g) before treatment and 289.3 g (±32.8 g) at the end of the treatments. The groups of 6 rats were treated as follows:
Group A was a negative control and therefore the animals received no treatment.
Group B, 0.1 ml 0.9% saline was administered to each animal as a carrier control.
Group C, 0.1 ml of peanut oil was administered as a carrier control.
Group D, a single 0.1 ml dose of 1.25 mg Clomiphene (CC) dissolved in saline was administered.

Group E, a single 0.1 ml dose of 5 mg progesterone (P_4) dissolved in peanut oil was administered (Table 2.1.).
Group F, the animals were treated with saline on the first day followed by oil on the second, third and fourth day. This acted as a carrier control.
Group G, the animals were hormonally primed by administering saline on the first day, 5 mg P_4 on the second day, 5 mg P_4 on the third day, 5 mg P_4 and 0.5 μg oestrogen (E_2) on the fourth day (PPPE).
Group H administered 1.25 mg clomiphene on the first day to PPPE treated animals (Table 2.2.).

2.2. Drug preparation and administration

2.2.1. Clomiphene citrate treatment

The treatment regime used was based on that of Hosie *et al.* (1992, 1995). The ovariectomised rats were injected with a single 1.25 mg dose of Clomiphene Citrate (CC) (40% cis- / 60% trans-isomers). This gave a concentration of approximately 4 mg/kg, which is considered a physiological dose level (Young *et al.*, 1991). Newberne *et al.* (1966) found that the LD_{50} for clomiphene in rats is 530 mg/kg.

Clomiphene was prepared by dissolving 5 mg CC (2-[4-(2-Chloro-1,2-diphenyl-ethenyl)phenoxy]-N,N-diethylethanamine) (Sigma-Aldrich Inc., St Louis, Mo., USA) in 100 μl absolute ethanol and 300 μl of 0.9% medical grade saline (Saarchem, Gauteng, South Africa), to give a final volume of 0.4 ml and a final concentration of 1.25 mg/ 0.1 ml. CC was administered by a 0.1 ml intraperitoneal injection using a 1 ml syringe (Surgi Plus Sterile Syringes, China) and 25 gauge needle (New Promex Corporation, Bergvlei, South Africa). (Group D).
Placebo treatment consisted of treating animals intraperitoneally with carrier alone (Group B).

2.2.2. Steroid hormone treatment

2.2.2.1. Progesterone treatment

The treatment regime used was based on that of Hosie *et al.* (1992, 1995). Progesterone (P_4) (17α-hydroxy-6α-methylpregn-4-ene-3,20-diole) was administered as a 5 mg dose. Ljungkvist (1971a), Psychoyos (1973), and Huet and Dey (1987) have shown this dose to elicit a normal physiological response in the rat uterus.

The progesterone was prepared by dissolving 120 mg P_4 (Sigma-Aldrich) in 0.9 ml benzyl alcohol (BDH, Poole, England). Once the P_4 had been dissolved, 3.9 ml peanut oil was added. Each animal was injected subcutaneously in the scruff of the neck with 0.2 ml of this solution to give a concentration of 5 mg/ml using a 1 ml syringe (Group E).
Placebo animals were treated subcutaneously in the scruff of the neck with carrier alone (Group C).

2.2.2.2. Oestrogen treatment

The treatment regime used was based on that of Brown-Grant *et al.* (1972), Murphy and Rogers (1981) and Hosie *et al.* (1992, 1995). 17-β Estradiol (E_2) (1,3,5[10]-Estratriene-3,17β-diol) was administered as a 0.5 μg dose. This dose has been shown to induce implantation in the pseudo-pregnant rat (Ljungkvist, 1971b, Psychoyos, 1973).

Oestrogen was prepared by dissolving 0.2 mg E_2 (Sigma-Aldrich) in 8 ml benzyl alcohol and then diluted in 32 ml peanut oil to give a concentration of 5 μg/ml. Placebo animals were treated subcutaneously in the scruff of the neck with carrier alone.

2.2.2.3. PPPE hormonal priming

Psychoyos (1966, 1967, 1973) developed a treatment regime in ovariectomised rats that replicated the expression of hormones in pregnant rats by a 3 day sequence of daily hormonal injections. This involved treating the animals for 3 days with 5 mg P_4 and treated on the third day with 0.5 μg E_2 (PPPE treatment) (Group G).

One group of animals received CC prior to the PPPE regime (group H), another group of animals received a saline treatment prior to the PPPE regime (Group G), and one group received carrier relevant to both CC and the hormones (Group F) (SOOO) (see Table 2.2).

2.3. Treatment regimes

Table 2.1.: Single Treatments
Animals were ovariectomised and given a single subcutaneous (SC) injection of 5 mg P_4, in carrier oil (O); or an intraperitoneal (IP) injection of 1.25 mg CC in saline (S) carrier. Control animals were given carrier alone or were untreated. The animals were killed (Kill) 24 hours after the last treatment. Groups A, B and C form part of the negative controls.

Group	No. of Animals	Day 1	Day 2	Carrier	Administration
A	6	-	Kill	-	-
B	6	Saline	Kill	Saline	IP
C	6	Oil	Kill	Oil	SC
D	6	1.25 mg CC	Kill	Saline	IP
E	6	5 mg P_4	Kill	Oil	SC

Table 2.2: Hormonally primed animals
The animals were ovariectomised, allowed to recover, then treated with a 3 day regime of hormones. The rats were given a series of SC injections of 5 mg P_4 in carrier oil over 3 days and a single injection of 0.5 µg E_2 on the third day and killed on day 4 (day of implantation receptivity). Clomiphene experimental animals: PPPE animals were given a single IP injection of 1.25 mg CC on day one. Control animals were given placebos. Animals were killed 24 hours after the final treatment.

Group	No	Day 1	Day 2	Day 3	Day 4	Day 5.5	Carrier	Admin.
F	6	S	O	O	O	Kill	O / S	SC / IP
G	6	-	5 mg P_4	5 mg P_4	5 mg P_4 / 0.5 µg E_2	Kill	O / S	SC / IP
H	6	1.25 mg CC	5 mg P_4	5 mg P_4	5 mg P_4 / 0.5 µg E_2	Kill	O / S	SC / IP

2.4. Sacrifice of animals

The animals were weighed and injected intraperitoneally with a 500 µl lethal dose of sodium pentabarbotone (Eutha-naze, Centaur Labs, Isando, South Africa). A central ventral incision was made to expose the uteri. Uteri were dissected from the attached fat and mesentery, cut above the cervix and removed. The tissue was cut into approximately 6 mm pieces. The combined pieces of tissue were all rinsed in phosphate buffered saline in a single container. Arbitrary pieces were removed for the following techniques:

1. Light microscopy: the tissue was cut into 2-3 mm pieces for histological sections analysed using H&E for morphometry;
2. Immunohistochemistry, and
3. Protein extraction: the proteins were analysed by ELISA.

2.5. Tissue preparation for light microscopy

2.5.1. Fixation

Arbitrary pieces (3 to 6 mm) of rat uteri were rinsed in phosphate buffered saline (PBS), pH 7.4 (appendix) and fixed in fresh 4% paraformaldehyde (Merck, Darmstadt, Germany) made up in PBS for 3 hours. The sections were rinsed 3 times in PBS x 2 minutes each and processed for wax embedding in an automatic tissue processor (Shandon Citadel 1000, Thermo Fisher Scientific, MA, USA).

2.5.2. Processing schedule

The tissue was dehydrated in 70% alcohol for half an hour to overnight, 95% alcohol for 2 hours followed by 2 changes of 95% alcohol for 1½ hours each, 3 changes of absolute alcohol; the first for 1 hour, the second for 2 hours and the final for 1 hour. The sections were cleared in two changes of chloroform, the first for 1 hour and the second for 2 hours, and finally the sections were left in 2 changes of paraffin wax for 2 hours each.

The tissue was embedded in fresh paraffin wax and orientated so cross sections of uteri could be cut. Sections (4-5 μm) were cut on a sledge microtome (Leica 1400, Germany) onto APES (3-aminopropyltriehoxysilane) treated slides (see Appendix B.1.). The sections were used either for Haemotoxylin and Eosin staining, or for immunohistochemistry.

2.6. Haematoxylin and eosin staining

The method was adapted from Mayer (1903) in Wilson and Gamble (2002). The sections were dewaxed in 2 changes of xylene for 5 minutes each and rehydrated through decreasing concentrations of alcohol (absolute alcohol 2 x 2 minutes, 95% alcohol for 2 minutes; and washed in water for 1 minute.

The sections were immersed in haematoxylin for 5 minutes, blued in running tap water, dipped once or twice in acid alcohol to differentiate the nuclei, left in running tap water, stained in 0.2% eosin for 1 minute and rinsed in running tap water.

The sections were then dehydrated through increasing concentrations of alcohol (95% alcohol for 2 minutes, 100% alcohol, 2 x 2 minutes), cleared in two changes of xylene (for 5 minutes each) and mounted in Entellan (Merck).

2.7. Morphometry

Morphometry was carried out on light microscopy sections stained with Haematoxylin and Eosin.

Two blocks were selected for each animal. Measurements were made on a binocular microscope (Kyowa, Tokyo). Measurements were made using a 5 x, 10 x or 40 x planar objective, with eyepiece micrometers. The eyepiece micrometers were always inserted into the left hand eyepiece tube. The diopter was maintained at a constant setting and the distance between the eyepieces was kept constant. These parameters were kept constant to minimise small magnification differences. When the 5 x and 10 x planar objectives were used, a 10 x eyepiece micrometer (Meopta) was used. The eyepiece micrometer was calibrated against a stage micrometer (Graticules Ltd, England) that was divided into 100 x 10 μm divisions. It was found that the eyepiece micrometer (Meopta) measured 385 μm per arbitrary unit using the 5 x planar objective. The eyepiece micrometer measured 147 μm per arbitrary unit using the 10 x planar objective
A 10 x Kellner (Kellner, patent 8395/75) eyepiece system was used when measurements were taken using the 40 x planar objective. The arbitrary units from the Kellner system measured 0.2167 μm when calibrated with the stage micrometer (Graticules Ltd., England).

2.7.1. Parameters measured

Fig. 2.7.1. shows the areas where measurements were taken. The measurements have been presented in μm.

The long (1) diameter and short (2) diameter of the entire uterus extending from the external myometrial layers were measured using the 10 x eyepiece micrometer from Meopta and the 10 x planar objective by default, or the 5 x objective if the sections were extremely large. The long (3) and short (4) internal diameters of the lumen were measured under the 10 x objective. Measurements were taken along the central axis as far as possible.

The stromal tissue extending from the basement membrane of the luminal epithelium to the inner myometrial layer was measured using the 10 x objective and 10 x micrometer eyepiece. Two measurements were taken when the axis was perpendicular to the mesometrial/anti-mesometrial pole (5), and one measurement each was taken for the stromal tissue at the mesometrial side (6) and anti-mesometrial side (7).

The luminal epithelial height (8) was measured with the Kellner micrometer eyepiece using the 40 x objective.

The total number of glands per section were counted (9); groups of glands together (10) indicating possible coiling of glands and glands that occurred singly were counted (11). These measurements were done using the 10 x planar objective. Glands that opened up into the luminal epithelium (12) were counted using the 40 x planar objective.

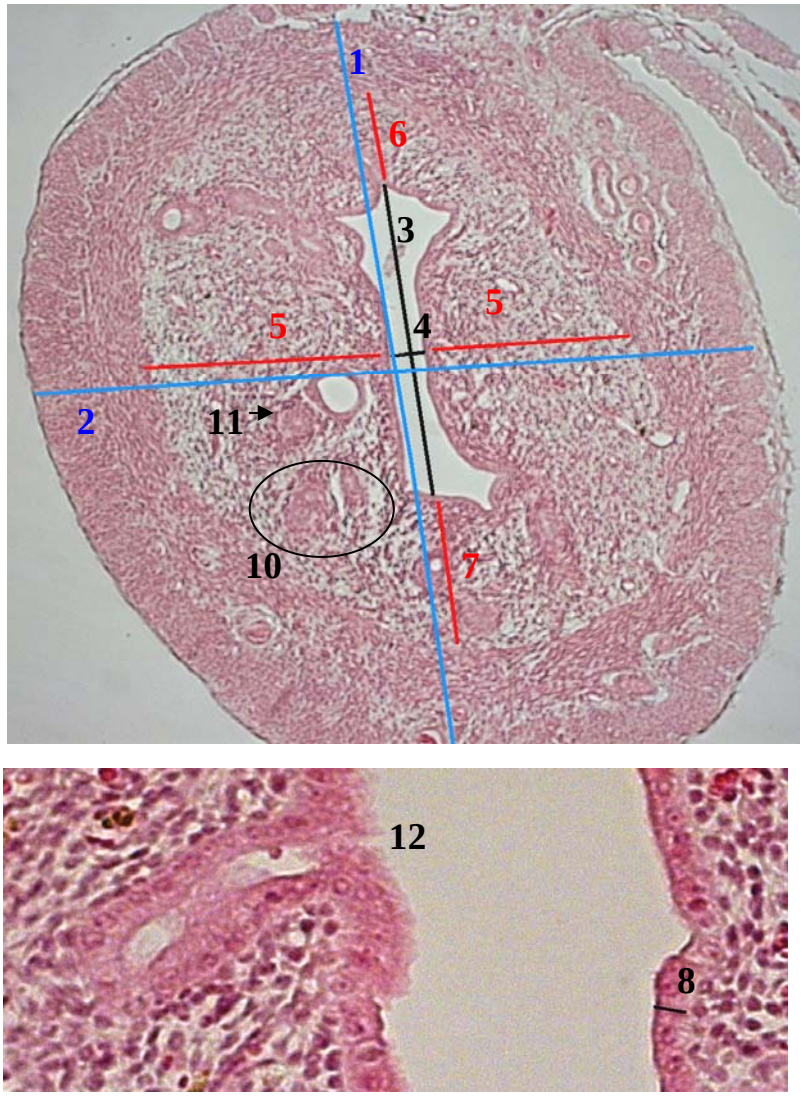

Figure 2.7.1. Parameters measured for morphometric analysis
The long (1) and short (2) diameters of the entire uterus as well as the internal lumen length (3) and lumen width (4) are indicated on the micrograph. The stroma was measured between the lumen and myometrium. Two measurements were taken perpendicular to the mesometrial/anti-mesometrial axis (5), one measurement taken at the mesometrial pole (6) and one measurement was taken at the anti-mesometrial pole (7).
All of the glands in the section were counted. The glands that existed in a group (10) as well as the glands that occurred alone (11) were counted.
The luminal epithelial height (8) was measured, and the glands that opened into the lumen were counted (12) using a 40 x objective.

2.7.2. Statistical analysis

The statistical analysis was performed using the JMP 5.0.1. statistical program (version 3.1.6.2., SAS Institute, Cary, NC). The data were analysed using non-parametric statistical methods as the sample size of each group was less than thirty individuals. The descriptive statistics were presented as medians with the upper (75%) and lower (25%) quartiles.

The data were first tested using the Wilcoxon / Kruskal-Wallis test (rank sums), followed by a 1-way Chi-squared approximation. If the value was significant, a Tukey-Kramer test was used to show the differences between groups. Significant results were presented with the means and standard error of the mean in addition to the medians and interquartiles.
The data have been presented in the text in a table or graphs in the Results.

2.8. Immunohistochemistry against the progesterone receptor (PR), Bcl-2 and Bax

Immunohistochemistry (IHC) was used to determine the immunolocalisation of the progesterone receptor, Bcl-2 and Bax in the rat endometrium. (Appendix C.1. shows the optimisation steps carried out.)

Two sections per animal were used. The uterine sections (4 μm) on 3-aminopropyltriehoxysilane coated (APES) slides were dewaxed and rehydrated and washed in distilled water for 1 minute, with stirring. The excess liquid was aspirated.

Antigen retrieval, adapted from Shi *et al.* (1995), was performed by placing the sections in a plastic container with Tris-EDTA buffer pH 9.0 (10 mM Tris Base, 1 mM EDTA, 0.05% Tween-20), (see appendix A.3.) and microwaved twice at 720 Watts for 6 minutes each and left to cool for at least 20 minutes.

After the slides had cooled, the area around the sections was wiped dry and the sections were delineated with a Dako pen (Dako, Glostrup, Denmark). The sections were washed 3 times in 0.01 M PBS, pH 7.2 (see appendix A.1.) with stirring for 2 minutes each. Endogenous peroxidase activity was quenched by incubating the sections in 1% H_2O_2 (Merck) in 0.01 M PBS for 10 minutes, washed with PBS (2 x 5 minutes) with stirring and aspirated. The sections were then incubated for 20 minutes in 1% goat serum made up in PBS.

The serum block was aspirated off the sections, but the sections were not washed. The antibodies, 1/50 anti-PR (A-0098, Dako), 1/50 anti-Bcl-2 (A-3533, Dako) and 1/50 anti-Bax (A-3533, Dako) were made up in antisera diluent (0.25% ($^{w}/_{v}$) sodium azide; 0.005% ($^{w}/_{v}$) BSA; 0.005% ($^{w}/_{v}$) thyroglobulin; 0.04% ($^{w}/_{v}$) EDTA; 1% ($^{w}/_{v}$) swine serum made up in Tris-Saline, (appendix A.1.) and left overnight at 4 ºC.

The following day, the sections were rinsed with PBS and then washed twice with PBS for 2 minutes each, with stirring. Excess liquid was aspirated and the sections were incubated for an hour at room temperature in 1/250 goat-anti-rabbit IgG/HRP (for PR), 1/200 goat-anti-mouse IgG/HRP (Dako, P-0447) (for Bcl-2) and 1/200 goat-anti-rabbit IgG/HRP (horse radish peroxidase) (Dako, P-0448) (for Bax) made up in PBS. The sections were rinsed with PBS and then washed with PBS (2 x 2 minutes with stirring).

The sections were incubated for 5 minutes in diaminobenzidine (DAB) (Roche Diagnostics Ltd., Mannheim, Germany) and rinsed in distilled water for 2 minutes with stirring, then dehydrated and cleared in 95% alcohol for 2 minutes, absolute alcohol 2 x 2 minutes, xylene 2 x 5 minutes and then mounted in Entellan (Merck).

Control sections used for IHC:

A pregnant rat uterus or colon tissue was used as a positive control.

The primary antibody was omitted, and diluent was used, on an adjacent section for every treated section as a negative control. The other negative controls used an adjacent section from the pregnant uterus or colon, incubated the primary antibody but did not incubate with the secondary antibody; or the adjacent section from the pregnant uterus or colon was incubated without either primary antibody or secondary antibodies.

Figure 2.8.1. Flow chart showing the steps for IHC against PR, Bcl-2 and Bax

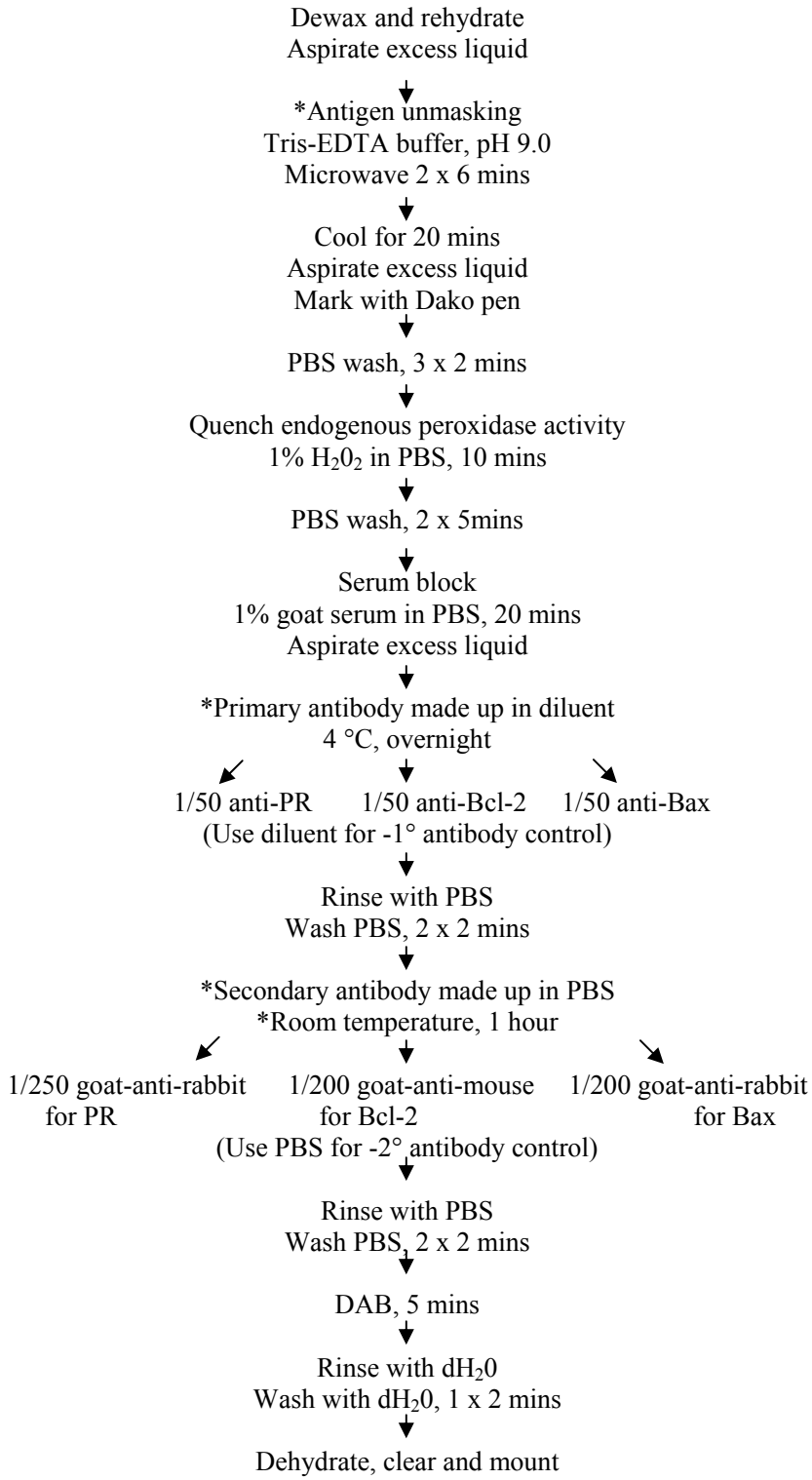

*The steps that were optimised were antigen retrieval, primary antibody, secondary antibody and DAB, which have been included in appendix C.1.

2.9. Protein extraction

Arbitrary pieces of tissue from the uterine horns were selected for protein extraction. The tissue was washed in cold PBS, pH 7.4, weighed, and cut up with sterile scissors. The tissue was placed in a clean Dounce homogeniser with 10 volumes of homogenising buffer (10% ($^{v}/_{v}$) glycerol, 5 mM magnesium acetate, 0.2 mM EDTA, 1% Triton-X-100, 50 mM Tris-HCl, pH 7.5, 0.5 M dithiothreitol, 0.5% Protease Inhibitor cocktail (Sigma-Aldrich).

The tissue was homogenised and then put into a microcentrifuge tube and centrifuged (HM2E Microfuge, Hagar Designs, Widerness, South Africa) at 15 000 g for 30 minutes at 4 ºC. The supernatant was removed, aliquoted and stored at -70 ºC.

The concentration of the protein homogenates was calculated using the Lowry-Folin method, and the relative expressions of the progesterone receptor, Bcl-2 and Bax was determined using the enzyme linked immunosorbent assay (ELISA).

2.10. Lowry-Folin method for protein determination

This assay was used according to manufacturer's instructions (Sigma-Aldrich) and based on the method of Lowry and co workers (1951). Bovine serum albumin (BSA) (Sigma-Aldrich) was used to make concentration standards (0, 31.25, 62.5, 125, 250, 500, 1 000 and 2 000 µg/ml BSA in PBS, pH 7.4). The protein samples were diluted 10 x or 20 x in PBS, pH 7.4.

Each sample of protein homogenate or BSA standard (50 µl) was added to an ELISA plate (96 well Nunc maxisorb plates, Nunc A/S, Roskilde, Denmark). Subsequently, 200 µl of 2% sodium carbonate in 0.1 M sodium hydroxide, 0.01% copper sulphate and 0.02% sodium potassium tartrate was added to the sample and incubated for 10 minutes with shaking. The samples were then incubated in

50 µl Folin-Ciocalteu's phenol Reagent (Sigma-Aldrich) diluted 1:4 in dH_2O and left on a shaker for 30 minutes. Absorbance was read on a plate reader (Multiskan Ascent, Helsinki, Finland) at 690nm.

2.11. Enzyme linked immunosorbent Assay (ELISA)

The ELISA method was used to determine the relative expression of PR, Bcl-2 and Bax. Section 10.1 shows the technique used, and appendix C.2. shows the optimisation steps used.

2.11.1. ELISA against PR, Bcl-2, Bax

Protein from the rat uterus was incubated in a 96 well Nunc maxisorb plates (Nunc A/S). The plates were coated with 100 µl of 10 µg/ml protein sample and incubated overnight at 4 ºC in a humidified chamber.

The following day, the plates were aspirated and washed 3 times with 0.9% saline, then blocked with 200 µl 0.1% BSA in PBS (appendix A.1.) and left on a shaker for an hour. The block was aspirated off and the wells washed 3 times in 0.9% saline. 100 µl primary antibody (1/100 anti-PR, sc-538; 1/500 anti-Bcl-2; 1/100 anti-Bax, sc-7480) (antibodies from Santa Cruz Biotechnology, Inc, Santa Cruz, Ca, USA) made up in block (0.1% BSA in PBS) was added to the wells and left to incubate overnight at 4 ºC in a humidified chamber.

On the third day, the primary antibodies were aspirated and the plates were washed x 4 with 0.9% saline. 100 µl secondary antisera made up in block (1/1000 donkey-anti-rabbit for Bax and PR, sc-2313, Santa Cruz; 1/1000 goat-anti-mouse for Bcl-2, sc-2005, Santa Cruz) was incubated for 1½ hours at room temperature on a shaker. The secondary antibodies were aspirated and the plate was washed 5 times with 0.9% saline. 70 µl soluble BM Blue POD substrate was added (Roche) and left to incubate in the dark. The reaction was stopped by adding 50 µl 0.5 M

sulphuric acid (see appendix A.5.) and optical density was read at 450nm (Multiskan Ascent, Labsystems, Helsinki, Finland).

2.11.2. Statistical analysis

The statistical analysis was performed using the JMP 5.0.1. statistical program (version 3.1.6.2., SAS Institute, Cary, NC). The data were analysed using non-parametric statistical methods as the sample size of each group was less than thirty individuals. The descriptive statistics were presented as medians with the upper (75%) and lower (25%) quartiles.
The data were first tested using the Wilcoxon / Kruskal-Wallis test (rank sums), followed by a 1-way Chi-squared approximation. The data have been presented in Table 3.4.1.1. in the Results section.

Figure 2.11. Flow chart for ELISA method used against PR, Bcl-2 and Bax

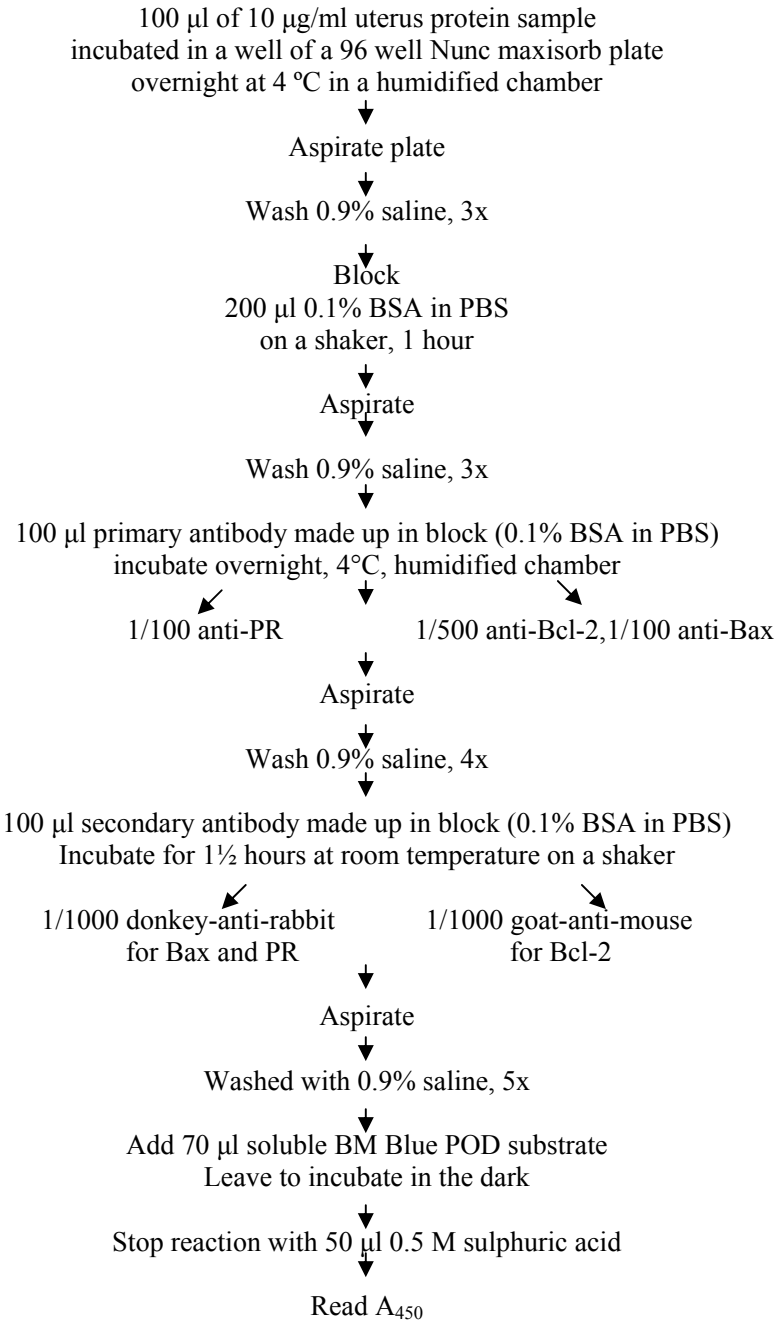

CHAPTER 3. RESULTS

3.1. Morphometric analysis of haematoxylin and eosin treated slides

3.1.1. Overview of the uterus measurements

Two random sections were analysed per animal. The uterine parameters measured included the long (1) and short (2) uterus diameters, the long (3) and short (4) luminal diameters, stroma perpendicular to the mesometrial plane (5), stroma at the mesometrial pole (6) and at the anti-mesometrial pole (7), the height of the luminal epithelium (8), total glands per section (9), groups of glands(10), single glands(11) and glands opening into the luminal epithelium (12). Wilcoxon / Kruskal Wallis rank sums tests were used to determine significance between the treatment groups, and the results have been presented in Table 3.1.1.1.
The level of significance was set at 5% level of significance. Significant differences were found between the samples for the uterine diameter measurements (1 and 2), the long luminal diameter (3), the perpendicular stroma (5) and the luminal epithelium height (8). These parameters were further tested using Tukey-Kramer *post hoc* analysis.

The results are presented in tables 3.1.1.1 to 3.1.2.6 and graphs 3.1.2.1 to 3.1.2.6.

Table 3.1.1.1. Results of the χ^2 approximation of the uterine measurements using the Wilcoxon / Kruskal Wallis rank sums tests

Two arbitrary sections were taken per animal, and the various uterine parameters were measured using an eye piece micrometer and light microscope, then tested using the Wilcoxon / Kruskal Wallis ranks sums at the 5% level of significance. For probability less than 0.05, the chi-squared approximation was used. Results that were significantly different have been indicated in bold type.

	Parameter	**χ^2 Approximation P> χ^2**
1	Long diameter uterus	**<0.001**
2	Short diameter uterus	**<0.001**
3	Long diameter lumen	**<0.001**
4	Short diameter lumen	0.117 *
5	Stroma perpendicular to mesometrial plane	**<0.001**
6	Stroma at mesometrial pole	0.0111
7	Stroma at anti-mesometrial pole	0.1789
8	Luminal epithelial height	**<0.001**
9	Total number of glands per section	0.0104
10	Groups of glands	0.3044
11	Single glands	0.119
12	Glands opening into luminal epithelium	0.4575

* The lumens of the CCPPPE treated animals were very convoluted. It was therefore not valid to measure the internal luminal diameter, as this could vary greatly depending on where the measurement was taken.

3.1.2. Results of the Tukey-Kramer *post hoc* analysis for the parameters that were significantly different

3.1.2.1. Tukey-Kramer *post hoc* analysis of uterine length

Uterine length refers to the long diameter of the cross section of the uterus, as seen in Fig 2.7.1. (1). The uterine lengths of the CCPPPE treated animals were not significantly different to SPPPE treated animals, but both were significantly different to SOOO treated animals. Therefore, the PPPE treatments appeared to increase uterine length, but CC with PPPE had no significant effects on uterine lengths.

CC alone did not significantly affect uterine length compared to saline treatment, and neither were significantly different to the ovariectomised treated group. Similarly, the uterine lengths of P_4 treated animals, oil treated animals and ovariectomised animals were not significantly different.

Generally, the CC treatment seemed to dampen the effect of the SPPPE treatment.

Table 3.1.2.1. and graph 3.1.2.1 show the mean and SEM (standard error of the mean) of the treatment groups. These show that the SPPPE treatment exhibited the greatest increase in uterine length, followed by CC alone and then CCPPPE. CC on its own seems to have an oestrogenic effect, whereas it seems to have an anti-oestrogenic effect when administered with PPPE.

Table 3.1.2.1. The median and mean for cross sectional uterine length by treatment and comparisons for all pairs using Tukey-Kramer *post hoc* analysis.

N indicates the number of samples, 25Q, the 25th interquartile, 75Q, the 75th interquartile, SEM, the standard error of the mean. Measurements in μm. For the Tukey Kramer *post hoc* analysis, levels that were not connected by the same letter are significantly different.

Treatment	N	Median and interquartiles			Mean and SEM		Tukey Kramer *post hoc* analysis		
		Median	25Q	75Q	Mean	SEM	Level		
Untreated	11	1352	1147	1470	1294	55		B	C
Saline	11	1397	1235	1470	1380	43		B	C
Oil	12	1301	1088	1580	1327	77		B	C
CC	11	1579	1323	1810	1588	78	A	B	
P_4	17	1323	1117	1636	1374	58		B	C
SOOO	11	1147	1058	1382	1196	48			C
SPPPE	12	1733	1485	1848	1734	73	A		
CCPPPE	9	1419	1286	1713	1466	82	A	B	C

Graph 3.1.2.1. The mean and SEM (black lines) for the uterine length by treatment.

Measurements in μm. For the Tukey Kramer *post hoc* analysis, levels that were not connected by the same letter (above graph) are significantly different.

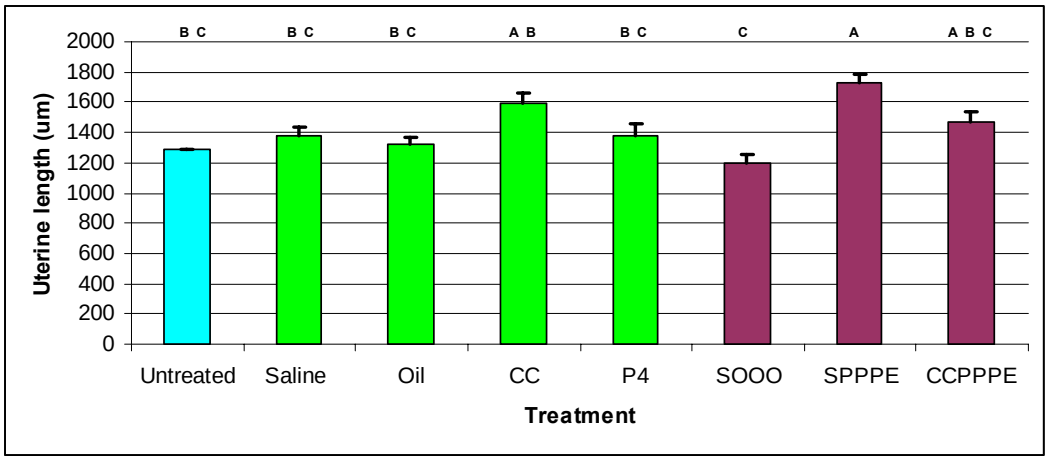

3.1.2.2. Tukey-Kramer *post hoc* analysis of uterine width

The uterine width refers to the short diameter of the cross section of the uterus, as seen in Fig. 2.7.1. (2). The uterine widths of the CCPPPE and SPPPE treated animals were not significantly different to each other, but were different to SOOO. Therefore, the hormonal treatments increased the width of the uterus, but CC treatment had no significant effect.

CC treatment alone had a significantly higher median value for uterine width than the saline treated animals, whereas the other single treatments were not significantly different.

Generally, the CC alone seemed to mimic the effect of the PPPE treatment for uterine width, but CC in conjunction with PPPE seemed to diminish the uterine width.

Table 3.1.2.2. and graph 3.1.2.2. show the mean and SEM of the treatment groups. These show that the SPPPE treatment displayed the greatest increase in uterine width, followed by CCPPPE and then CC alone. CC on its own seems to have an oestrogenic effect, whereas it seems to have an anti-oestrogenic effect when administered with PPPE.

Table 3.1.2.2. The median and mean for the uterine width by treatment and comparisons for all pairs using Tukey-Kramer *post hoc* analysis.
N indicates the number of samples, 25Q, the 25th interquartile, 75Q, the 75th interquartile, SEM, the standard error of the mean. Measurements in μm. For the Tukey Kramer *post hoc* analysis, levels that were not connected by the same letter are significantly different.

Treatment	N	Median and interquartiles			Mean and SEM		Tukey Kramer *post hoc* analysis	
		Median	25Q	75Q	Mean	SEM	Level	
Untreated	10	1014	911	1055	998	28	A	B
Saline	12	904	764	1029	908	46		B
Oil	11	956	911	1205	1006	44	A	B
CC	12	1154	1047	1246	1237	83	A	
P4	18	1047	1018	1165	1078	44	A	B
SOOO	12	849	680	1040	861	51		B
SPPPE	12	1198	1088	1308	1205	35	A	
CCPPPE	10	1161	957	1409	1174	87	A	

Graph 3.1.2.2. The mean and SEM (black lines) for the uterine width by treatment.
Measurements in μm. For the Tukey Kramer *post hoc* analysis, levels that were not connected by the same letter (above graph) are significantly different.

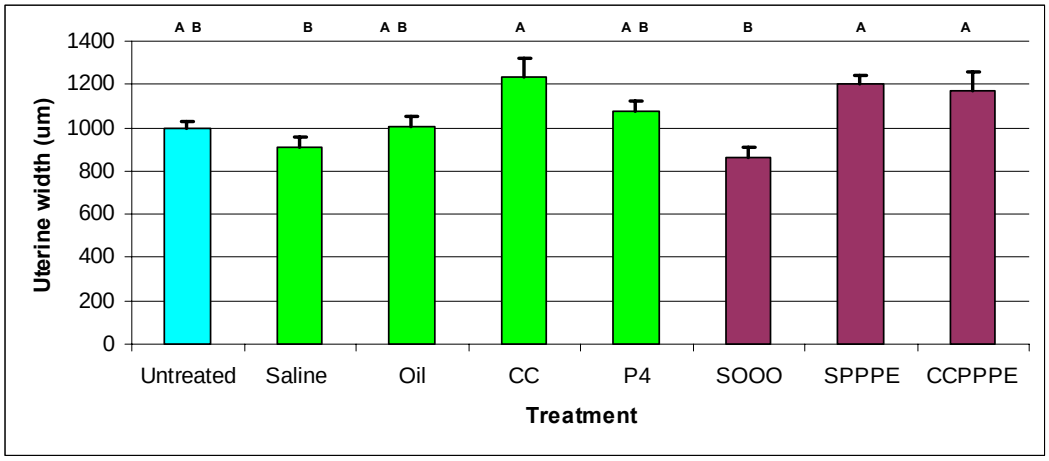

3.1.2.3. Tukey-Kramer *post hoc* analysis of luminal length

Luminal length refers to the long diameter of the internal lumen, as seen in Fig. 2.7.1. (3). The luminal lengths of the CCPPPE and SPPPE treated animals were significantly different to SOOO, but not to each other. Any effect, therefore, was influenced by the PPPE treatment, and not by the addition of CC.

The luminal length of the single CC treatment was significantly different to the saline treatment and the untreated, ovariectomised animals. Therefore, a single CC treatment significantly increased the length of the lumen.

The P_4, oil treated and the ovariectomised animals did not have significantly different luminal lengths. Therefore, P_4 did not appear to cause a significant change to the length of the lumen.

Table 3.1.2.3. and graph 3.1.2.3. show the mean and SEM of the treatment groups. These show that the CC treatment appeared to have the greatest increase in luminal length, followed by SPPPE and then CCPPPE. CC on its own seems to have an oestrogenic effect, whereas it seems to have an anti-oestrogenic effect when administered with PPPE.

Table 3.1.2.3. The median and mean for the lumen length by treatment and comparisons for all pairs using Tukey-Kramer *post hoc* analysis.
N indicates the number of samples, 25Q, the 25th interquartile, 75Q, the 75th interquartile, SEM, the standard error of mean. Measurements in μm. For the Tukey Kramer *post hoc* analysis, levels that were not connected by the same letter are significantly different.

Treatment	N	Median and interquartiles			Mean and SEM		Tukey Kramer *post hoc* analysis		
		Median	25Q	75Q	Mean	SEM	Level		
Untreated	10	411.6	376.7	457.5	414.5	15.7			C
Saline	11	485.1	411.6	529.2	477.1	27.3		B	C
Oil	11	411.6	323.4	588.0	459.0	48.1			C
CC	11	690.9	602.7	793.8	673.5	43.0	A		
P_4	18	573.3	396.9	635.8	513.7	32.7		B	C
SOOO	12	441.0	402.4	531.0	457.5	26.7			C
SPPPE	11	676.2	588.0	690.9	660.2	19.6	A		
CCPPPE	10	617.4	518.2	690.9	626.2	43.3	A	B	

Graph 3.1.2.3. The mean and SEM (black lines) for the lumen length by treatment.
Measurements in μm. For the Tukey Kramer *post hoc* analysis, levels that were not connected by the same letter (above graph) are significantly different.

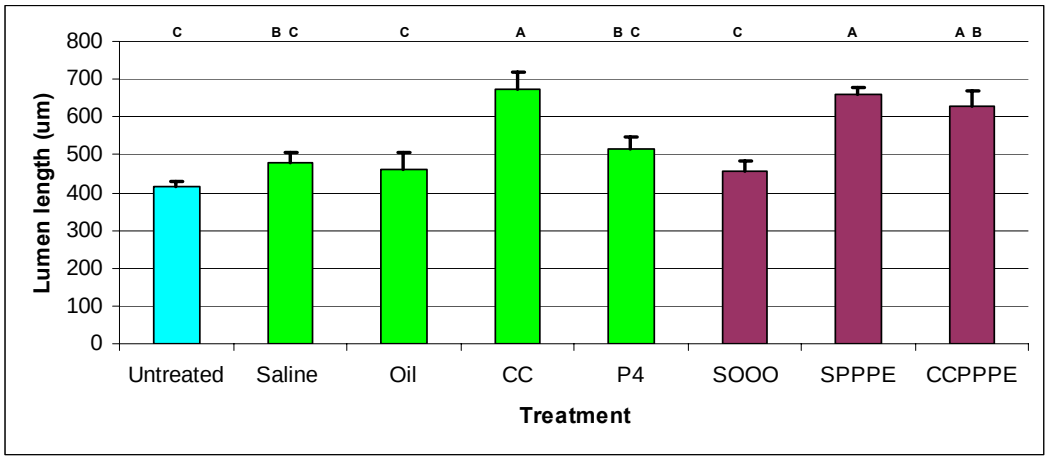

3.1.2.4. Tukey-Kramer *post hoc* analysis of the stroma perpendicular to mesometrial / anti-mesometrial pole

The wide stroma of the animals treated with CCPPPE and SPPPE were significantly different to SOOO, but not to each other. The hormonal treatments appeared to increase the stroma width, but CC in conjunction with SPPPE had no significant effect on stromal width.

The CC alone had significant differences to the stromal width compared to the saline control and the ovariectomised treated animals. Therefore, a single CC treatment demonstrably increased the stromal width.
However, P_4, oil and the ovariectomised animals did not have significantly different stromal widths from each other.

Table 3.1.2.4. and graph 3.1.2.4. show the mean and SEM of the treatment groups. These show that the SPPPE treatment displayed the greatest increase in stromal width, followed by CC alone and then CCPPPE. CC on its own seems to have an oestrogenic effect, whereas it seems to have an anti-oestrogenic effect when administered with PPPE.

Table 3.1.2.4. The median and mean for the stroma width by treatment and comparisons for all pairs using Tukey-Kramer *post hoc* analysis.
N indicates the number of samples, 25Q, the 25th interquartile, 75Q, the 75th interquartile, SEM, the standard error of the mean. Measurements in μm. For the Tukey Kramer *post hoc* analysis, levels that were not connected by the same letter are significantly different.

Treatment	N	Median and interquartiles			Mean and SEM		Tukey Kramer *post hoc* analysis				
		Median	25Q	75Q	Mean	SEM	Level				
Untreated	11	286.7	242.6	301.4	277.6	14.2			C	D	E
Saline	11	220.5	176.4	279.3	227.2	18.2					E
Oil	12	294.0	250.8	363.8	300.7	20.0		B	C	D	E
CC	12	371.2	338.1	464.9	387.1	23.4	A				
P_4	18	330.8	284.8	428.1	353.2	17.8	A	B	C		
SOOO	11	257.3	220.5	338.1	268.9	20.1				D	E
SPPPE	12	393.2	314.2	433.7	381.6	17.0	A	B			
CCPPPE	10	341.8	283.0	380.4	336.6	20.3	A	B	C	D	

Graph 3.1.2.4. The mean and SEM (black lines) for the stroma width by treatment.
Measurements in μm. For the Tukey Kramer *post hoc* analysis, levels that were not connected by the same letter (above graph) are significantly different.

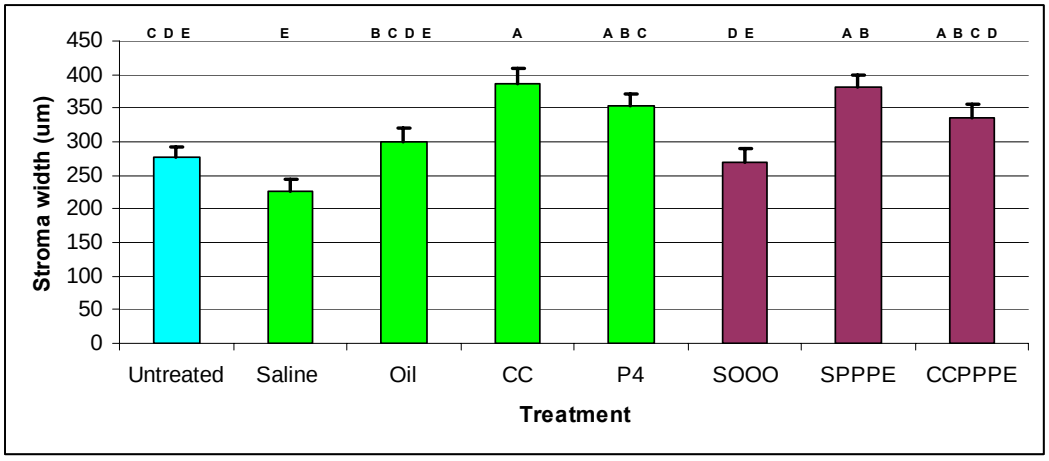

3.1.2.5. Tukey-Kramer *post hoc* analysis of the stroma at the mesometrial pole

The SPPPE treatment and P_4 treatment alone were significantly different from each other in terms of the stromal length at the mesometrial pole. SPPPE was not significantly different to the other treatments. P_4 was not significantly different to the other treatments.

Table 3.1.2.5 and graph 3.1.2.5 show the mean and SEM of the treatment groups. The stroma with the CCPPPE treatment was smaller than that seen in the controls and seemed to approach the stromal length at the mesometrial side of the uterus at a level similar to that seen in P_4 treatment alone. It almost appeared to have an effect similar to that of P_4 alone.

Table 3.1.2.5. The median and mean for the stroma at the mesometrial pole, by treatment and comparisons for all pairs using Tukey-Kramer *post hoc* analysis.

N indicates the number of samples, 25Q, the 25th interquartile, 75Q, the 75th interquartile, SEM, the standard error of the mean. Measurements in μm. For the Tukey Kramer *post hoc* analysis, levels that were not connected by the same letter are significantly different.

Treatment	N	Median and interquartiles			Mean and SEM		Tukey Kramer *post hoc* analysis	
		Median	25Q	75Q	Mean	SEM	Level	
Untreated	11	102.9	88.2	102.9	96.2	7.5	A	B
Saline	12	102.9	66.2	132.3	104.1	11.4	A	B
Oil	11	102.9	73.5	161.7	114.9	14.5	A	B
CC	12	110.3	102.9	176.4	131.1	16.1	A	B
P_4	17	88.2	73.5	102.9	88.6	3.7		B
SOOO	12	102.9	77.2	128.6	107.8	10.3	A	B
SPPPE	10	147.0	117.6	161.7	147.0	10.3	A	
CCPPPE	12	91.9	77.2	154.4	110.3	12.9	A	B

Graph 3.1.2.5. The mean and SEM (black lines) for the stroma at the mesometrial pole by treatment.

Measurements in μm. For the Tukey Kramer *post hoc* analysis, levels that were not connected by the same letter (above graph) are significantly different.

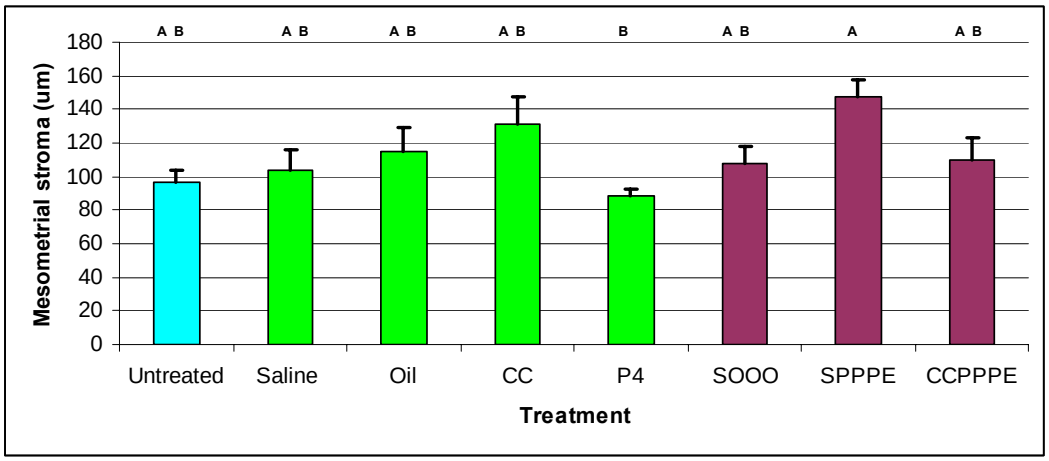

3.1.2.6. Tukey-Kramer *post hoc* analysis of the luminal epithelium height

The CCPPPE and SPPPE treatments had significantly greater luminal epithelial heights than the SOOO control, but were not significantly different to each other. Therefore, the PPPE treatment had an effect on luminal epithelial height, and the effect of CC in conjunction with the hormonal treatments was negligible.

The effect of CC alone on uterine luminal epithelial height was significantly different to the saline and ovariectomised treated animals. A single dose of CC increased the height of the luminal epithelium (LE), almost by double.

The P_4 treatment significantly increased epithelial height when compared to the oil vehicle and ovariectomised treated animals

Table 3.1.2.6. and graph 3.1.2.6. show the mean and SEM of the treatment groups. These show that the CC treatment alone had the greatest increase in epithelial height, followed by CCPPPE and then SPPPE. CC on its own seemed to have an oestrogenic effect, whereas it seemed to have an anti-oestrogenic effect when administered with PPPE. The progesterone on its own was significantly different to the controls.

Table 3.1.2.6. The median and mean for the luminal epithelial height by treatment and comparisons for all pairs using Tukey-Kramer *post hoc* analysis.

N indicates the number of samples, 25Q, the 25th interquartile, 75Q, the 75th interquartile, SEM, the standard error of the mean. Measurements in μm. For the Tukey Kramer *post hoc* analysis, levels that were not connected by the same letter are significantly different.

Treatment	N	Median and interquartiles			Mean and SEM		Tukey Kramer *post hoc* analysis			
		Median	25Q	75Q	Mean	SEM	Level			
Untreated	11	6.501	5.905	7.801	6.604	0.296				D
Saline	12	6.366	5.851	7.219	6.551	0.232				D
Oil	11	6.230	6.122	6.826	6.457	0.177				D
CC	11	11.431	10.185	12.352	11.337	0.315	A			
P_4	15	8.451	7.747	8.614	8.336	0.170			C	
SOOO	12	6.095	5.661	6.677	6.203	0.158				D
SPPPE	10	9.968	8.803	11.485	10.104	0.438		B		
CCPPPE	11	10.239	9.968	10.618	10.441	0.266	A	B		

Graph 3.1.2.6. The mean and SEM (black lines) for the luminal epithelial height by treatment.

Measurements in μm. For the Tukey Kramer *post hoc* analysis, levels that were not connected by the same letter (above graph) are significantly different.

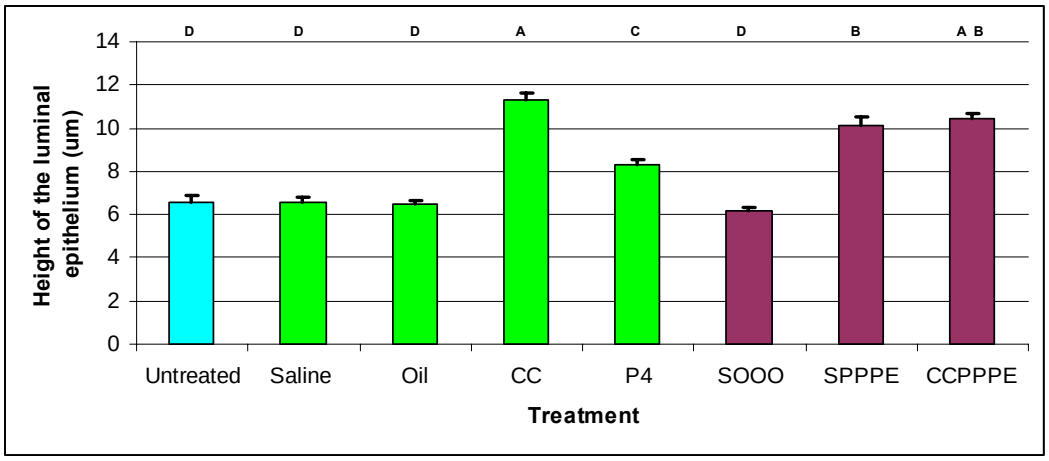

3.2. Descriptive analysis of H&E stained slides

3.2.1. H&E of control animals

The morphometric analysis of the uterine parameters measured showed no significant differences using rank sums analyses between the ovariectomised (Group A), saline treated (Group B), oil treated (Group C) and SOOO treated (Group F) animals, as evident in tables 3.1.1.1. to 3.1.2.6. Therefore, the control groups have been presented together. The results reported here concur and extend those reported by Ljungkvist (1971a, 1971b), Hosie and Murphy (1995), Hosie (1997).

The overall size of the uterine profile was small, showing a short diameter at a median (interquartile range) of 941 μm (790-1043 μm) and long diameter of 1294 μm (1117-1470 μm). The oil control demonstrated a slightly larger average diameter when compared to the other control tissue.

The uterine lumens in this group of animals were generally narrow and straight with no evidence of closure or tissue folding. An expansion at the mesometrial pole of the lumen was noted, which was often T-shaped. More stromal tissue was present at the antimesometrial pole than the mesometrial pole. Fig. 3.2.1., of an SOOO treated animal, shows a typical low power uterine profile from a control animal.

The uterine luminal epithelium seen in this group of animals typically had a single layer of low cuboidal cells with central to apically placed round nuclei. A narrow band of pale eosinophilic cytoplasm was seen above and below the nucleus. Fig. 3.2.2. shows the uterine luminal epithelium typically seen in this group of animals.

The stroma was indistinctly divided into two zones; a narrow darkly stained zone of six to eight cell layers directly below the epithelium (dark layer, DL,

Fig. 3.2.2.) where the fibroblasts were generally triangular or elongated; and a wider, paler stained layer radiating out to the myometrial layers. In this layer the fibroblasts were more flattened in appearance and not as densely packed with more ground substance evident.

Glands were generally seen more often at the antimesometrial pole of the uterus, as seen in Fig. 3.2.1. The glands generally had wide lumens that sometimes showed evidence of secretion (Fig. 3.2.3.). The epithelium lining the glands was cuboidal in shape with central to basally placed nuclei. There was little evidence of mitosis or apoptosis in the epithelium. The glands were straight with coiling evident in the deeper stroma as groups of gland profiles are clustered together (Figs. 3.2.1 and 3.2.3.).

Figure 3.2.1.
Uterine profile of an SOOO control animal
The lumen of a control animal was narrow and had an expansion at the mesometrial pole. Glands were more concentrated at the anti-mesometrial pole.

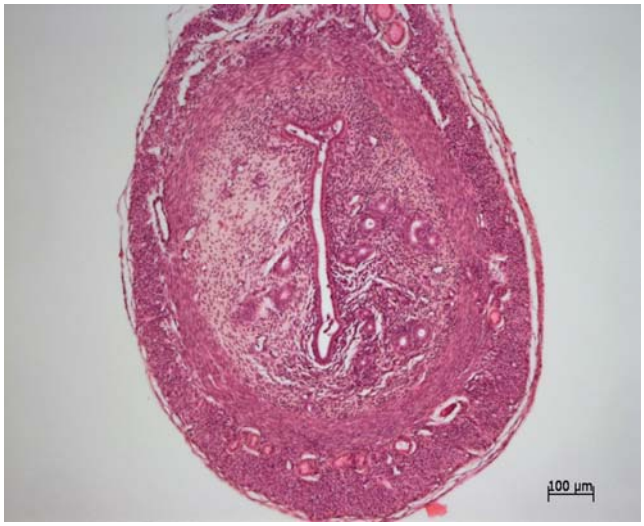

Figure 3.2.2.
Luminal epithelium of an oil control animal
The luminal epithelial cells were cuboidal, with central to apical nuclei.
The dark layer (DL) of the stroma was about six to eight layers, directly surrounding the luminal epithelium.

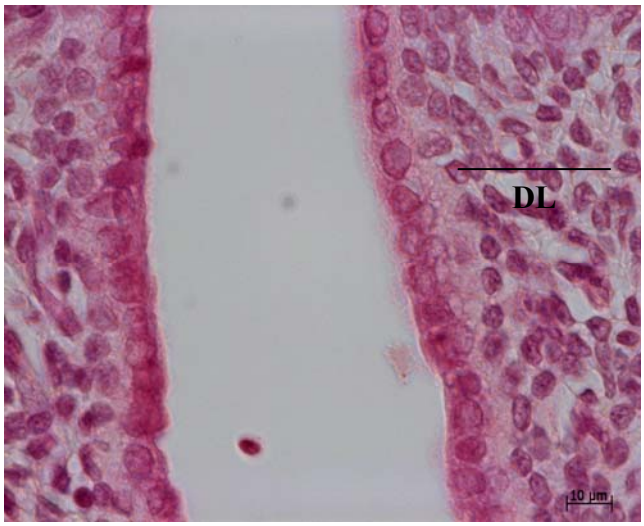

Figure 3.2.3.
Glandular tissue of an oil treated control
The epithelium lining the glands was cuboidal with basally placed nuclei.

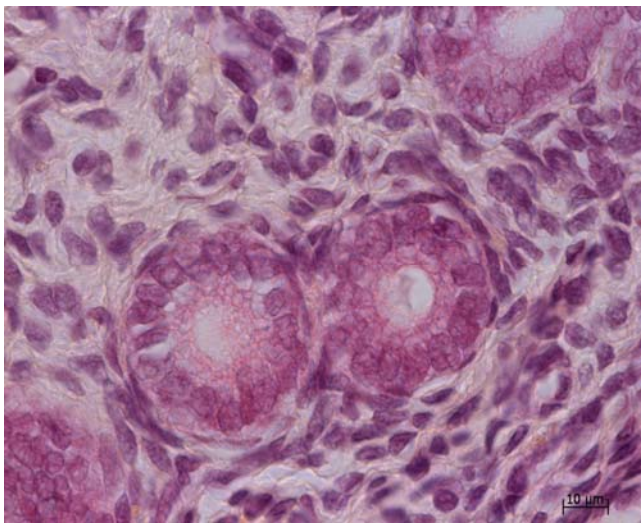

3.2.2. H&E of animals treated with a single 1.25 mg CC dose

The overall size of the uterine profile of CC treated animals was large compared to the controls and the P_4 treated tissue. The short diameter showed a median (interquartile range) of 1154 μm (1047-1246 μm) and long diameter of 1579 μm (1323-1810 μm). The uterine lumens in this group of animals were generally wide and extended at the mesometrial pole of the uterus. Fig. 3.2.4. shows a typical low power uterine profile from a CC treated animal.

The uterine luminal epithelium seen in this group of animals was typically a single layer of columnar cells which sometimes appeared closely packed and pseudostratified or stratified, indicative of hyperplasia. The epithelium had a beaded appearance with basally placed ovoid nuclei with darkly stained nuclear membranes and prominent nucleoli. A wide band of eosinophilic cytoplasm was seen above the nucleus. Long dense microvilli were evident on the surface of this epithelium. Fig. 3.2.5. is typical of the luminal epithelium of this group.

The stroma was indistinctly divided into two zones, a wide darkly stained zone (DL) extending more than half way into the tissue (Fig. 3.2.4.), where the fibroblasts were generally quite densely packed and rounded. The external stromal layer was less densely stained and quite cellular (Fig. 3.2.4.). The fibroblasts in this layer were flattened. Blood vessels were numerous and seen throughout the stroma (Fig. 3.2.5.).

Gland profiles were more numerous in this tissue when compared to the control and P_4 treated uteri, as the glands were more dispersed throughout the stroma, rather than clumped at the anti-mesometrial pole of the uterus. Coiling also appeared more extensive when compared to the other single treatment animals. The epithelium lining the glands was columnar in shape, although generally not as tall as the uterine luminal epithelium (Fig. 3.2.6.). The glandular cells had basally placed nuclei and darkly stained nuclear membranes. Nucleoli were also present

in this epithelium. Apoptotic bodies were also noted (not shown). Flattened fibroblasts often surrounded the gland profiles (Fig. 3.2.6.).

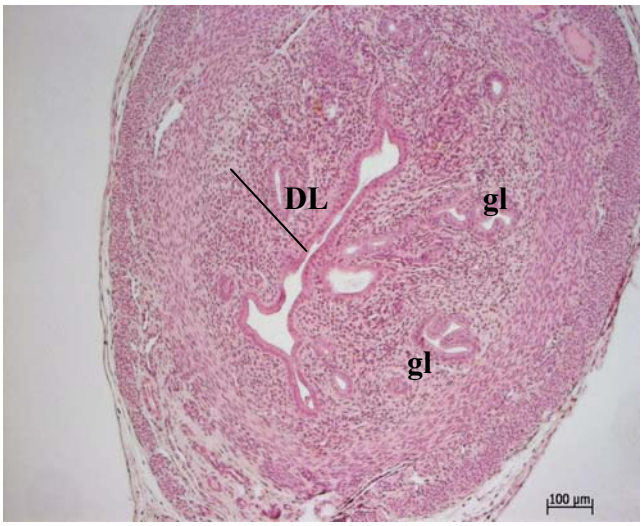

Figure 3.2.4.
Uterine profile of a 1.25 mg CC treated animal
The uterine lumens of CC treated animals were generally larger than the control or P_4 treated animals. The dark layer (DL) extended more than half way into the stroma, and the glands (gl) were dispersed throughout the stroma, and not concentrated towards the anti-mesometrial pole.

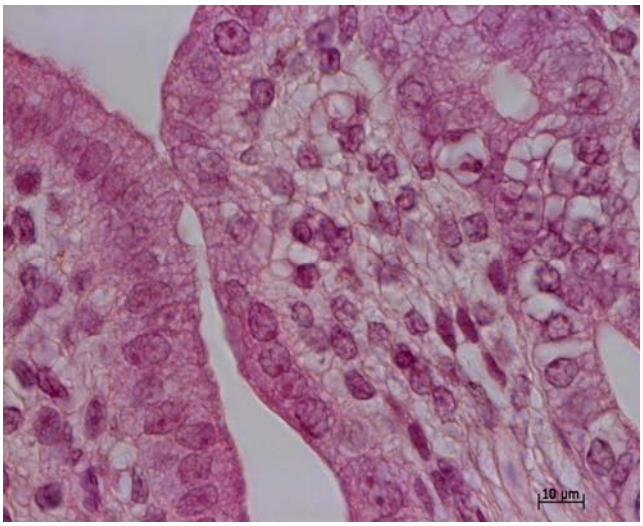

Figure 3.2.5.
Luminal epithelium of a CC treated animal
The columnar luminal epithelial cells showed some pseudostratification. Microvilli were evident on the edge of these cells. The nuclei were basally situated, with dark nuclear membranes and prominent nucleoli. Capillaries were seen in this micrograph.

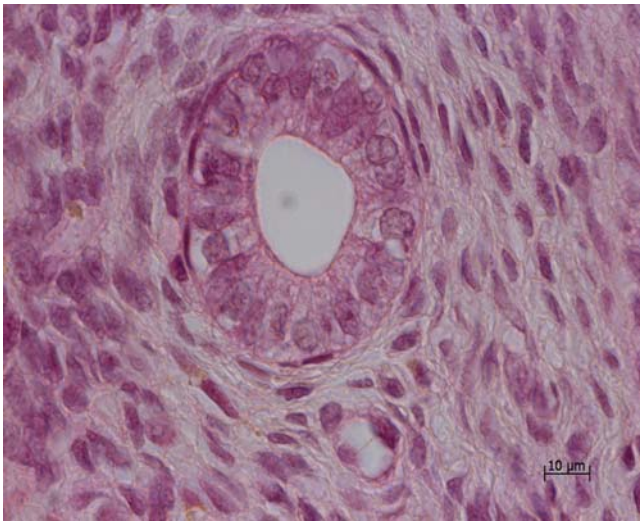

Figure 3.2.6.
A gland of a single CC treated animal
The glandular cells were elongated, with basally placed nuclei that had prominent nuclear membranes and nucleoli.

3.2.3. H& E of a single dose of 5 mg P_4

The overall size of the uterine profile of a P_4 treated animal was small and not significantly different to those seen in the control animals (tables 3.1.2.1. and 3.1.2.2.) showing a short diameter with a median (interquartile range) of 1047 μm (1018-1165 μm) and long diameter 1323 μm (1117-1636 μm). The uterine lumens in this group of animals were generally narrow and straight and usually occluded with no tissue folding, in accordance with the work by Ljunkvist (1971a). At the mesometrial pole of the tissue the lumen was T-shaped. Fig. 3.2.7. shows a typical low power uterine profile from a P_4 treated animal.

The uterine luminal epithelium seen in this group of animals was typically a single layer of cuboidal cells with central to basally placed round nuclei, with a darkly stained nuclear membrane often displaying nucleoli. A narrow band of eosinophilic cytoplasm was seen above and below the nucleus, as seen in Fig. 3.2.8.

The stroma was indistinctly divided into two zones, a narrow darkly stained zone (DL) of six to eight cell layers directly below the epithelium (Figs. 3.2.7. and 3.2.8.) where the fibroblasts were generally rounded, and a wider paler stained layer radiating out to the myometrial layers. Numerous small blood vessels were seen just below the luminal epithelium.

As seen in the control tissue, the majority of gland profiles were seen at the anti-mesometrial pole of the uterus (Fig. 3.2.7.) with similar wide lumens sometimes showing evidence of secretion. The epithelium lining the glands was more columnar in shape with more basally placed nuclei, and darkly stained nuclear membranes (Fig. 3.2.9.). Nucleoli were also present in this epithelium. Apoptotic bodies were also noted (Fig. 3.2.9.). The glands were straight with less coiling evident in the deeper stroma when compared to the control tissue. Flattened fibroblasts often surrounded the gland profiles (Fig. 3.2.9).

Figure 3.2.7.
Uterine profile of a 5 mg P_4 treated animal
The lumen of the P_4 treated animals tended to have a T-shape at the mesometrial pole, with occlusion of the luminal epithelium further into the stroma. The dark layer (DL) was about six to eight cell layers beneath the luminal epithelium. Glands tended to concentrate at the anti-mesometrial pole.

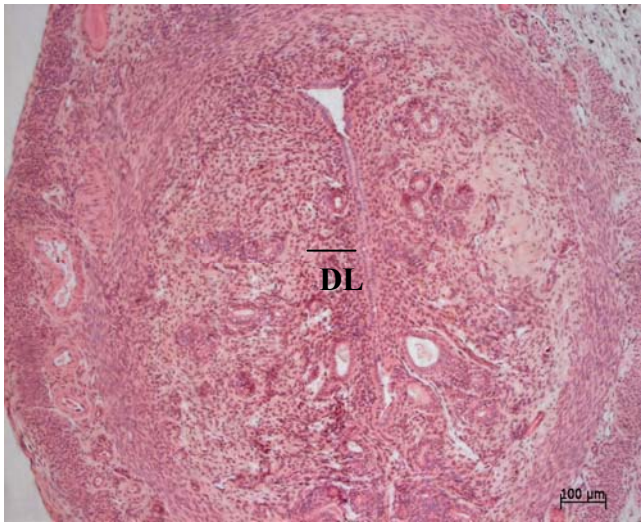

Figure 3.2.8.
Luminal epithelium of a P_4 treated animal
The nuclei of the luminal epithelia tended to be basally to centrally positioned with dark nuclear membranes.
Eosinophilic cytoplasm surrounded the nuclei.
The fibroblasts surrounding the luminal epithelium tended to be rounded.

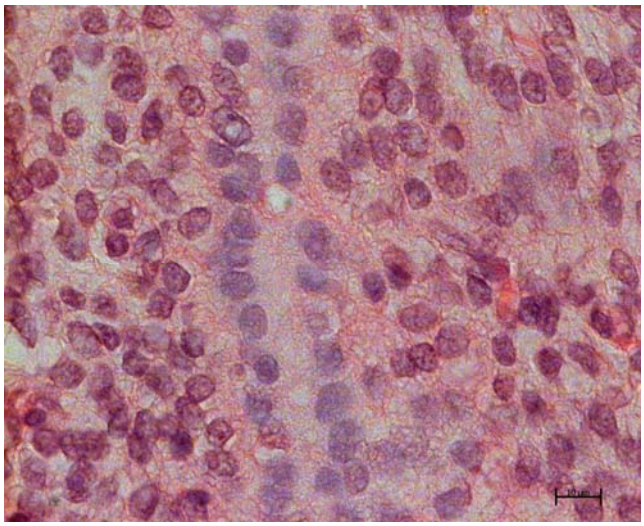

Figure 3.2.9.
Glands of a 5 mg P_4 treated animal
The epithelia lining the glands was columnar, with basally placed nuclei.
An apoptotic cell (ApC) has been indicated with the arrow.
Flattened fibroblasts surrounded the tissue.

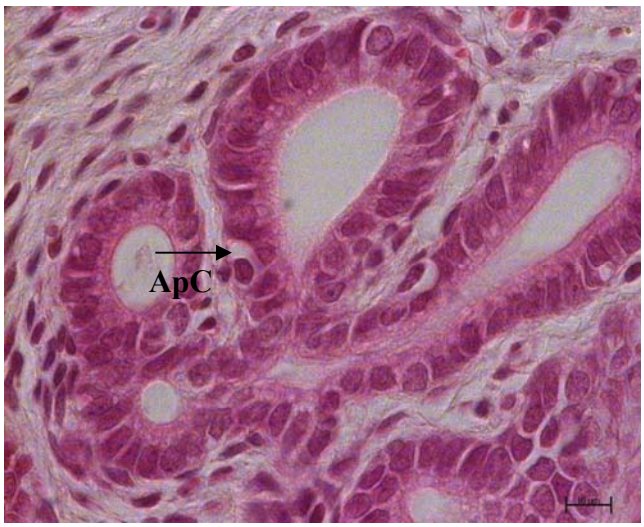

3.2.4. Hormonally induced receptivity, SPPPE

The results concur and extend those reported by Ljungvist (1971a).
The overall size of the uterine profile of SPPPE treated animals was large when compared to the control tissue, with a short diameter median (interquartile range) of 1198 μm (1088-1308 μm) and long diameter of 1733 μm (1485-1848 μm). The uterine lumens in this group of animals were generally narrow and straight and were largely occluded. At the mesometrial pole of the tissue the lumen was expanded. Fig. 3.2.10. shows a typical low power uterine profile from an SPPPE treated animal.

The uterine luminal epithelium seen in this group of animals was typically a single layer of cuboidal cells with basally placed round nuclei surrounded by a darkly stained nuclear membrane. A narrow band of eosinophilic cytoplasm was prominent above the nucleus, as seen in Fig. 3.2.11.

The stroma was divided into two zones, a narrow darkly stained zone of six to eight cell layers directly below the epithelium (dark layer DL) and extending with the glandular epithelium and so surrounding it. The fibroblasts in this area were generally rounded. Surrounding the DL was a wider paler stained layer radiating out to the myometriun where the fibroblasts also appeared somewhat rounded and active. Large blood vessels were evident in the stroma. Fig. 3.2.11. shows the stroma surrounding the luminal epithelium.

In this tissue, the majority of gland profiles were seen at the anti-mesometrial pole of the uterus, although in some sections, gland profiles were also seen at the mesometrial pole. The glands had wide lumens mostly filled with secretions (Fig. 3.2.12.). The epithelium lining the glands was more columnar in shape than that of the luminal epithelium, with basally placed nuclei, and darkly stained nuclear membranes. The gland profiles were numerous, demonstrating extensive coiling when compared to the control tissue and single treatment tissue (Fig. 3.2.12.).

Figure 3.2.10.
Uterine profile of an SPPPE animal
The lumen was expanded at the mesometrial pole.
The dark layer (DL) surrounding the lumen was about six to eight layers deep.
There were numerous gland profiles, concentrated mainly at the anti-mesometrial pole.

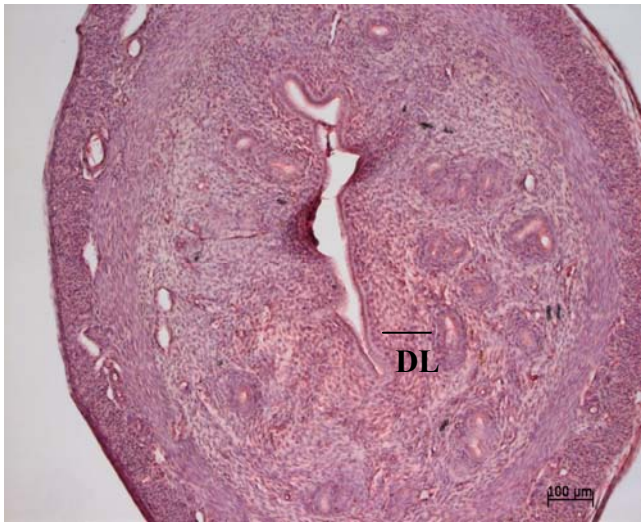

Figure 3.2.11.
Luminal epithelium of an SPPPE animal
The uterine epithelium had cuboidal cells with round nuclei and darkly stained nuclear membranes. Prominent eosinophilic cytoplasm was evident above the nuclei. The fibroblasts surrounding the uterine luminal epithelium were generally rounded.

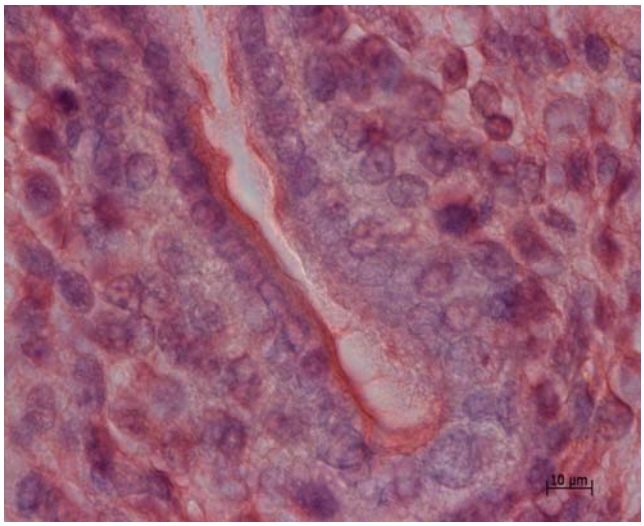

Figure 3.2.12.
Gland profile of an SPPPE animal
The glands generally had wide lumens filled with eosinophilic secretions. The glandular epithelia had rounded, basally placed nuclei with dark nuclear membranes and the glandular cells were more columnar than the luminal epithelial cells.

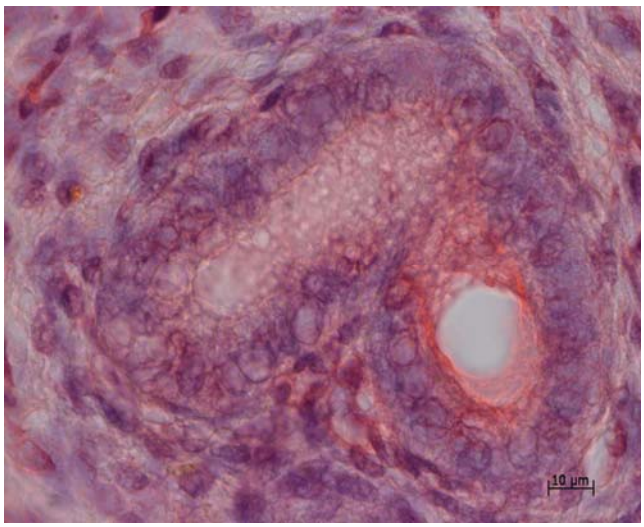

3.2.5. CCPPPE Hormonally induced receptivity

The overall size of the uterine profile of the CCPPPE treated tissue was smaller when compared to the SPPPE treated tissue, but not significantly smaller (tables 3.1.2.1 – 3.1.2.2). The short diameter median (interquartile range) was 1161 μm (957-1409 μm) and long diameter was 1419 μm (1286-1713 μm).

The uterine lumens in this group of animals were invaginated, forming pockets or large diameter glandular structures and to some extent folding was apparent. There was also no obvious expansion of the lumen at the mesometrial pole as seen in the other tissue analysed in this study. Fig. 3.2.13. shows a typical low power uterine profile from a CCPPPE treated animal.

The uterine luminal epithelium seen in this group of animals was typically a single layer of tall columnar cells, sometimes appearing pseudostratified. The cells displayed centrally to basally placed granular nuclei that were oval to irregularly shaped. The nuclei had a darkly stained nuclear membrane and nucleoli were also noted. A band of eosinophilic cytoplasm was prominent below the nucleus. The cytoplasm of these cells appeared bubbly or granular. The cells also displayed a prominent band on the apical membrane indicative of a brush border or at least dense long microvilli as reported by Hosie and Murphy (1992) and Hosie (1997). Fig. 3.2.14. shows a typical micrograph of a CCPPPE treated luminal epithelium.

The dark layer (DL) of the stroma extended to the end of the glands as seen in the SPPPE treated tissue. Similarly, the fibroblasts in this area were rounded, suggestive of activity. Surrounding the DL was a wider, paler stained layer of stroma radiating out to the myometrium, where the fibroblasts also appeared rounded and active (Fig. 3.2.13.).

In this tissue the majority of gland profiles were seen at the anti-mesometrial pole of the uterus, or dispersed throughout the stroma, with few or no gland profiles

seen at the mesometrial pole (Fig. 3.2.13.). The glands had wide lumens that usually lacked eosinophilically stained secretions (Fig. 3.2.15.). The epithelium lining the glands was cuboidal in shape with darkly stained basally placed nuclei. In contrast, the SPPPE treated tissue had more columnar glandular epithelia. Apoptotic cells were often seen in this tissue (Fig. 3.2.15.). Gland profiles were numerous, demonstrating extensive coiling when compared to other tissue examined in this study (Fig. 3.2.10 and 3.2.12. of SPPPE treated tissue, and 3.2.13 and 3.2.15 of CCPPPE treated tissue).

Figure 3.2.13.
Uterine profile of a CCPPPE treated animal
At low power, the lumen showed extensive folding. The gland profiles were found at the anti-mesometrial pole, or dispersed through the stroma. The dark layer (DL) of fibroblasts extended to the glands.

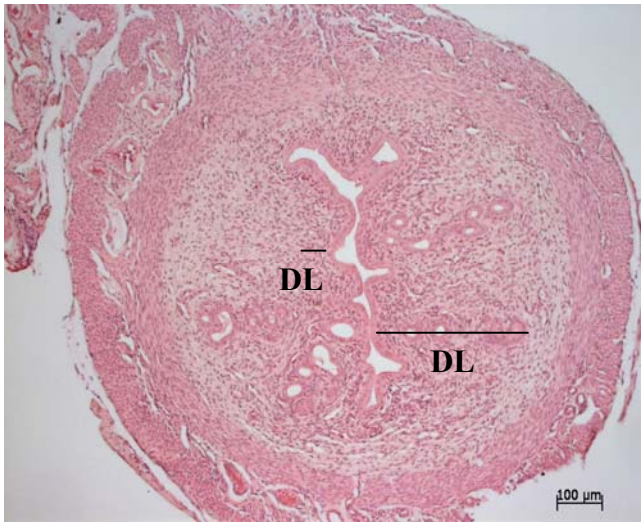

Figure 3.2.14.
Luminal epithelium of CCPPPE treated tissue
The luminal epithelial (LE) cells were columnar in shape. They had centrally placed nuclei with dark nuclear membranes and dark nucleoli. The cells had a prominent apical membrane. Fibroblasts surrounding the LE were rounded, suggesting that they were active.

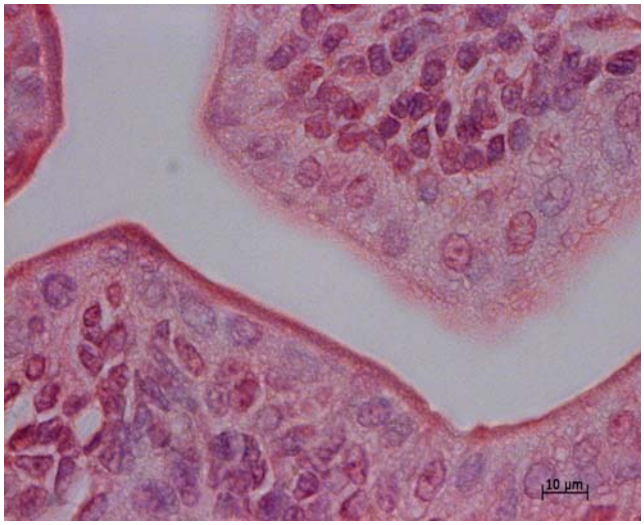

Figure 3.2.15.
Glandular tissue of a CCPPPE treated animal
The glands had wide lumens that usually lacked secretions. The epithelium lining the glands was cuboidal in shape with darkly stained, basally placed nucleoli. Two apoptotic cells (ApC) situated next to each other have been indicated with the arrow.

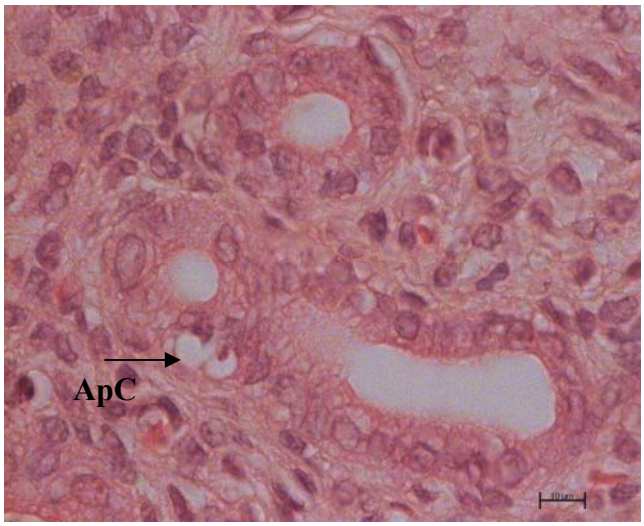

3.3. Immunohistochemistry against the progesterone receptor, Bcl-2 and Bax

3.3.1. Immunohistochemistry (IHC) of the Progesterone Receptor (PR)

3.3.1.1. PR expression in ovariectomised, control or placebo rat uteri

The results of immunohistochemistry against the progesterone receptor for the ovariectomised, saline treated, oil treated and SOOO treated control animals were generally similar and have been presented together.

PR expression in the control tissues was generally most concentrated in the luminal epithelium, less concentrated in the stromal tissue and least concentrated in the glandular tissue. In the stromal tissue, PR tended to be concentrated in the dark layer immediately surrounding the lumen. Fig. 3.3.1.1. of an ovariectomised, untreated animal shows a typical uterine profile of a control animal.

In the luminal epithelium, PR expression was localised in the nuclei, with a concentration of expression in the nuclear membrane. (Fig. 3.3.1.2 of a saline treated control animal shows a high power micrograph of PR expression in the luminal epithelium.) In the ovariectomised untreated and saline treated controls, there was little expression of PR in the cytoplasm of the uterine luminal epithelium (Fig. 3.3.1.2). By contrast, the oil and SOOO controls had PR expression in the cytoplasm which was lower than in the nuclei. The oil controls and SOOO controls also had PR expression concentrated at the apical membrane of the luminal epithelium (Fig. 3.3.1.3.).

PR expression in the glandular epithelium of the control tissues was concentrated in the nuclear membranes (Fig. 3.3.1.4.). Expression of PR was greater in the nuclei than the cytoplasm for the ovariectomised, saline treated and oil treated controls (Fig. 3.3.1.4.). The SOOO controls had a similar expression of PR in the

nuclei and the cytoplasm, and the SOOO controls tended to have a frothy appearance at high power (Fig. 3.3.1.5.).

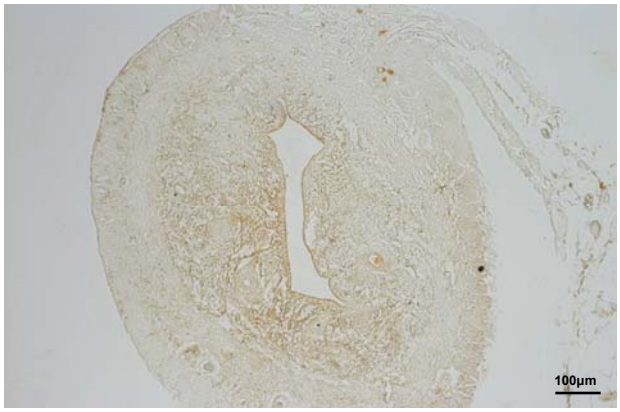

Figure 3.3.1.1.
IHC of PR in an ovariectomised, untreated control rat uterus
Generally, the PR expression in the control tissues was greatest in the luminal epithelium, followed by the stroma, and the least expression in the glands. In the stroma, PR expression was greatest in the area immediately surrounding the lumen.

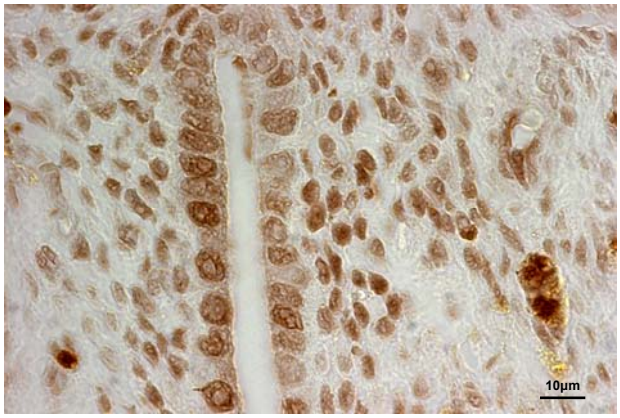

Figure 3.3.1.2.
Expression of PR in the luminal epithelium of a saline treated control animal
The PR was localised in the nucleus of the luminal epithelium, with a concentration at the nuclear membrane.
Ovariectomised and saline treated control animals had low expression of PR in the cytoplasm.

Figure 3.3.1.3.
Expression of PR in the luminal epithelium of an oil treated control animal
PR expression in cytoplasm of the oil and SOOO treated animals was greater than that in the ovariectomised, untreated and saline treated controls. The expression of PR in the cytoplasm was concentrated at the apex of the luminal cells.

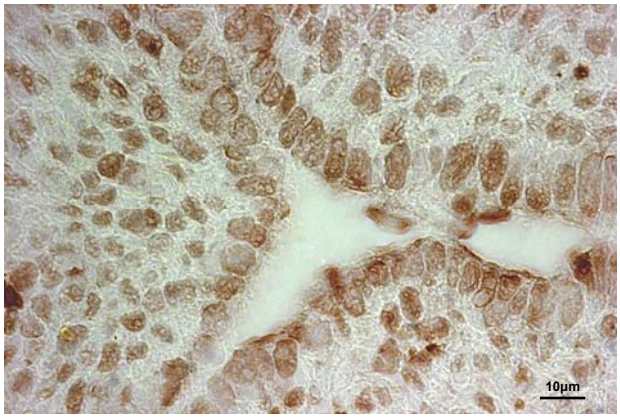

Figure 3.3.1.4.
Expression of PR in the glandular epithelium of an oil treated control animal
PR expression in the glandular epithelium was concentrated in the nuclei, with distinct nuclear membranes. In the untreated, saline and oil treated animals, the PR expression was greater in the nuclei than in the cytoplasm. PR expression in the cytoplasm was concentrated to the apex of the glandular cells.

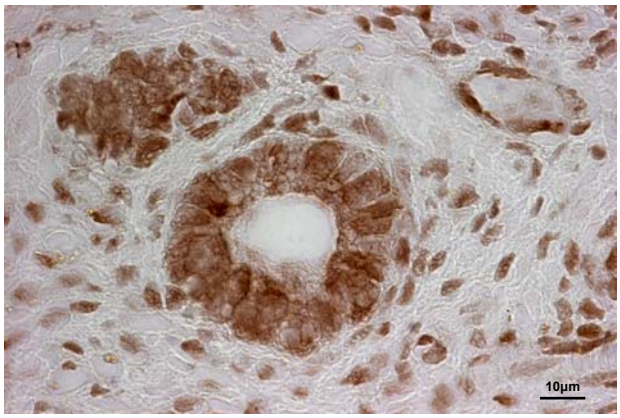

Figure 3.3.1.5.
Expression of PR in the glandular epithelium of an SOOO treated control animal
Expression of PR in SOOO animals was similar in the nuclei and cytoplasm. This gave the glands a frothy appearance.

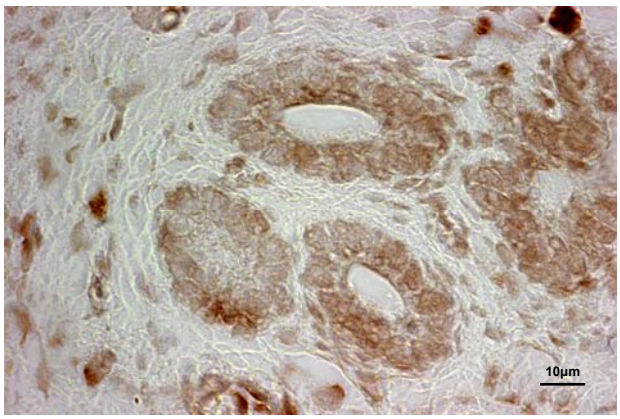

3.3.1.2. PR expression in 1.25 mg CC treated rat uteri

Expression of PR in the 1.25 mg CC treated rat uteri was greatest in the stroma, followed by the luminal epithelium, and the glands had the lowest expression of PR. In the stroma, PR expression had the greatest intensity immediately surrounding the lumen, with a decrease of expression in the stroma between the glandular tissue and myometrium. Fig. 3.3.1.6. shows a typical uterine profile of a single CC treated animal. The control tissues differed from the single CC treated tissue, as the controls had the greatest expression of PR in the luminal epithelium, followed by the stromal tissue and least expression in the glandular tissue (Fig. 3.3.1.1.).

PR expression in the luminal epithelium of single CC treated animals was localised in the nuclei, which had a granular appearance, and was concentrated at the nuclear membrane (Fig. 3.3.1.7.). Some nuclei in the luminal epithelium contained a distinct, dark, concentrated spot when treated with PR antibody, which may have been a concentration of PR expression at the nucleolus. The cytoplasm of the uterine luminal epithelium had the greatest expression of PR at the apex of the cell membrane. By contrast, the base of the cells below the epithelium did not appear to express PR.

In the glandular epithelium, as with the uterine luminal epithelium, PR expression was greater in the nuclei than in the cytoplasm (Fig. 3.3.1.8.). The nuclei in the glands appeared granular with a dark membrane and some nuclei expressed PR in the nucleolus.

Figure 3.3.1.6.
IHC of PR in a 1.25 mg CC treated rat uterus
The expression of PR in the CC treated rat uterus was greatest in the stroma, less in the uterine luminal epithelium and least in the glands. PR expression in the stroma was greatest in the dark layer surrounding the lumen, and diminished in intensity past the glands.

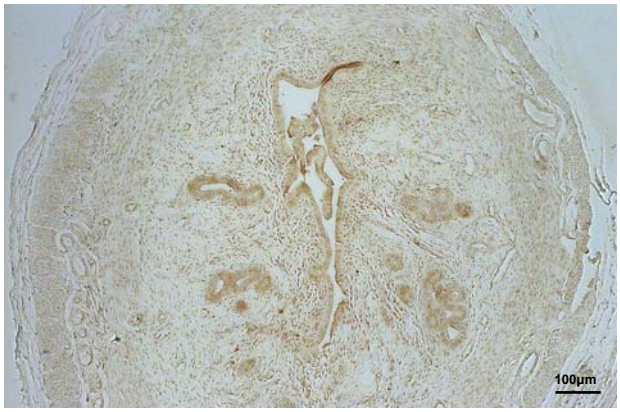

Figure 3.3.1.7.
Expression of PR in the luminal epithelium of a CC treated animal
PR expression was greatest in the nuclei of the luminal epithelial cells, with a concentration at the nuclear membranes. In the cytoplasm, PR was expressed at the apex of the cells, but not at the base of the cells. The stromal cells surrounding the lumen had a greater expression of PR than the luminal epithelium.

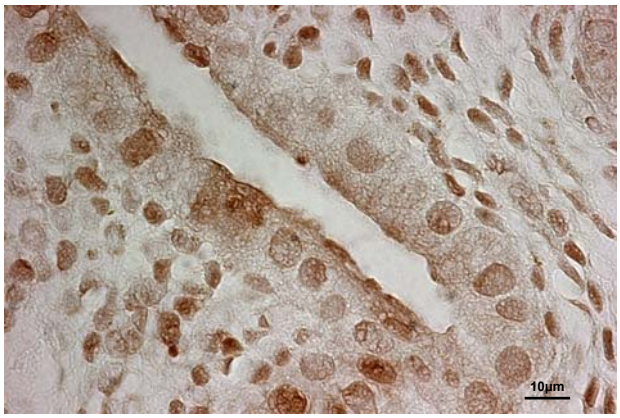

Figure 3.3.1.8.
Expression of PR in the glandular tissue of a CC treated animal
PR expression in the glandular epithelium was greatest in the nucleus, with a concentration at the nuclear membranes. In the cytoplasm, there was a concentration of PR expression at the apex of the cells.

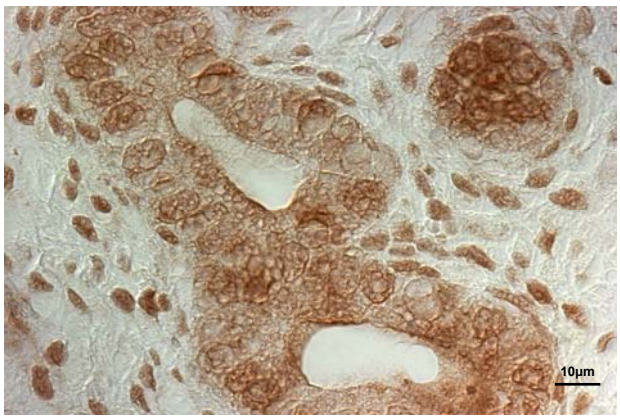

3.3.1.3. PR expression in 5 mg progesterone treated rat uteri

Expression of PR in the 5 mg P_4 treated animals was slightly greater in the luminal epithelium than the glands and both structures had greater P_4 expression than the stroma. PR expression in the stroma was localised around the lumen. This was similar to the expression of PR in the control tissues (Fig. 3.3.1.1.), but different to the expression in the single CC treated animals (Fig. 3.3.1.6.). Fig. 3.3.1.9. shows a typical uterine profile of PR expression in a P_4 treated animal.

Generally, PR in the luminal epithelium was expressed as a granular nuclear stain. In some sections, the PR expressed in the nuclei, and in other sections it did not appear to localise (Fig. 3.3.1.10.). PR in the cytoplasm concentrated toward the apex of the cells (Fig. 3.3.1.10.).

In the glandular epithelium of P_4 treated animals, the nuclei were similar in intensity of expression of PR when compared to the cytoplasm (Fig. 3.3.1.11.). Some animals showed expression of PR in the apex of the glandular cells (Fig. 3.3.1.11.), whereas some animals did not (not shown), and some of the glandular secretions expressed PR (not shown).

Figure 3.3.1.9.
IHC of PR in a 5 mg P_4 treated rat uterus
Expression of PR was similar in the luminal epithelium and the glands, and lower in the stroma in a single P_4 treated animal. Expression in the stroma occurred in the dark layer surrounding the uterine lumen.

Figure 3.3.1.10.
Expression of PR in the luminal epithelium of a P_4 treated animal
PR in the luminal epithelial cells was generally expressed in the nuclei.

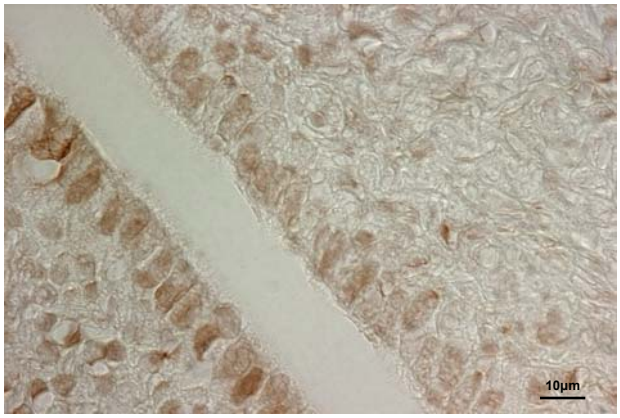

Figure 3.3.1.11.
Expression of PR in the glandular tissue of a P_4 treated animal
Expression of PR in the glands was similar in the nuclei and the cytoplasm. This section shows a concentration of PR towards the apex of the cells.

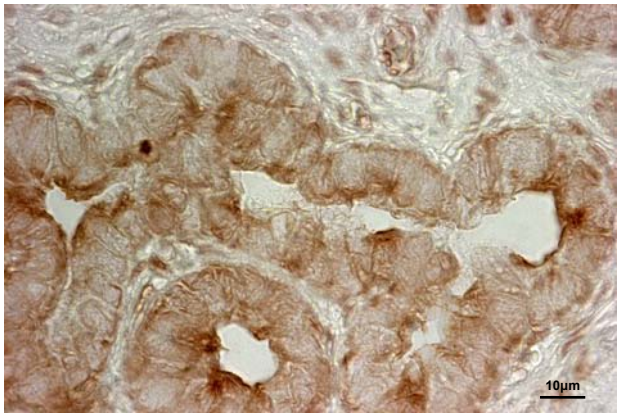

3.3.1.4. PR expression in SPPPE treated rat uteri

Expression of PR in SPPPE treated animals was greatest in the stroma, followed by the luminal epithelium and the least expression was in the glands. This profile was similar to that of the single CC treatment (Fig. 3.3.1.6.). In the stroma of SPPPE animals, PR expression was diffused, with the greatest concentration around the uterine luminal epithelium, less expression around the glandular epithelium and low (or absent) expression immediately below the myometrium. Fig. 3.3.1.12. shows a typical profile of PR expression in an SPPPE treated rat uterus.

PR expression in the uterine luminal epithelium was greatest at the nuclear membranes (Fig. 3.3.1.13.). The nuclei in the epithelial cells had greater or similar expression of PR to the cytoplasm, although both were pale (Fig. 3.3.1.13.). There was an intermittent expression of PR at the apex of the cells and there was no expression of PR in the basement membrane below the luminal epithelium.

In some of the glands, the nuclei had greater expression of PR and the cytoplasm had less expression, whereas in other glands, expression of PR was greater in the cytoplasm than the nuclei (Fig. 3.3.1.14.). The nuclei was generally pale in comparison to the nuclear membrane, although sometimes one could not distinguish between the cytoplasm and nucleus, as both structures were pale.

Figure 3.3.1.12.
IHC of PR in an SPPPE treated rat uterus
Expression of PR in SPPPE treated animals was greatest in the stroma, and equivalent in the luminal epithelium and the glands. In the stroma, PR expression was greatest in the area surrounding the lumen and was less concentrated towards the myometrium.

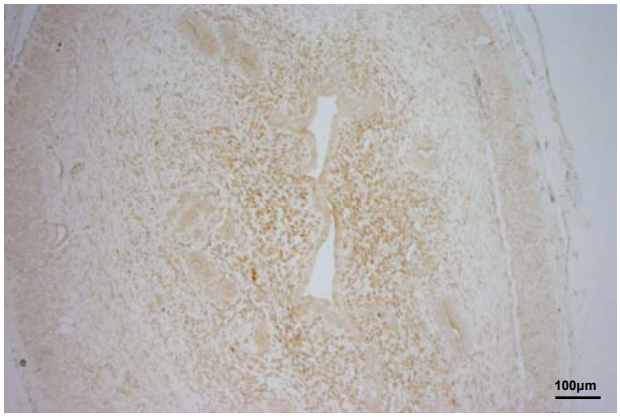

Figure 3.3.1.13.
Expression of PR in the luminal epithelium of an SPPPE treated animal
PR was most concentrated at the nuclear membranes in the luminal epithelium. Expression of PR in the nuclei was slightly greater than the cytoplasm. There was a concentration of PR towards the apex of the cells.

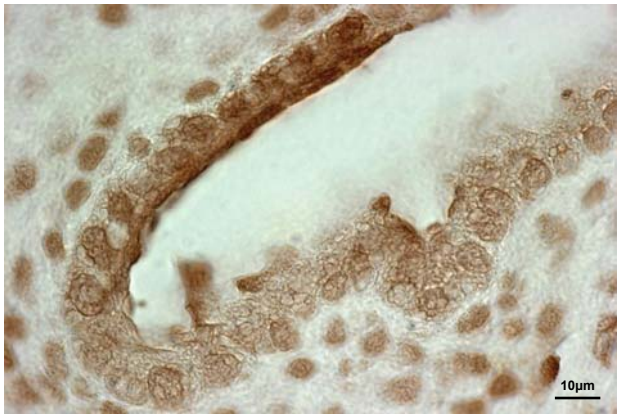

Figure 3.3.1.14.
Expression of PR in the glandular tissue of an SPPPE treated animal
PR expression was equivalent in the nuclei and cytoplasm of the glandular epithelium, with greater expression at the nuclear membranes.

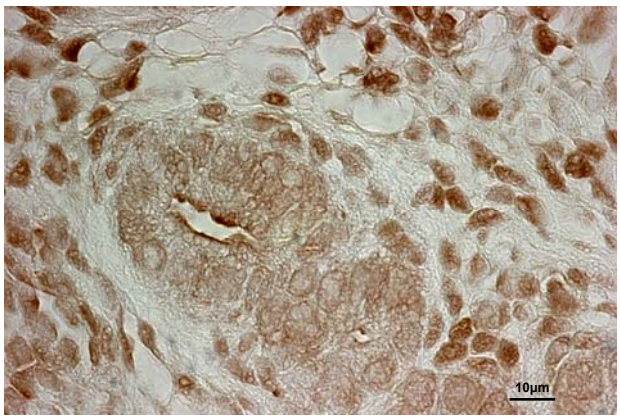

3.3.1.5. PR expression in CCPPPE treated rat uteri

Expression of PR was greatest in the stroma of CCPPPE treated animals, followed by the luminal epithelium and least in the glandular epithelium. Expression of PR in the stroma was most concentrated around the lumen, and diminished in the stromal tissue in the region between the glands and the myometrium. This result was similar to the expression of PR in SPPPE treated animals (Fig. 3.3.1.12.). Fig. 3.3.1.15. shows a typical profile of PR expression in a CCPPPE treated rat uterus.

The nuclei in the luminal epithelium of CCPPPE treated animals had greater expression of PR than the cytoplasm (Fig. 3.3.1.16.). There was a concentration of PR expression at the apex of the cells (Fig. 3.3.1.16.). This was in contrast to the SPPPE treated animals, which had less intense expression of PR in the luminal epithelium and did not show much difference in expression between the nuclei and cytoplasm.

Similarly to the luminal epithelium, PR expression in the glandular epithelium was more concentrated in the nuclei than in the glands (Fig. 3.3.1.17.). The nuclei appeared granular and had a concentration of PR expression at the nuclear membranes, although the nuclei did not always express PR (Fig. 3.3.1.17.). PR expression in the cytoplasm was greater towards the apex of the cells (Fig. 3.3.1.17.).

Figure 3.3.1.15.
IHC of PR in a CCPPPE treated rat uterus
Expression of PR was greatest in the stroma, followed by the luminal epithelium and the glands. PR expression in the stroma was greatest around the lumen and diffused past the glands.

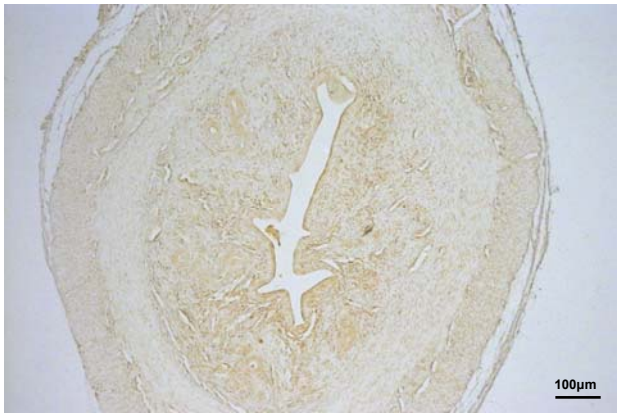

Figure 3.3.1.16.
Expression of PR in the luminal epithelium of a CCPPPE treated animal
PR expression in the luminal epithelium was greater in the nuclei than the cytoplasm. There was a concentration of PR expression at the apical membranes.

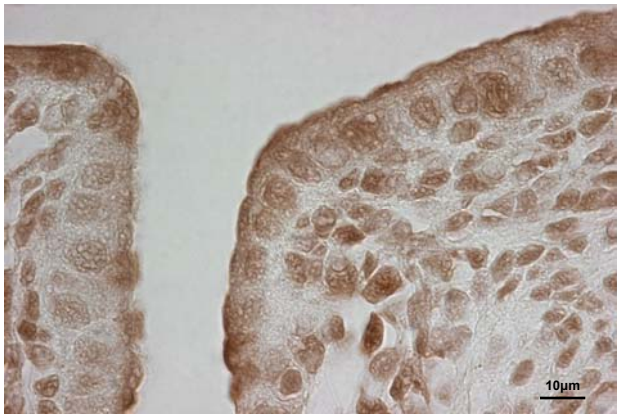

Figure 3.3.1.17.
Expression of PR in the glandular tissue of a CCPPPE treated animal
PR expression in the glands was greater in the nucleus than the cytoplasm and PR aggregated at the nuclear membranes. PR expression in the cytoplasm was most concentrated at the apex of the cells.

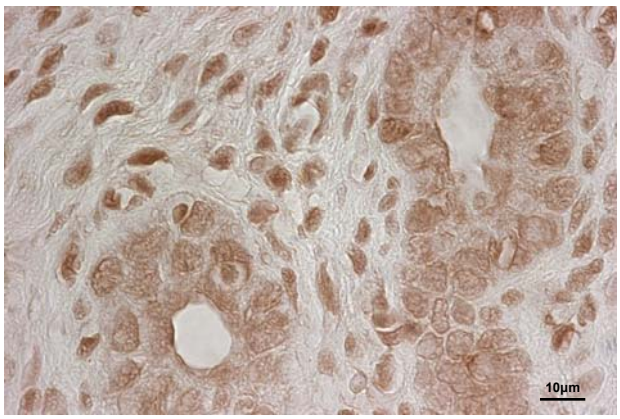

3.3.1.6. Summary of IHC against PR in rat uteri

PR expression in the uterine profiles of the control tissues was greatest at the uterine luminal epithelium, followed by the stroma and least expression in the glandular epithelium. The CC, SPPPE and CCPPPE treated tissue had the greatest expression of PR in the stroma, followed by the luminal epithelium and least in the glandular epithelium. P_4 treated tissues had a greater or similar expression of PR in the luminal epithelium and glandular epithelium, with less expression in the stroma.

PR expression in the stroma of the controls and the P_4 treated animals was concentrated in the dark layer around the lumen, the expression of PR in the single CC and SPPPE treated tissues extended to the glandular epithelium, and expression of PR in CCPPPE treated tissues extended to beneath the myometrium.

Expression of PR in the uterine luminal epithelium of ovariectomised untreated and saline treated controls was greater in the nuclear membranes than the nuclei, and there was little expression in the cytoplasm. Neither of these controls showed a concentration of PR expression towards the apex of the cells. The oil and SOOO controls as well as the CC, P_4, SPPPE and CCPPPE treated tissues had the greatest expression of PR in the nuclear membranes, followed by the nuclei and least in the cytoplasm. These controls and treatment groups had PR expression in the apex of the luminal epithelial cells.

PR expression in the glandular epithelium of the control tissues as well as the CC and CCPPPE treated tissues was greatest at the nuclear membranes followed by the nuclei and least in the cytoplasm. The P_4 treated tissue had similar expression of PR in the nuclei and cytoplasm. The SPPPE treated tissue had greater expression of PR in the nuclei and less in the cytoplasm in some sections, and in other sections the expression of PR was greater in the cytoplasm than the nuclei. The controls (except for the SOOO control) did not generally show a

concentration of PR in the apex of the glandular cells and the treatment groups had a concentration of PR at the apex of the cells.

3.3.2. IHC against Bcl-2 (B cell lymphoma/leukemia-2)

3.3.2.1. Bcl-2 expression in ovariectomised, control or placebo rat uteri

The results of the immunohistochemistry against Bcl-2 expression in the ovariectomised untreated, saline control, oil control and SOOO control treated animals was similar and have been presented together.

Bcl-2 expression in the untreated or placebo treated rat uteri was concentrated in the luminal epithelium, less concentrated in the glandular tissue and least concentrated in the stroma. Fig. 3.3.2.1. shows Bcl-2 expression in the uterus of an SOOO treated animal. Expression of Bcl-2 was dispersed throughout the stromal tissue and there was not a distinct concentration of Bcl-2 in the dark layer surrounding the lumen.

Expression of Bcl-2 in the control tissues of the luminal epithelium appeared bubbly. Bcl-2 expression was distinct on the nuclear membranes in some sections (Fig. 3.3.2.2.), but its expression was absent in other sections. The nucleus had a similar or slightly greater expression of Bcl-2 than the cytoplasm, so if the nuclear membrane was not apparent, it was difficult to distinguish between these cellular components. The Bcl-2 in the cytoplasm tended to concentrate towards the apex of the luminal epithelial cells (Fig. 3.3.2.2.).

Bcl-2 expression in the control tissues appeared frothy in the glandular epithelium (Fig. 3.3.2.3.). The nuclei had a greater or similar expression of Bcl-2 compared to the cytoplasm (Fig. 3.3.2.3.), although it was not always possible to distinguish between the two cellular structures. The nuclear membrane was sometimes, although not always, distinguishable, and there was sometimes a concentration of Bcl-2 towards the lumen of the gland.

Figure 3.3.2.1.
IHC of Bcl-2 in an SOOO treated rat uterus
Generally,in the control sections, the Bcl-2 had the greatest expression in the luminal epithelium, followed by the glands and the least expression in the stroma. Bcl-2 expression was distributed in the stroma with some concentration close to the lumen.

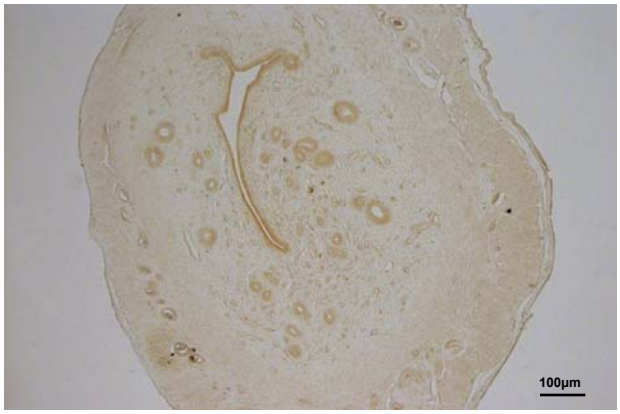

Figure 3.3.2.2.
Expression of Bcl-2 in the luminal epithelium of an ovariectomised control animal
Bcl-2 expression in the luminal epithelium of the control animals was similar in the nucleus and cytoplasm and had a bubbly appearance. There was some concentration of Bcl-2 expression toward the apex of the cells.

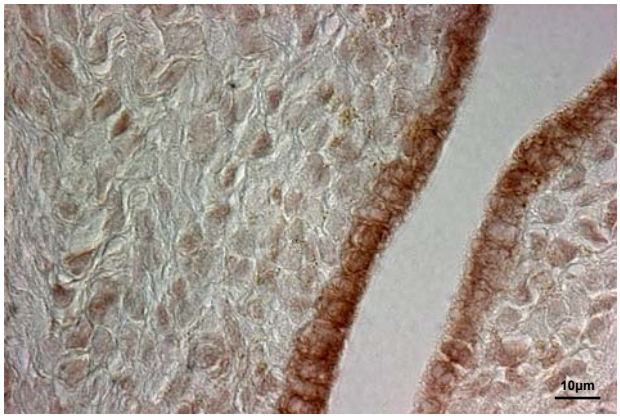

Figure 3.3.2.3.
Expression of Bcl-2 in the glandular tissue of an SOOO control animal
Bcl-2 expression in the glandular epithelium of the control tissues was similar between the nuclei and cytoplasm, and the glands appeared frothy. The nuclear membranes were sometimes, but not always, distinct.

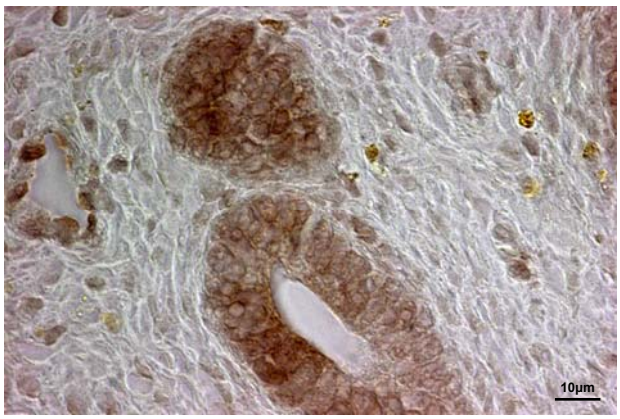

3.3.2.2. Bcl-2 expression in 1.25 mg CC treated rat uteri

Bcl-2 expression in the CC treated rat uteri sections was noticeably different to those of the controls (Figs. 3.3.2.1-3.3.2.3). The luminal epithelium of the CC treated tissue had a far more concentrated localisation than the glands and the stroma had very little localisation. In addition, the luminal epithelium had a patchy expression of Bcl-2, which was apparent, even at low power. Fig. 3.3.2.4.. shows a typical low power micrograph of CC treated tissue that has been immunolocalised against Bcl-2. Bcl-2 expression in the stroma was dispersed, but sometimes had a higher concentration surrounding the lumen (Figs. 3.3.3.4 and 3.3.2.4.).

At higher magnification, it was apparent that the luminal epithelium was characterised by patches of Bcl-2 localisation, where some portions of the epithelium were localised, and adjacent portions did not express Bcl-2 (Fig. 3.3.2.5).
The cytoplasm of the luminal epithelium generally had a greater or equal concentration of Bcl-2 when compared to the nuclei, and some nuclei stained, whereas others did not (Fig. 3.3.2.5.). The nuclear membrane was usually distinct. In some sections, there was a dark spot visible in the nucleus, which was probably the nucleolus (not shown).

Bcl-2 expression in CC treated animals appeared frothy in the glandular epithelium (Fig. 3.3.2.6.). The cytoplasm and nuclei were generally pale. The nuclear membranes were sometimes, but not always, distinct (Fig. 3.3.2.6.). Occasionally, there was a concentration of stain in the nucleolus.

Figure 3.3.2.4.
IHC of Bcl-2 in a 1.25 mg CC treated rat uterus
Patchiness of Bcl-2 expression was evident around the luminal epithelium of a CC treated animal. The expression of Bcl-2 was greatest in the luminal epithelium, followed by the glands and least in the stroma . Bcl-2 expression was dispersed throughout the stroma.

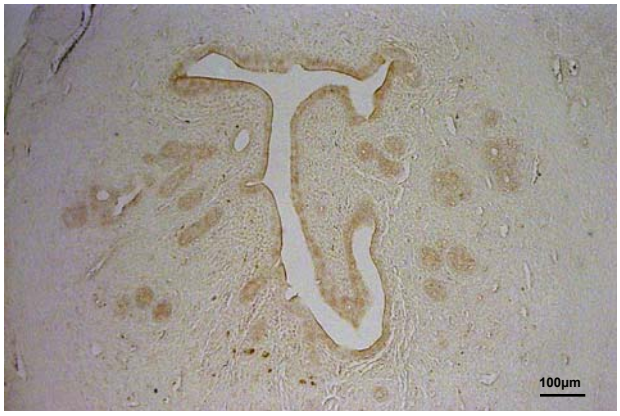

Figure 3.3.2.5.
Expression of Bcl-2 in the luminal epithelium of a CC treated animal
Expression of Bcl-2 was patchy in the luminal epithelium, where some sections expressed Bcl-2 and adjacent sections did not express Bcl-2.

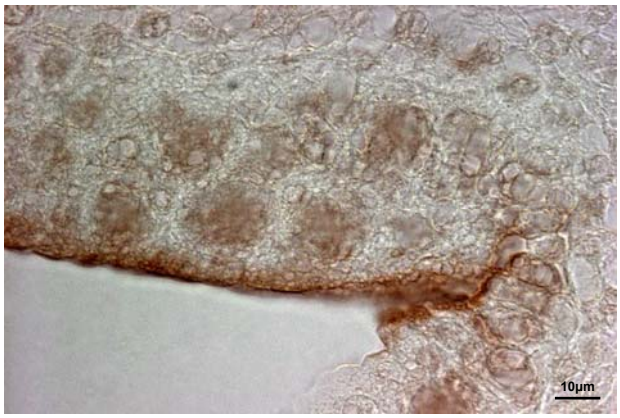

Figure 3.3.2.6.
Expression of Bcl-2 in the glandular tissue of a CC treated animal
Bcl-2 expression in the glandular epithelium of CC treated animals appeared frothy. The cytoplasm and nuclei were similar in expression, although both cellular components were generally pale. The nuclear membranes were sometimes, but not always, distinct.

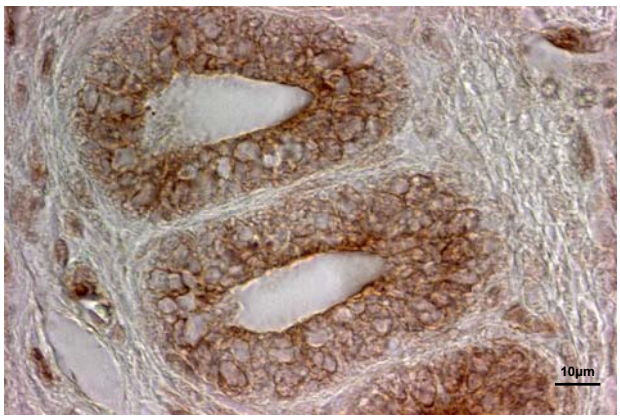

3.3.2.3. Bcl-2 expression in 5 mg P_4 treated rat uteri

Bcl-2 expression in the uteri of the P_4 treated tissue was greatest in the luminal epithelium, followed by the glandular epithelium and had the least expression in the stroma. Although Bcl-2 was dispersed throughout the stroma, it was localised more intensely around the luminal epithelium. The expression of Bcl-2 in the P_4 treated animals was similar to that seen in the control animals. Fig. 3.3.2.7. shows a typical micrograph of Bcl-2 in P_4 treated rat uterus tissue.

Unlike the untreated and placebo controls, as well as the CC treated tissue, Bcl-2 in the P_4 treated uterine luminal epithelium was usually concentrated in the nuclei (Figs 3.3.2.2, 3.3.2.5 and 3.3.2.8.). The nucleus had a greater concentration than the cytoplasm and the nuclear membrane was dark. Bcl-2 in the cytoplasm concentrated to the apex of the cells (Fig. 3.3.2.8.).

The nuclei in the uterine glands expressed Bcl-2 at a more concentrated, or equivalent level, to the cytoplasm (Fig. 3.3.2.9.). The glandular tissue did not appear bubbly, as was the case with the control tissues. The nuclei in P_4 treated rat uteri were granular and frothy, and a distinct nuclear membrane was observed. The glandular contents also localised Bcl-2 strongly (Fig. 3.3.2.9.).

Figure 3.3.2.7.
IHC of Bcl-2 in a 5 mg P_4 treated rat uterus
Expression of Bcl-2 in P_4 treated animals was greatest in the luminal epithelium, followed by the glands and least in the stroma.

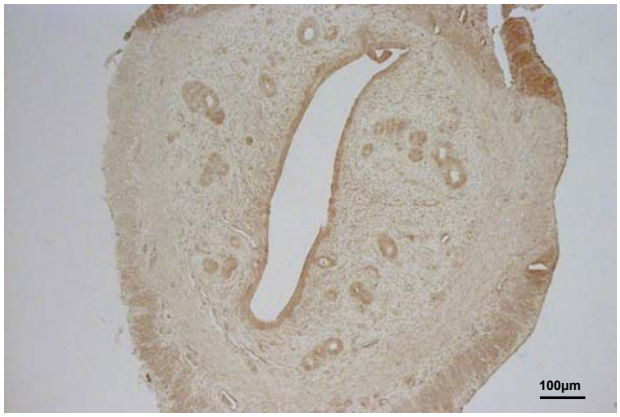

Figure 3.3.2.8.
Expression of Bcl-2 in the luminal epithelium of a P_4 treated animal
In the luminal epithelial cells, Bcl-2 expression was concentrated in the nuclear membranes and the apex of the epithelial cells. The nuclei had a greater expression of Bcl-2 than the cytoplasm.

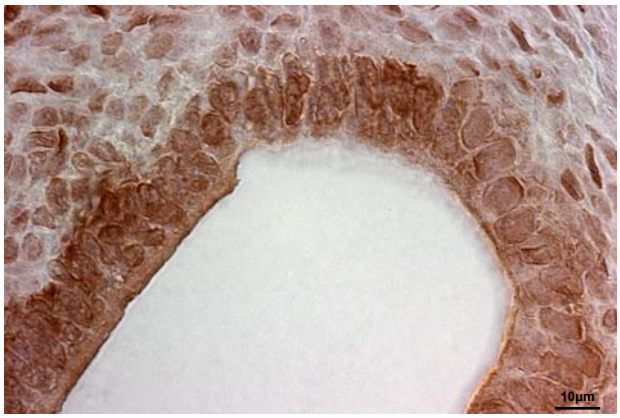

Figure 3.3.2.9.
Expression of Bcl-2 in the glandular tissue of a P_4 treated animal
Expression of Bcl-2 in the glandular epithelium was greatest at the nuclear membranes. The nuclei had a greater or similar expression of Bcl-2 compared to the cytoplasm.

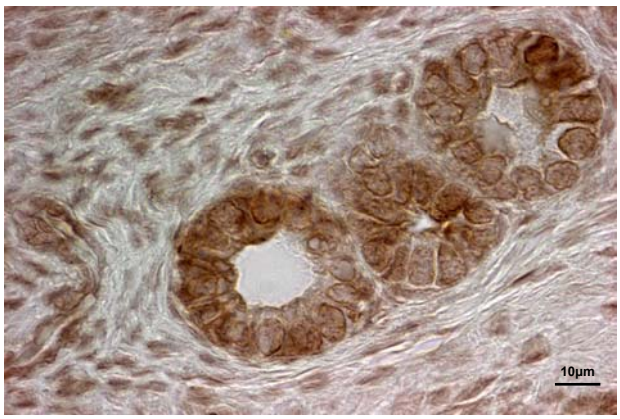

3.3.2.4. Bcl-2 expression in SPPPE treated rat uteri

Unlike the controls, Bcl-2 expression in SPPPE treated tissue was greatest in the stromal tissue, followed by expression in the luminal epithelium, which was similar to the glands. Bcl-2 expression in the stroma concentrated around the luminal epithelium, and decreased in intensity to beyond the glands. Localisation did not appear to occur in the tissue immediately surrounding the glands. Fig. 3.3.2.10. shows the expression of Bcl-2 in the uterine profile of an SPPPE treated animal.

Bcl-2 expression in the luminal epithelium of the SPPPE treated tissue was concentrated in two "layers", the first layer was at the apex of the epithelial cells, and the second at the basal portion of the cells. The middle section of the luminal epithelium was far paler. This gave the epithelium a sandwich-like appearance. The basement membrane below the epithelium did not express Bcl-2.

In the uterine luminal epithelium, the nuclei localised Bcl-2 slightly more than the cytoplasm, and there was a greater concentration of Bcl-2 along the nuclear membrane. Fig. 3.3.2.11. shows a micrograph of Bcl-2 expression in the luminal epithelium of an SPPPE treated animal.

The glandular epithelium of SPPPE treated tissue had similar expression of Bcl-2 in the nuclei and cytoplasm, and both cellular components had a frothy appearance (Fig. 3.3.2.12.). The nuclear membranes in the glandular cells were not always distinct. Occasionally there was a concentration of Bcl-2 toward the apex of the glandular cells.

Figure 3.3.2.10.
IHC of Bcl-2 in an SPPPE treated rat uterus
Expression of Bcl-2 in SPPPE treated animals was greatest in the dark layer of stroma, and the luminal epithelium was darker or similar in intensity to the glands.

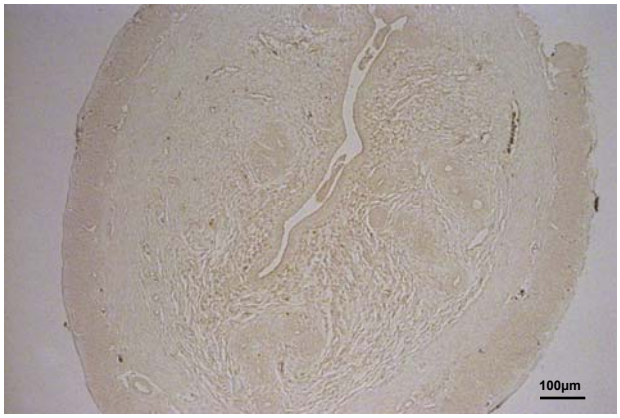

Figure 3.3.2.11.
Expression of Bcl-2 in the luminal epithelium of an SPPPE treated animal
Bcl-2 expression was greatest at the nuclear membranes, and expression in the nuclei was similar or greater than the expression in the cytoplasm. Expression of Bcl-2 in the cytoplasm was concentrated towards both the apex and base of the cells.

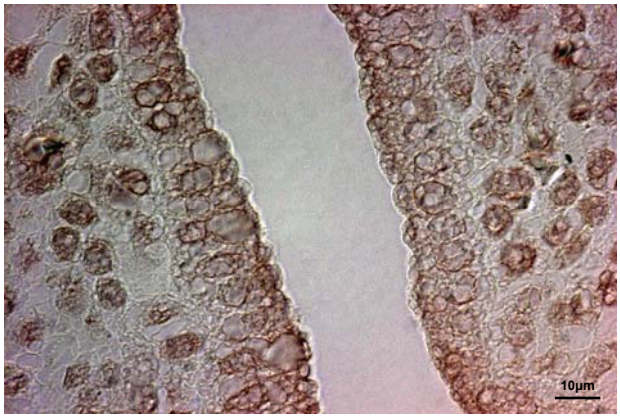

Figure 3.3.2.12.
Expression of Bcl-2 in the glandular tissue of an SPPPE treated animal
Bcl-2 expression in the glandular cells was similar between the nuclei and cytoplasm. The nuclear membranes were not always distinct and the glandular epithelium appeared frothy. There was a slight concentration of Bcl-2 expression at the apex of the glandular cells.

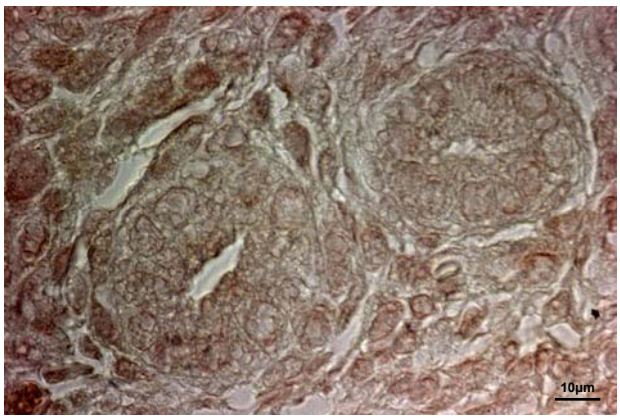

3.3.2.5. Bcl-2 expression in CCPPPE treated rat uteri

Expression of Bcl-2 in the CCPPPE treated rat tissue was greatest in the luminal epithelium, followed by the glands, followed by the stromal tissue. Bcl-2 was dispersed in the stroma, and was sometimes more concentrated around the luminal epithelium. Fig. 3.3.2.13. shows Bcl-2 expression in a CCPPPE treated rat uterus. This was more comparable to the expression in the SOOO control than to the SPPPE treated tissue. Patchiness of expression was evident at the lumen, but it was not as obvious as in the single CC treatment (Figs 3.3.2.5. and 3.3.2.13.).

The luminal epithelium of CCPPPE treated tissue generally had a greater expression of Bax in the cytoplasm than in the nuclei of the epithelial cells (Fig. 3.3.2.14.). The cytoplasm had a frothy appearance and Bcl-2 expression was concentrated towards the luminal aspect of the cells. Some of the nuclei showed localisation of Bcl-2, whereas others did not. Bcl-2 was concentrated along the nuclear membranes.

The glands appeared bubbly when localised with Bcl-2. The cytoplasm of glandular cells generally had a greater expression of Bcl-2 compared to the nuclei, and both had a frothy appearance (Fig. 3.3.2.15.). The nuclei were generally pale or unstained, with dark nuclear membranes. Bcl-2 in the cytoplasm was concentrated in the apex of the glandular cells.

Figure 3.3.2.13.
IHC of Bcl-2 in a CCPPPE treated rat uterus
Expression of Bcl-2 was greatest in the luminal epithelium, followed by the glands and least in the stroma. Patchiness was evident in the luminal epithelium of CCPPPE treated animals, although not to the same extent as in the single CC treated animals.

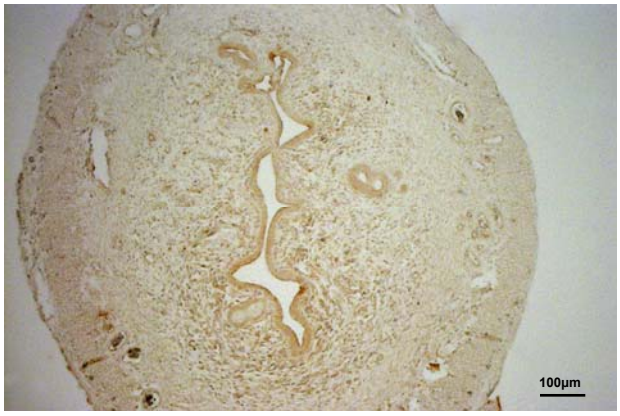

Figure 3.3.2.14.
Expression of Bcl-2 in the luminal epithelium of a CCPPPE treated animal
In the luminal epithelial cells, Bcl-2 expression was greater in the cytoplasm than the nuclei, and there were obvious nuclear membranes. The cytoplasm had a concentration of Bcl-2 towards the apex of the cells.

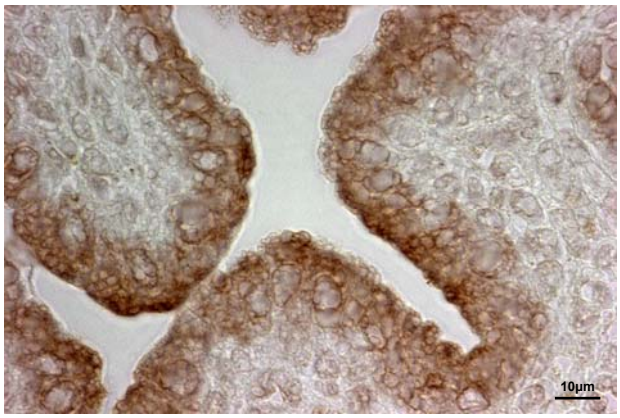

Figure 3.3.2.15.
Expression of Bcl-2 in the glandular tissue of a CCPPPE treated animal
Bcl-2 expression in the CCPPPE treated animals was greater in the cytoplasm than the nucleus, with an aggregation towards the lumen of the glands. The nuclear membranes were distinct. The glandular cells had a foamy appearance in both the cytoplasm and nucleus.

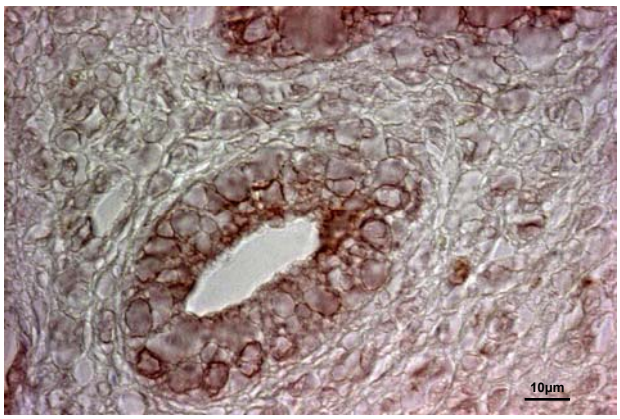

3.3.2.6. Summary of IHC against Bcl-2 in rat uteri

The most striking feature of the uteri treated against Bcl-2 was the patchy expression of Bcl-2 in the uterine luminal epithelium of the single CC treated, and to a lesser extent in the CCPPPE treated tissues. The patchiness was absent from the other treatments and controls.

The expression of Bcl-2 in the controls, single CC, P_4 and CCPPPE treated tissues was greatest in the luminal epithelium, followed by the glandular epithelium and lowest in the stroma. The SPPPE tissue had the greatest expression of Bcl-2 in the stroma, followed by the luminal epithelium which was greater or similar in expression to the glandular epithelium.

The control tissues had pale stroma when treated against Bcl-2 and the Bcl-2 expression was concentrated around the dark layer of the lumen, if at all. The single CC, P_4 and CCPPPE treated tissues had Bcl-2 expression distributed throughout the stromal tissue with some concentration at the dark layer. Bcl-2 expression in the stroma of SPPPE treated tissues extended to the glandular epithelium.

Bcl-2 expression in the control tissues was greatest at the nuclear membranes, followed by the cytoplasm which had greater or similar expression to the nuclei. The CC and CCPPPE tissues were similar to the controls, although these treatments had a greater expression of Bcl-2 in the cytoplasm than in the nuclei. The P_4 and SPPPE treated tissues had the greatest expression at the nuclear membranes, followed by the nuclei which were greater or similar to the expression in the cytoplasm. All treatment groups had a concentration of Bcl-2 towards the apex of the luminal epithelial cells, although SPPPE treatment also had a concentration of Bcl-2 toward the base of the cells.

In the glandular epithelium, the controls, P_4 and SPPPE treated tissues had some expression of Bcl-2 at the nuclear membranes, and the nuclei had a greater or

similar expression of Bcl-2 than the cytoplasm. The CCPPPE had a greater expression of Bcl-2 in the cytoplasm than in the nuclei. The nuclei of the single CC treated animals showed more expression of Bcl-2 than the cytoplasm in some sections, and less expression in other sections, although generally both the nuclei and the cytoplasm were pale. The glandular tissue of all of the treatment groups, except for the P_4 treated animals, appeared frothy.

3.3.3. IHC against Bax (Bcl-2 – associated X protein)

3.3.3.1 Bax expression in ovariectomised, control or placebo untreated rat uteri

The results for the immunohistochemistry against Bax in the ovariectomised untreated, saline treated, oil treated and SOOO treated control animals were similar and have been presented together.

The uterine profiles of the control or placebo treated tissue generally had a greater or similar concentration of Bax expression in the uterine luminal epithelium compared to the concentration of Bax in the glands, as seen by the intensity of chromagen deposition in these regions. This was similar to the expression of Bcl-2 in the untreated rat uterus, which also had the greatest expression of Bcl-2 in the luminal epithelium, followed by the glandular epithelium and lowest expression of Bcl-2 in the stroma (Fig. 3.3.2.1.). Expression of Bax was greater in both the epithelium and the glands than in the stroma. Bax expression in the stroma was most apparent in the dark layer surrounding the uterine lumen. Fig.. 3.3.3.1. shows a low power micrograph of Bax expression in a saline treated uterus, which is typical of the control tissues. By contrast, Bcl-2 was lightly dispersed throughout the stromal tissue and was not concentrated in the dark layer surrounding the lumen.

The distribution of Bax in the control tissues was localised in the nucleus with a concentration towards the nuclear membrane in both the uterine luminal epithelium and the glandular epithelium. In the cytoplasm, Bax expression was concentrated towards the apex of the cells, showing an edge effect. Fig. 3.3.3.2. shows a typical micrograph of the luminal epithelium of the control tissues and Fig. 3.3.3.3. shows a typical micrograph of the glandular epithelium.

The glandular epithelium had greater expression of Bax in the nuclei than in the cytoplasm of the ovariectomised untreated and saline treated animals (Fig.

3.3.3.3.), whereas the oil treated and SOOO treated animals had similar expression of Bax in both the nucleus and cytoplasm, giving the glandular epithelium a frothy appearance (not shown).

Figure 3.3.3.1.
IHC of Bax in a saline treated rat uterus
Generally, in control tissues, Bax had the greatest expression in the luminal epithelium, followed by the glands and the least expression in the stroma. Bax in the stroma was localised in a dark layer close to the lumen. There was very little expression of Bax in the myometrium.

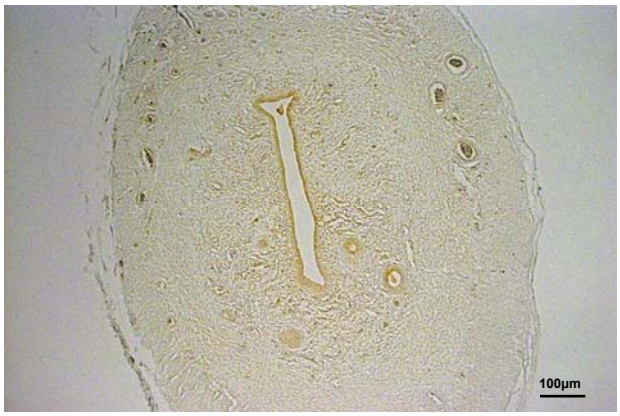

Figure 3.3.3.2.
Expression of Bax in the luminal epithelium of an ovariectomised control animal
The Bax was localised in the nucleus of the luminal epithelium, with a concentration at the nuclear membrane. In the cytoplasm, the Bax was concentrated towards the apex of the cells.

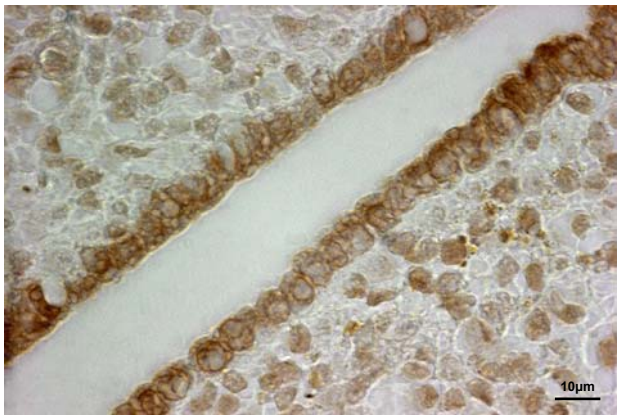

Figure 3.3.3.3.
Expression of Bax in the ovariectomised control animal
Bax was more concentrated in the nucleus than the cytoplasm, particularly in the nuclear membranes.
In the cytoplasm, Bax was more concentrated towards the apex of the cells.

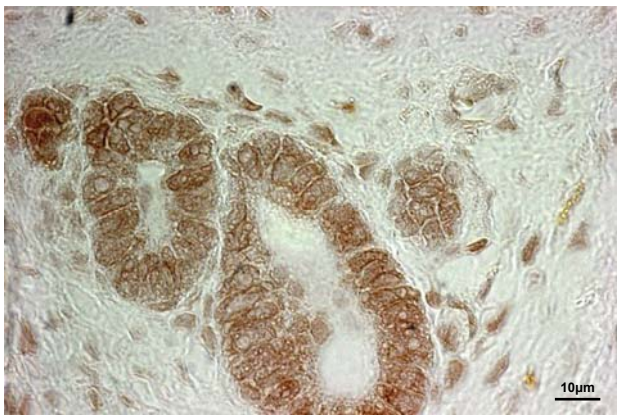

3.3.3.2. Bax expression in 1.25 mg CC treated animals

Expression of Bax in the uteri of CC treated animals was similar in the luminal epithelium and the glandular epithelium. Both types of epithelia were darker than the stroma. In the stroma, Bax was expressed closer to the lumen of the uterus, but extended in tendrils to the glandular epithelium. There was a noticeable expression of Bax in the myometrium, especially when compared to the control animals. This can be seen in Fig. 3.3.3.4. Localisation of Bax was more distinct in CC treated animals when compared to the control animals (ovariectomised, saline treated and oil treated). However, in comparison with the control sections, the luminal epithelium and the glandular tissue was generally far paler, indicative of a lower expression of Bax.

Expression of Bax in the luminal epithelium was patchy (Figs. 3.3.3.4 and 3.3.3.5.). The nucleus in the luminal epithelium appeared granular or frothy when treated against Bax antibody, with a concentration towards the nuclear membrane (Fig. 3.3.3.5.). The cytoplasm also appeared frothy, and was concentrated toward the apex of the cell. Bax expression was greater in the nucleus than the cytoplasm (Fig. 3.3.3.5.). The patchiness evident in these sections was less pronounced than the sections treated for Bcl-2 expression (Fig. 3.3.2.4.). Bcl-2 expression in the stroma was dispersed, but sometimes had a higher concentration surrounding the lumen. Expression of Bax, by contrast, extended about halfway into the endometrium (Figs 3.3.2.4. and 3.3.3.4.).

In the glands, Bax expression seemed concentrated in some nuclei, while other nuclei had a lower expression of Bax. The cytoplasm generally had a frothy appearance and localised toward the lumen of the glands (Fig. 3.3.3.6.). Generally, this edge seemed equivalent in expression to that of the nuclear membrane. In the glandular tissue, Bax was most highly expressed in the cytoplasmic edge and nuclear membranes, followed by the cytoplasm, and least expressed in the nucleus (Fig. 3.3.3.6.). By contrast, the control tissues had greater expression in the nuclei than in the cytoplasm (section 3.3.1.1.).

Figure 3.3.3.4.
IHC of Bax in a 1.25 mg CC treated rat uterus
The expression of Bax in CC treated sections was similar in the luminal epithelium and glands, and lower in the stroma. Bax expression in the stroma extended from the lumen to the glandular tissue (indicated by the arrows). There was a noticeable expression of Bax in the myometrium.

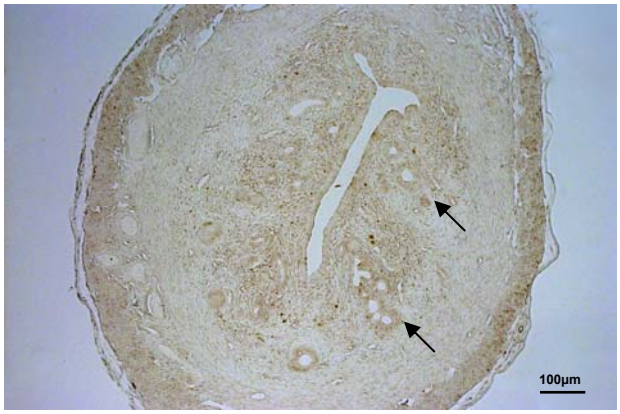

Figure 3.3.3.5.
Expression of Bax in the luminal epithelium of a CC treated animal
Expression of Bax appeared patchy in the luminal epithelium.
Bax was concentrated in the nuclear membrane as well as the apical edge of the luminal epithelium.
The stromal nuclei surrounding the luminal epithelium were darkly stained and numerous.

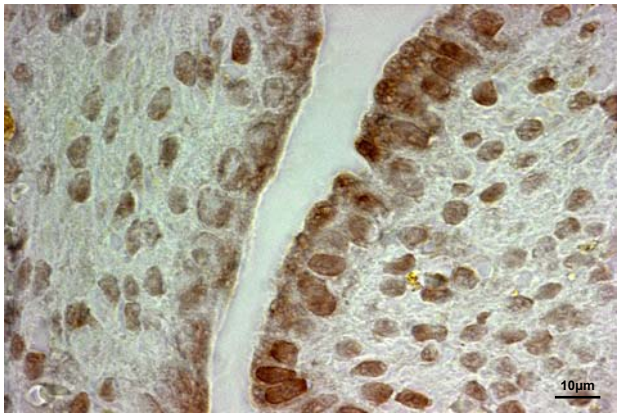

Figure 3.3.3.6.
Expression of Bax in the glandular tissue of a CC treated animal
Bax was most concentrated in the nuclear membranes, and had a bubbly appearance in the glandular tissue. The stromal cells surrounding the glands show expression of Bax. An apoptotic cell (ApC) showed Bax concentrated in the nucleus.

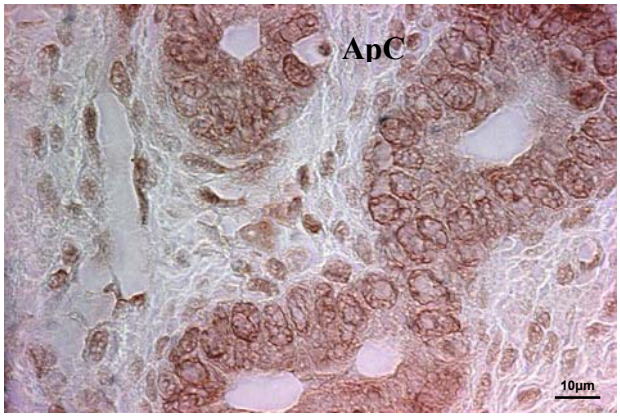

3.3.3.3. Bax in 5 mg P_4 treated animals

Expression of Bax in P_4 treated animals was greatest in the glandular epithelium, followed by the uterine luminal epithelium and least in the stroma. This was different to the control tissues, which had the greatest expression of Bax in the luminal epithelia. The P_4 treated animals did not appear to have localisation of Bax in the myometrium. Bax in the stroma was expressed approximately 4-5 layers deep in the dark layer surrounding the lumen. Fig. 3.3.3.7. shows a typical uterus immunolocalised against Bax.

Some nuclei in the luminal epithelium expressed high levels of Bax, whereas other nuclei had a lower expression of Bax. Bax was most concentrated in the nuclear membranes. Bax was localised in the apex of the luminal epithelium and this expression of Bax was similar to the nuclear membranes (Fig. 3.3.3.8.).

In the glands, Bax was expressed intermittently with a granular appearance and concentrated towards the nuclear membrane. The cytoplasm appeared frothy and Bax was concentrated toward the apex of the cell. Generally, expression of Bax was greater in the cytoplasm than the nuclei. Many glandular nuclei of P_4 treated animals did not express Bax (Fig. 3.3.3.9.).

Figure 3.3.3.7.
IHC of Bax in a 5 mg P_4 treated rat uterus
Expression of Bax in P_4 treated animals was greatest in the glands, followed by the luminal epithelium and least in the stroma. Expression in the stroma occurred in 4-5 layers around the uterine lumen.

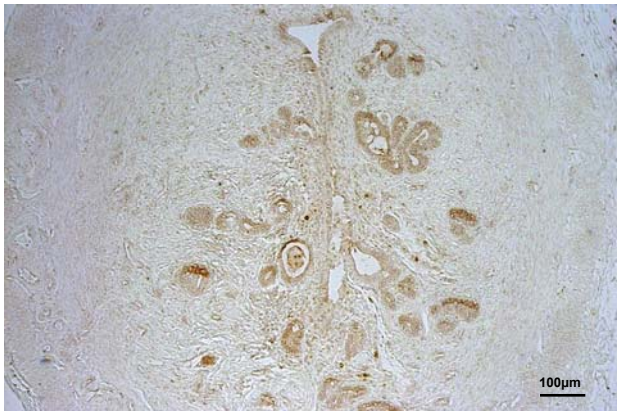

Figure 3.3.3.8.
Expression of Bax in the luminal epithelium of a P_4 treated animal
In the luminal epithelial cells, Bax was concentrated in the nuclear membranes and the apex of the epithelial cells. The cytoplasm had a greater or similar expression of Bax compared to the nuclear contents.

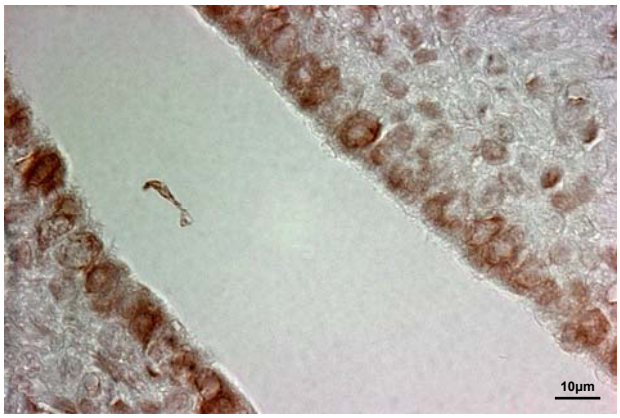

Figure 3.3.3.9.
Expression of Bax in the glandular tissue of a P_4 treated animal
Expression of Bax in the glands was greatest at the nuclear membranes and the luminal edge of the glandular cells. The nuclei did not always express Bax.
The glandular cells had a foamy appearance after immunolocalisation with Bax.

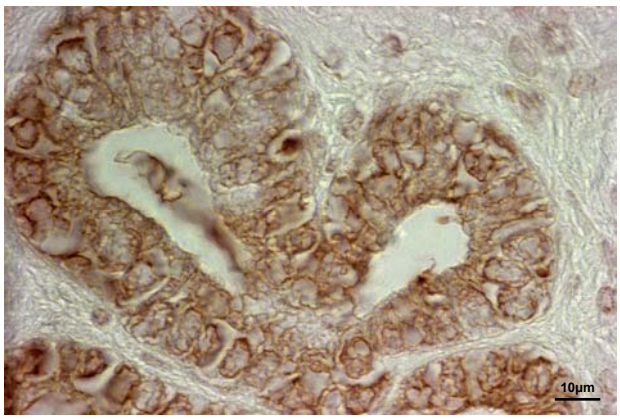

3.3.3.4. Bax in SPPPE treated animals

Expression of Bax in SPPPE treated animals was greatest in the stroma, followed by the luminal epithelium, which was slightly darker than the glands. Expression in the stroma extended halfway into the uterus, extending into the stroma beyond some of the glands. The area of stroma immediately surrounding the glands did not have a strong reaction to the Bax. Fig. 3.3.3.10. shows a typical micrograph of Bax expression in an SPPPE treated uterus. The SPPPE tissue was different to the control tissue, as the control tissue had the greatest expression of Bax in the luminal epithelium and the least in the stroma.

At a superficial level, the expression of Bcl-2 and Bax mimic each other with strong immunolocalisation of both proteins in the stroma and less in the luminal epithelium and glands (figures 3.3.2.10 and 3.3.3.10.). However, these similarities diminish when details of the glands and the luminal epithelium were examined.

Bax expression in the uterine luminal epithelium was prominent in the nuclei with a concentration at the nuclear membranes. Bax expression in the cytoplasm was concentrated toward the apex of the cell. The luminal epithelium nuclei were darker than the cytoplasm and the nucleus appeared more granular, while the cytoplasm appeared smoother. There did not appear to be a cytoplasmic concentration of Bax toward the lumen. Fig. 3.3.3.11. shows Bax in the luminal epithelium of an SPPPE treated animal.

Bax expression in the glands appeared uneven. The cytoplasm had a greater expression of Bax than the nuclei in the glands, and the nuclear membranes were clearly defined. Bax expression in the cytoplasm was not concentrated at the apex of the glandular epithelium (Fig. 3.3.3.12.).

Figure 3.3.3.10.
IHC of Bax in an SPPPE treated rat uterus
Expression of Bax in SPPPE treated animals was greatest in the dark layer of stroma, and equivalent in the uterine luminal epithelium and the glands.

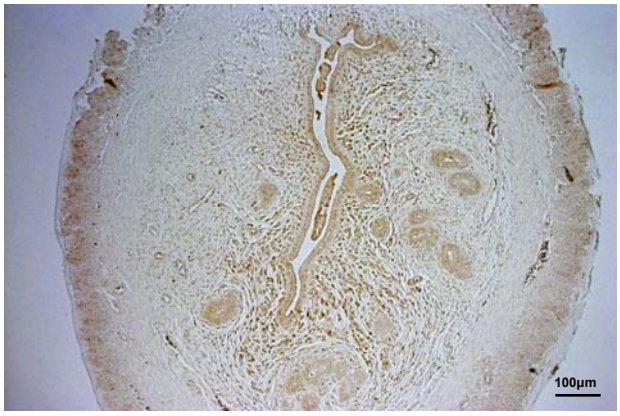

Figure 3.3.3.11.
Expression of Bax in the luminal epithelium of an SPPPE treated animal
Bax was expressed mainly in the nuclei of the luminal epithelium, particularly at the nuclear membranes, with less expression in the cytoplasm. The nuclei appeared smooth and the cytoplasm appeared granular.

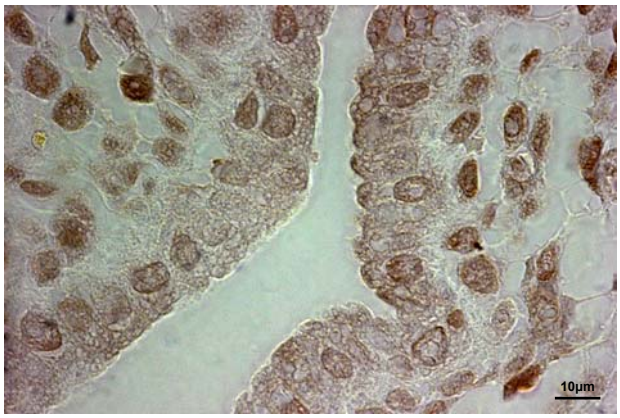

Figure 3.3.3.12.
Expression of Bax in the glandular tissue of an SPPPE treated animal
Bax expression in the SPPPE treated animals gave the glands a frothy appearance. Expression seemed to be greater in the cytoplasm than in the nuclei, although Bax localised in the nuclear membranes. Bax in the cytoplasm did not seem to especially localise at the glandular lumen.

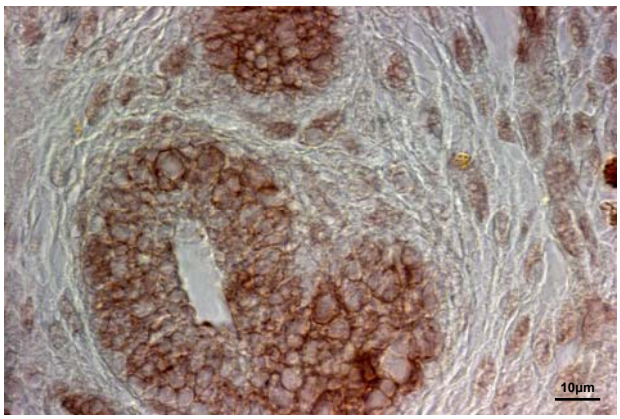

3.3.3.5. Bax in CCPPPE treated animals

In CCPPPE treated animals, Bax expression was generally most concentrated in the stroma, followed by the luminal epithelium, which was similar to the glands. The Bax expressed in the stroma was concentrated around the lumen, but extended to the glands, especially those closer to the lumen (approximately two thirds of the stroma immunolocalised against Bax) (Fig. 3.3.3.13.). This expression of Bax was similar to that seen in the SPPPE treated animals, although the CCPPPE treated animals had a greater intensity of chromagen in the uterine luminal epithelium and glandular tissue (Figs 3.3.3.10. and 3.3.3.13.).

Some of the nuclei in the luminal epithelium immunolocalised against Bax and some did not, but they all had a dark nuclear membrane (Fig. 3.3.3.14.). The luminal epithelial cytoplasm was sometimes darker, and sometimes lighter when compared with the nucleus, and there was some expression of Bax towards the apex of the epithelial cells (Fig. 3.3.3.14.).

Bax expression in the glandular tissue was more concentrated in the cytoplasm than in the nuclei, and the nucleus had a darker nuclear membrane. The cytoplasm seemed to concentrate to the apical end of the glandular cells. Both the nucleus and the cytoplasm had a frothy appearance. This can be seen in Fig. 3.3.3.15.

Figure 3.3.3.13.
IHC of Bax in a CCPPPE treated rat uterus
Expression of Bax in CCPPPE treated sections was greatest in the stroma, followed by the luminal epithelium and least in the glandular epithelium.

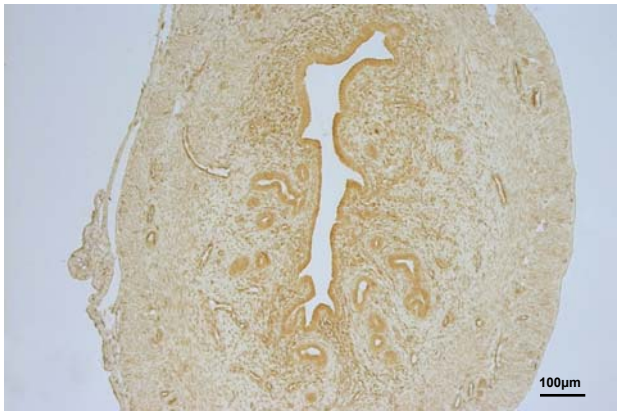

Figure 3.3.3.14.
Expression of Bax in the luminal epithelium of an CCPPPE treated animal
In the uterine luminal epithelial cells, Bax was obvious at the nuclear membranes. The nuclei were sometimes darker and sometimes lighter than cytoplasm. The cytoplasm had a concentration of Bax towards the apex of the cells.

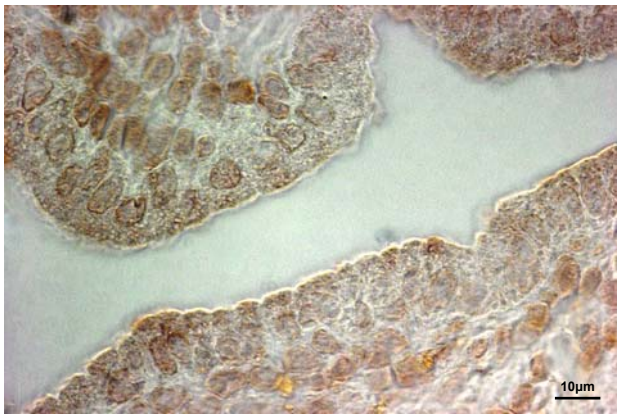

Figure 3.3.3.15.
Expression of Bax in the glandular tissue of a CCPPPE treated animal
Expression of Bax in the glands was greater in the cytoplasm than the nucleus, with an aggregation towards the lumen of the glands. The nuclear membranes were distinct. The glandular cells had a foamy appearance in both the cytoplasm and nucleus.

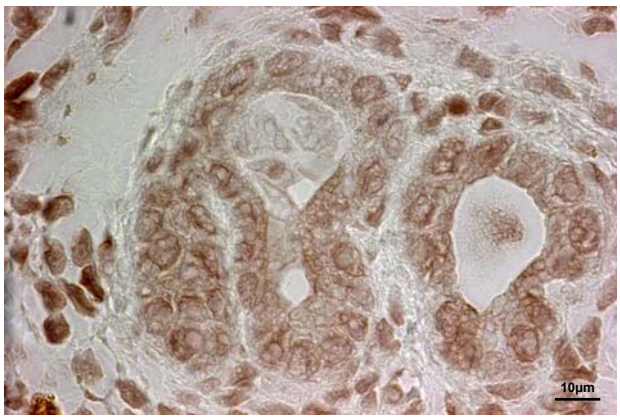

3.3.3.6. Summary of IHC against Bax in rat uteri

Bax expression in the uterine profiles of the control tissues was greatest at the uterine luminal epithelium, which was similar to the glandular epithelium, and the least expression in the stroma. The single CC treated animal had a similar expression of Bax, with the glandular epithelium and luminal epithelium having similar concentrations, and the stroma having a lower expression of Bax. Notably, the single CC treated tissue had Bax expression in the myometrium. Expression of Bax in the P_4 treated animals was greatest in the glands, followed by the luminal epithelium and lowest in the stroma. By contrast, both the SPPPE and CCPPPE treated tissues had the greatest expression of Bax in the stroma, followed by the luminal epithelium which was greater or similar in expression of Bax to the glandular epithelium.

Bax expression in the stroma of the control tissues and P_4 treated tissues was mainly concentrated in the dark layer surrounding the lumen, whereas the single CC, SPPPE and CCPPPE treated animals had expression of Bax extending to the glandular epithelium.

The luminal epithelium expressed the greatest concentration of Bax at the nuclear membranes, followed by the nuclei and least in the cytoplasm for the control tissues, single CC, P_4 and SPPPE treated tissues. The CCPPPE tissue had the greatest expression of Bax in the nuclear membranes, followed by the cytoplasm which was greater or similar in expression to the nuclei. All of the treatments, except for the SPPPE treated animals, had a concentration of Bax towards the apex of the cells. The single CC treated animals had a patchy expression of Bax at the luminal epithelium.

Bax expression in the glandular epithelium of the control tissues was greatest in the nuclear membranes, followed by the nuclei which was greater (ovariectomised untreated or saline treated) or similar (oil treated and SOOO treated) to the cytoplasm. The single CC, P_4, SPPPE and CCPPE treatments had the greatest

expression of Bax at the nuclear membranes, followed by the cytoplasm and least in the nuclei. Bax expression was localised in the apex of the glandular cells for all of the treatments except for the SPPPE treatment, and the localisation in the apex was particularly noticeable in the single CC treated animals. The oil, SOOO, single CC and CCPPPE treated tissues appeared frothy after localisation with Bax antibody.

3.3.4. Overview of IHC in rat uterine compartments

Table 3.3.1. Summary of expression of antibody in rat uterine structures.

The table shows a comparison between treatment groups against antibody.
The uterine profile indicates the relative levels of expression of antibody in the uterine luminal epithelium (LE), glandular epithelium (GE) or stroma (S). Concentration of expression in the stroma has been indicated, showing expression predominantly in the dark layer (dl), to the glandular epithelium or extending to the myometrium.
Both the uterine luminal and glandular epithelium show the relative expression of the antibodies at the nuclear membranes (nmb), nuclei (n) and cytoplasm (c). The expression of the antibodies towards the apex of the epithelial cells has also been indicated.

Expression has beeen indicated as greater than (>), greater or equal to (≥), equal to (=) or in some cases expression was found to be greater in a structure in one section, and the same structure was found to have less expression in a different section, which has been assigned the symbol "≅".

Treatment		Uterine Profile	Stroma	Luminal Epithelium	C. to apex	Glandular Epithelium	C. to apex	Other
Ovex	PR	LE > S > GE	Some dl	nmb > n	None	nmb = n	No apex	
	Bcl-2	LE > GE > S	Some dl	nmb > n = c	To apex	nmb > n = c	No apex	
	Bax	LE ≥ GE > S	Around dl	nmb > n > c	To apex	nmb > n > c	To apex	
Saline	PR	LE > S > GE	Around dl	nmb > n	None	nmb ≥ n	No apex	
	Bcl-2	LE > GE > S	Some dl	nmb > n = c	To apex	nmb > n = c	Some apex	
	Bax	LE ≥ GE > S	Around dl	nmb > n > c	To apex	nmb > n > c	To apex	
Oil	PR	LE > S > GE	Around dl	nmb > n > c	To apex	nmb > n > c	To apex	
	Bcl-2	LE > GE > S	Some dl	nmb > n = c	To apex	nmb > n = c	Some apex	
	Bax	LE ≥ GE > S	Around dl	nmb > n ≥ c	To apex	nmb > n > c	To apex; Foamy appearance	
SOOO	PR	LE > S > GE	Around dl	nmb > n > c	To apex	nmb > n = c	To apex	
	Bcl-2	LE > GE > S	Some dl	nmb > n = c	To apex	nmb > n = c	Some apex	
	Bax	LE ≥ GE > S	Around dl	nmb > n > c	To apex	nmb > n > c	To apex; Foamy appearance	
CC	PR	S > LE > GE	To glands	nmb > n > c	To apex	nmb > n > c	To apex	
	Bcl-2	LE > GE > S	Some dl	nmb > c > n	To apex	nmb > n = c	Some apex	LE patchy
	Bax	LE = GE > S	To glands	nmb > n > c	To apex	nmb = apex > c > n	To apex; Foamy appearance	LE patchy Myometrium stained
P_4	PR	LE ≥ GE > S	Around dl	n ≥ c		n = c	To apex	
	Bcl-2	LE > GE > S	Around dl	nmb > n = c	To apex	nmb > n = c	Some apex	
	Bax	GE > LE >S	Around dl	nmb > c ≥ n	To apex	nmb > c > n	To apex	
SPPPE	PR	S > LE > GE	To glands	nmb > n ≥ c	To apex	nmb > n ≅ c	Some apex	
	Bcl-2	S > LE ≥ GE	To glands	nmb > n ≥ c	To apex and base	nmb > n = c	Some apex	
	Bax	S > LE ≥ GE	To glands	nmb > n > c	Not to apex	nmb > c > n	Not to apex	
CCPPPE	PR	S > LE > GE	To myometrium	nmb > n > c	To apex	nmb > n > c	To apex	
	Bcl-2	LE > GE > S	Some dl	nmb > c > n	To apex	nmb > c > n	To apex	
	Bax	S > LE = GE	To glands	nmb > c ≅ n	To apex	nmb > c > n	To apex	

3.4. Enzyme linked immunosorbent assay (ELISA)

3.4.1. Overview of the ELISA analysis

Two technical replicates were analysed per animal and the controls omitting primary antibody, secondary antibody and protein homogenate have been included. ELISA was performed against PR, Bcl-2 and Bax. The data have been presented as medians with the upper (75%) and lower (25%) quartiles.
Significance was set at the 5% significance level using the Wilcoxon / Kruskal Wallis rank sums tests.
Significant differences were found between the samples for the ELISA against Bax, which was further tested using Tukey-Kramer *post hoc* analysis.
The results are presented in tables 3.4.1.1 to 3.4.3.3.

Table 3.4.1.1. Results of the χ^2 approximation of the ELISA data using the Wilcoxon / Kruskal-Wallis rank sums test
Two technical replicates were taken per animal and tested using the Wilcoxon / Kruskal Wallis ranks sums at the 5% level of significance. For probability less than 0.05, the chi-squared approximation was used. Results that were significantly different have been indicated in bold type.

	Parameter	**χ^2 Approximation P> χ^2**
1	ELISA against PR	0.1534
2	ELISA against Bcl-2	0.098
3	ELISA against Bax	**<0.001**

3.4.2. Results of the Tukey-Kramer *post hoc* analysis for the parameter that was significantly different

3.4.2.1. Tukey-Kramer *post hoc* analysis of ELISA against Bax

The treatment groups were not significantly different to each other, or to the controls that omitted primary antibody or omitted protein, but all of the treatment groups were different to the control that omitted secondary antibody.

Table 3.4.2.1 Comparisons for all pairs using Tukey-Kramer *post hoc* analysis of ELISA against Bax

Levels that were not connected by the same letter are significantly different.

Treatment	Level	
CCPPPE	A	
SPPPE	A	
Oil	A	
P_4	A	
CC	A	
Untreated	A	
SOOO	A	
Saline	A	B
Omit primary antibody (anti-Bcl-2)	A	B
Omit protein	A	B
Omit secondary antibody (anti-rabbit)		B

3.4.3. Medians and interquartiles of ELISA results

3.4.3.1. Median and interquartiles of ELISA against PR

Table 3.4.3.1. shows the median and interquartiles of the treatment groups against PR. These show that the CCPPPE treatment results in the greatest expression of Bcl-2, followed by the oil control and P_4 and then SPPPE treatment. However, these results were not significantly different to each other at the 5% level.

Table 3.4.3.1. The median and interquartiles for ELISA against PR by treatment.
25Q refers to the 25th interquartile, 75Q refers to the 75th interquartile.
Measurements were taken as absorbance at 450 nm per 1 μg protein sample.

Treatment	Median	25Q	75Q
Untreated	0.1055	-0.0994	0.5710
Saline	-0.0038	-0.0516	0.2530
Oil	0.0058	-0.0294	0.4790
CC	0.0233	-0.0079	0.4102
P_4	0.1262	-0.0236	0.4948
SOOO	0.1815	-0.0362	0.3597
SPPPE	0.1322	0.0992	0.5202
CCPPPE	0.2607	0.0580	0.5489
Omit protein	-0.0004	-0.0008	-0.0001
Omit anti-PR	0.2004	0.0769	0.3239
Omit anti-rabbit	-0.1716	-0.2647	-0.0785

3.4.3.2. Median and interquartiles of ELISA against Bcl-2

Table 3.4.3.2. shows the median and interquartiles of the treatment groups against Bcl-2. These show that the CCPPPE treatment results in the greatest expression of Bcl-2, followed by P_4 and SPPPE, and then the untreated and oil controls. However, these results were not significantly different to each other at the 5% level.

Table 3.4.3.2. The median and interquartiles for ELISA against Bcl-2 by treatment.
25Q refers to the 25th interquartile, 75Q refers to the 75th interquartile.
Measurements were taken as absorbance at 450 nm per 1 μg protein sample.

Treatment	Median	25Q	75Q
Untreated	0.2206	-0.0035	0.6499
Saline	0.0048	-0.0533	0.3185
Oil	0.2140	0.0238	0.6623
CC	0.0629	-0.0095	0.4468
P_4	0.2428	0.1077	0.6863
SOOO	0.1123	0.0000	0.4035
SPPPE	0.2365	0.1155	0.3777
CCPPPE	0.2771	0.1234	0.3877
Omit protein	-0.0001	-0.0002	0.0001
Omit anti-Bcl-2	0.4187	0.1616	0.6759
Omit anti-mouse	-0.1410	-0.3089	0.0270

3.4.3.3. Median and interquartiles of ELISA against Bax

Table 3.4.3.3. shows the median and interquartiles of the treatment groups against Bax. These show that the CCPPPE treatment results in the greatest expression of Bax, followed by the oil control and P_4, then SPPPE, and the single CC treatment. However, these results were not significantly different to each other at the 5% level.

Table 3.4.3.3. The median and interquartiles for ELISA against Bax by treatment.
25Q refers to the 25th interquartile, 75Q refers to the 75th interquartile.
Measurements were taken as absorbance at 450 nm per 1 μg protein sample.

Treatment	Median	25Q	75Q
Untreated	0.0458	-0.0385	0.5805
Saline	-0.0025	-0.0902	0.3482
Oil	0.2792	0.0001	0.6462
CC	0.0673	0.0120	0.6700
P_4	0.2590	0.0261	0.5263
SOOO	0.0970	-0.0110	0.4861
SPPPE	0.1990	0.1324	0.6713
CCPPPE	0.3213	0.1344	0.6834
Omit protein	0.0003	-0.0040	0.0042
Omit anti-Bax	0.0508	-0.0137	0.0746
Omit anti-rabbit	-0.3394	-0.4227	-0.2092

3.4.4. Summary of the ELISA analysis

Generally, the results for the ELISA against PR, Bcl-2 and Bax did not show any significant differences between the different treatment groups or the controls. The immunohistochemical results against PR, Bcl-2 and Bax showed marked differences between the various uterine compartments. Retrospectively, it would have been ideal to isolate the uterine luminal epithelium, glandular epithelium, stromal tissue and myometrium and perform ELISA against the uterine compartments.

CHAPTER 4. DISCUSSION

4.1. Histological and morphometric differences between ovariectomised animals treated with CC, P_4, SOOO, CCPPPE or the vehicle control

There is a brief period during the reproductive cycle when a uterus is receptive to a functional blastocyst, known as the window of implantation, and is controlled by the ovarian hormones, E_2 and P_4 (Wang and Dey, 2006). Progesterone binding to its receptor affects the downstream events of this process, and the levels of progesterone receptors are affected through feedback loops driven by oestrogen (Psychoyos, 1967). Clomiphene citrate binds to oestrogen receptors and has both oestrogenic and anti-oestrogenic effects on tissues, depending on the tissue and on the species (Clark and Markaverich, 1982, Hosie and Murphy, 1995). The binding of CC to ERβ acts as an anti-oestrogen (Kurosawa *et al.*, 2010). ERβ has been implicated in the decidualisation of the stroma in the rat uterus (Peters *et al*., 1995, Tessier *et al*., 2000), and so the binding of CC with PPPE inhibits the decidualisation seen in PPPE treatments via the ERβ receptor. Decidualisation is vital to sustain a growing conceptus and animals without a decidual response were unable to maintain a viable blastocyst. (Rider *et al.*, 1985)

The aim of this study was to determine some of the effects of a single, high CC dose on ovariectomised tissues, and how it compared to a single progesterone treatment on ovariectomised tissues. Psychoyos (1973) found that PPPE treatment in ovariectomised animals reflected the hormonal regime typical of a pregnant rat, and this study also looked at how CC affected PPPE treated animals.

4.1.1. Effects of CC, P_4, PPPE and CCPPPE on uterine length and breadth

The rat endometrium undergoes a well described plasma membrane transformation prior to implantation. The apical membrane of the uterine luminal epithelial cells tends to have long, regular microvilli. During early pregnancy, the microvilli become flattened and less dense and the membranes of the uterine epithelial and trophoblast cells have a flattened area of contact (Murphy and Shaw, 1994, Murphy, 2004). This suggests that pregnancy only becomes possible with a flattening of microvilli (Murphy, 2004). Moreover, the tight junctions between the luminal epithelial cells alter during early pregnancy, with deeper lateral tight junctions and disassembly of some focal adhesion molecules under the influence of progesterone (Murphy, 2004, Kaneko *et al.*, 2009). Psychoyos (1967) found that the hormonal milieu of the oestrus cycle could be replicated in ovariectomised rats by a PPPE treatment regime. In this study, the PPPE treated animals showed an increase in the long uterine diameter (uterine length) that was significantly different to the animals treated with either vehicle controls or a single P_4 (table 3.1.2.1. and graph 3.1.2.2.). As expected, uterine length is probably progesterone dependant requiring multiple doses of progesterone and a nidatory oestrogen dose.

The single CC treatment and the CCPPPE treated animals were not significantly different to the PPPE treated animals in terms of uterine length, and were not different to most of the vehicle controls or to the single P_4 treated animals. Although the uterine length of the CCPPPE treated animals was not significantly different, the CC treatment with PPPE had a reduced uterine length than either SPPPE or CC alone, which suggests that the CC dampens the effect of the PPPE treatment and may act as an oestrogen antagonist, possibly blocking the nidatory oestrogenic effect.

The treatments were not significantly different from each other in terms of the short uterine diameter (uterine width). However, they had a greater uterine diameter compared to the controls.

The single CC treatment animals had a greater uterine width when compared to the other treatments (table 3.1.2.2. and graph 3.1.2.2.) and had a distinct oestrogenic-like response on uterine width. The parameters of both uterine length and uterine width were greater in PPPE treated animals and CCPPPE treated animals than the vehicle control animals, and the CC dose tended to decrease the length and breadth of the uterus when used in conjunction with PPPE. This effect may have been caused by the CC binding to the oestrogen receptors and behaving, in this case, as an oestrogen antagonist. Similarly, Brown *et al*. (1991) found that clomiphene blocked oestrogenic-induced increase in uterine weight when both oestrogen and clomiphene were administered concurrently over an extended period of time.

4.1.2. Effects of CC, P_4, PPPE and CCPPPE on the lumen

Lumen length refers to the long luminal diameter as previouslyμ stated in Section 2.7.1. The results for the lumen length were similar to those of the uterine length and width. The CC, SPPPE and CCPPPE treated animals were similar to each other and different to the controls in terms of lumen length. The animals treated with SPPPE had increased lumen length compared to the controls and single P_4, but not to the animals treated with a single CC, and the animals treated with CCPPPE were similar to the SPPPE treated animals (tables 3.1.1.1., 3.1.2.3. and graph 3.1.2.3.). The single CC treatment therefore seemed to affect the luminal length similar to that of the PPPE treatment regime animals, and the CC in conjunction with the PPPE seems to diminish the luminal length, possibly indicating an anti-oestrogenic effect.

The short luminal diameter was not significantly different between the different treatment groups, or the controls (table 3.1.1.1.). Morphologically, however, the lumens of the control tissues tended to be narrow and straight without tissue folding. By contrast the P_4 and SPPPE treated animals exhibited occlusion of the lumen, which suggests that progesterone promotes the closure of the lumen in a normal cycle, and concurs with the results of Ljunkvist (1972). The animals

treated with a single CC had a slightly wider lumen than the controls, but not significantly so. This would suggest that in terms of lumen occlusion, the CC behaves in an oestrogenic manner. The CCPPPE treatment caused extensive branching or folding of the lumen (Fig. 3.2.4.), and so increased the surface area of the luminal epithelium, possibly diminishing the ability of the implanting blastocyst to adhere to the luminal epithelium at the anti-mesometrial pole. Similarly, in ovariectomised animals treated with E_2 alone, folding of the lumen is apparent, suggesting that this folding is oestrogen dependant (Ljungkvist, 1971c, Hosie and Murphy, 1992, Hosie and Murphy, 1995). In day 5.5 pregnant animals (at the time of implantation), there is tissue folding seen in non-implantation sites, whereas implantation sites do not have folding (Scholtz *et al.*, 2008), suggesting that a smooth uterine surface may be required for successful implantation.

4.1.3. Effects of CC, P_4, PPPE and CCPPPE on the stroma

The stromal width (i.e. stroma perpendicular to the mesometrial/anti-mesometrial pole) of the PPPE and CCPPPE treated animals were similar to each other and significantly greater than the SOOO control. This result was not unexpected as it has been well documented that hyperplasia of the endometrium is under the control of the ovarian hormones (Lee and DeMayo, 2004, Paria *et al*., 2001, Wood *et al*., 2007). The hormones therefore caused an increase in stromal width, as previously reported. The stromal width of the CCPPPE treated tissue was slightly, although not significantly, lower than the PPPE treated tissue.

A single 1.25 mg CC treatment resulted in significantly greater stromal width than the vehicle controls. The CC treatment may act as an oestrogen agonist causing cell division in the stromal tissue (Hosie and Murphy, 1992, Hosie and Murphy, 1995). Implantation in rats occurs at the anti-mesometrial pole (Enders and Schlafke, 1967, Abrahamsohn and Zorn, 1993, Tessier *et al*., 2000), and the various treatments did not cause any significant differences of stromal tissue at the anti-mesometrial pole (table 3.1.1.1.). The SPPPE treated animals had significantly more stromal tissue at the mesometrial pole than the P_4 treated

animals, although neither treatment group on its own was significantly different to the other treatment groups or to the controls. (tables 3.1.1.1. and 3.1.2.5.). The CCPPPE treatment, although not significantly different, had less tissue at the mesometrial pole than the SPPPE treated tissue. The increase in tissue at the mesometrial pole may therefore be inhibited by progesterone, or driven by oestrogen, and the CC in conjunction with the PPPE treatment may have an anti-oestrogenic effect. Expression of PR was lowest in the stroma in animals treated with P_4 alone, and highest in the stroma of PPPE treated animals (figures 3.3.1.9. and 3.3.1.12.).

The dark layer of the control treated tissues extended for 6 to 8 layers beyond the lumen and the fibroblasts were triangular or rectangular (Fig. 3.2.1.). The P_4 treated and SPPPE treated animals also had the dark layer extending 6 to 8 layers beyond the lumen, but did not extend beyond the glands. The fibroblasts were rounded, indicative of decidualisation (Figs 3.2.7. and 3.2.10.). The dark layer of the CC and CCPPPE treated animals extended beyond 6 to 8 layers, and was seen around the glands (Figs 3.2.4. and 3.2.13.). The fibroblasts were also rounded after CC treatment. The decidual reaction does not appear to be diminished by CC, but also extended to around the glands. Although not examined in this work, it is known that blood supply in the uterus is largely affected by the ovarian hormones oestrogen and progesterone. Oestrogens increase blood supply to the uterus while progesterone decreases blood supply. To a lesser extent, blood supply is also influenced by luteinising hormone, oxytocin, cytokines, neurotransmitters and other factors. (Krzymowski and Stefanczyk-Krzymowska, 2004)

4.1.4. Effects of CC, P_4, PPPE and CCPPPE on the luminal epithelium

The single CC, CCPPPE, PPPE and P_4 treated animals had a significantly greater luminal epithelial height than the vehicle controls (table 3.1.2.6. and graph 3.1.2.6.). The treatments with CC displayed an epithelium that appeared columnar with basal nuclei and obvious long microvilli and the epithelium appeared

pseudostratified, suggestive of hyperplasia (Figs 3.2.5. and 3.2.14.). These features are usually associated with oestrogen treatment alone (Ljungkvist, 1971c, Hosie and Murphy, 1992, Hosie and Murphy, 1995). The PPPE and P_4 treatments had a single layer of cuboidal epithelium and basally placed nuclei, and correlate with the nuclear polarity seen in both rat (Glasser *et al.*, 1988) and human (Bentin-Ley *et al.*, 1994) luminal epithelial cells (Figs 3.2.8. and 3.2.11.). Interestingly, the CCPPPE had a slightly greater height of epithelial cells than the PPPE alone. Oestrogen treatment has been shown to increase the uterine epithelial cells from cuboidal to columnar in canine endometria (Ilesanmi *et al.*, 1993), and so the CC in this case seemed to have enhanced, rather than diminished, the oestrogen agonistic effect in this uterine compartment. The action of progesterone contributes to luminal epithelial height, but CC treatment has a far greater effect on luminal epithelial height. These features, including the long microvilli, may decrease the ability of the blastocyst to implant, possibly by masking the adhesion molecules associated with apposition and attachment of the blastocyst (Wang and Dey, 2006). The morphology seen in the luminal epithelial height and especially the presence of the long microvilli, does not conform to the morphology of the plasma membrane transformation. Normally, at the time of implantation, the apical surface of the luminal epithelial cells display short or few microvilli and may even have pinopods (Murphy, 2004).

4.1.5. Effects of CC, P_4, PPPE and CCPPPE on the glandular tissue

In this study, the different treatments did not seem to affect the number of glands seen in a section, whether the glands occurred in groups or singly, or how many glands opened into the luminal epithelium (table 3.1.1.1.). Hosie and Murphy (1992) found that CC treatment resulted in an increase in number of glands opening into the uterus. However, these results were obtained using a low physiological dose of CC (0.25 mg), whereas the results presented here were at the maximal physiological dose of CC (1.25 mg). In humans, the proliferative stage (increased oestrogen) is associated with increased nuclear and mitotic activity in the glandular tissue, while the secretory stage (high progesterone) is

associated with an increase of gland size and increased secretory product (Maksem *et al.,* 2007). The control tissues had a concentration of glands at the anti-mesometrial pole, as did the P_4 treated tissues (Figs 3.2.1. and 3.2.7.). The SPPPE treated animals had glands at the anti-mesometrial and mesometrial poles (Fig. 3.2.10). The single CC treatment and the CCPPPE treatment had glandular tissue at the anti-mesometrial pole as well as dispersed throughout the stroma (Figs 3.2.4. and 3.2.13.). This seems to suggest that progesterone, oestrogen and CC treatments do not have a noticeable effect on the number of glands seen, but the CC and CCPPPE treatments affected the location of the glandular tissues. This change in glandular location may also contribute to the low implantation rates associated with CC administration.

4.2. Immunoassays against PR, Bcl-2 and Bax between ovariectomised animals treated with CC, P_4, SPPPE, CCPPPE or the vehicle control

4.2.1. Expression of PR in the rat endometrium

As mentioned earlier, attachment of the blastocyst to the endometrium occurs during a brief window of implantation that is largely controlled by the ovarian hormones, oestrogen and progesterone. The action of these hormones is modulated by their receptors, ER and PR (Psychoyos, 1969). Progesterone receptor expression is mainly controlled by oestrogen and progesterone. Increased levels of oestrogen upregulate the levels of PR and increased levels of progesterone result in a down regulation of PR expression (Tibbetts *et al.*, 1998; Tan *et al.*, 1999, Critchley and Saunders, 2009). Ohna and Fujimoto (1998) found that ER, but not PR, levels were lower in clomiphene stimulated cycles in women than in normal cycles.

In this study, PR expression in the PPPE, CCPPE and CC treated animals was greatest in the stroma followed by the luminal epithelium and least in the glandular tissue. In contrast, expression of PR in the P_4 treated tissue had the greatest expression in the luminal epithelium, followed by the glands and least in the stroma. Oestrogen has been reported to decrease PR levels in the uterine luminal epithelium and increase levels in the myometrium and stroma (Tibbetts *et al.*, 1998, Tan *et al.*, 1999). The results suggest that the CC has an oestrogenic effect on PR expression in the uterine compartments and that CCPPPE does not inhibit the oestrogen like effect, while P_4 has the opposite effect on PR expression when compared to E_2.

The controls also had the greatest expression of PR in the luminal epithelium, but this expression was reduced in the stroma and lowest in the glands suggesting that control of PR in the different uterine compartments is not exclusively determined by the ovarian hormone levels, but may be affected by other factors. This finding

concurs with that of Parczyk and co-workers (1997) who found a 50% decrease in PR levels after ovariectomy in hamsters, showing that progesterone and oestrogen do not exclusively regulate PR expression. The increased levels of PR in the uterine luminal epithelium of ovariectomised animals may be caused by a lack of oestrogen or possibly as a result of progesterone depletion or another consequence of ovariectomy (Ohta *et al.*, 1993, Parczyk *et al.*, 1997).

Tibbetts *et al*. (1998) found that PR protein expression in ovariectomised mice was intense in the luminal and glandular epithelium, and greatly reduced in the stroma and myometrium. This result is reflected in the present study, except that control tissue showed low expression in the glandular epithelium.

Expression of PR in CCPPPE treated animals was noticeably extended beyond the dark layer, to the limit of the stroma. The P_4 treated animals had a concentration of PR in the dark cell layer, while CC and SPPPE treatment extended to the glandular epithelium. Clomiphene, in conjunction with PPPE, upregulated PR expression. As oestrogen upregulates the expression of PR (Critchley and Saunders, 2009), the CC, in this case, seems to be acting as an oestrogen agonist, by upregulating PR expression on its own and also in conjunction with the PPPE treatment. Possibly the initial upregulation of PR by clomiphene is further upregulated after the nidatory oestrogen dose in the PPPE treatment.

The expression of PR in the luminal epithelium of CC treated animals was apparent along the apical plasma membrane when compared to the single P_4 and the PPPE treatments, which expressed PR around the nuclear membranes. The vehicle control tissue also showed a concentration of PR at the apex of the luminal epithelial cells. In the hormone-free state, the expression of PR at the apical nuclear membrane is moderate, while the treatment with P_4 and PPPE diminishes the expression of PR at the apical plasma membrane. However, treatment with CC or CCPPPE seems to mimic the hormone-free state, in that PR expression is still seen and is more concentrated at the apex of the luminal cells, although PR expression is also seen around the nuclear membrane. In the uterine luminal

epithelium, CC is in some way inhibiting the movement of the PR from the apical membrane and thus possibly preventing the downstream effects of progesterone. As PRs are not obvious on the apical surface of the uterine luminal epithelium in the PPPE treated tissue, their presence in CCPPPE tissue may in some way impede implantation, accounting for the possible low implantation rates seen with CC use.

Although PRs have been reported to be present in the implantation sites during early pregnancy (Theron, 2010), CC may cause an overexpression of PR in the epithelium. This may change the spatial expression of PR such that implantation is impaired.

It was noted when viewing the sections treated with CC that the myometrium, and particularly, the muscularis externa showed an increased expression of PR. Oestrogen has been shown to increase PR levels in the myometrium of ovariectomised rats (McCormack and Glasser, 1980) and mice (Tibbetts *et al.*, 1998, Kurita *et al.*, 2001). Farnell and Ing (2003) showed that the SERMS, 4-OH-tamoxifen, GW 5638 and EM-800 caused an oestrogenic effect in the outer myometrium of ovariectomised ewes. Similarly, the results here show that CC caused an oestrogenic agonist effect in the outer myometrium of ovariectomised rats.

The expression of PR in the glandular epithelium seems to be unchanged when treatment groups are compared to each other, or to the vehicle controls.

Traditionally, the activation of PR has been reported to be induced by oestrogen via the oestrogen receptor (ER) (Tan *et al.*, 1999). However, the discovery of the two isoforms of ER, i.e. ERα and ERβ have allowed for different possible actions of E_2 and SERMS on the receptors. Kurosawa *et al*. (2010) found that CC had both an oestrogenic and anti-oestrogenic effect on ERα using 293T cells, whereas CC had an anti-oestrogenic effect on ERβ. They postulated that CC may inhibit the action of progesterone in the endometrium by the antagonistic effect of CC.

Moreover, the work by Ohna and Fujimoto (1998), using sonograms to measure endometrial thickness in women, showed that extended CC treatments decreased endometrial thickness. This decrease in endometrial thickness had a correlative relationship with increased probability of miscarriage. They also found, by immunoassay, that CC diminished the numbers of ERs in the endometria in women, but did not have a significant effect on PR levels, when compared to natural cycles. They postulated that the reduction of oestrogen receptors was more important for low pregnancy rates than the decrease in progesterone receptors. However, they did not distinguish the expression of the receptors in the different uterine compartments and so did not comment on expression in compartments as a possibility for low implantation rates.

Published literature shows that CC does not significantly diminish the levels of PR in the endometrium (Fritz *et al.*, 1991, Ohno and Fujimoto, 1998, Palomino *et al.*, 2005). The results of the ELISA performed concur with these results. However, the immunohistochemical analysis of PR expression patently showed that treatment with the steroid hormones affected expression in the various uterine compartments. Had these compartments been separated, the effects may have been better elucidated.

The knockout PRKO (-/-) mice did not show PR expression in the decidual areas during early pregnancy (Lydon *et al.*, 1995). Furthermore, the decidual response in ovariectomised animals is absent, which is probably caused by the lack of circulating progesterone. Therefore, the absence of binding between progesterone and PR probably inhibits the transcription of progesterone dependent genes (Mahajan and London, 1997) and thus does not allow for decidualisation to occur. The decidual response can, however, be induced by progesterone and increased levels of PR in mice deficient in ERα expression, suggesting that oestrogen does not affect PR expression during decidualisation (Curtis *et al.*, 1999, Paria *et al.*, 1999). In contrast, the decidualisation reaction in wild type mice (that were not ERα deficient) was oestrogen dependent (Curtis *et al.*, 1999).

4.2.2. Expression of Bcl-2 and Bax in ovariectomised rat endometria

Tissue remodelling is important during the window of implantation to allow the blastocyst to adhere and implant in the receptive endometrium (Wang and Dey, 2006). Apoptosis is involved in this homeostatic process and the Bcl-2/Bax pathways are important to intrinsic apoptosis (Harada *et al.*, 2004, Wang and Dey, 2006). Bcl-2 protects cells against some forms of apoptosis, but does not promote cell proliferation. Bax promotes apoptosis and counters the anti-apoptotic properties of Bcl-2 by forming heterodimers with Bcl-2 (Korsmeyer *et al.*, 1993, Oltvai *et al.*, 1993, Oltvai and Korsmeyer, 1994). Bcl-2 is localised on the outer membranes of the mitochondria, endoplasmic reticulum and nuclear membranes. Bax is located in the cytoplasm under cell survival conditions, but translocates to the mitochondria during apoptotic conditions (Ogle, 2002).

Shifts in expression of Bcl-2 and Bax in the various endometrial compartments

In this study, expression of Bcl-2 in the CC treated and CCPPPE treated animals was arbitrarily patchy around the luminal epithelium. The expression of Bcl-2 in the CC, P_4, CCPPPE and control animals was greatest in the luminal epithelium, and lowest in the stroma, where localisation was only seen in the dark layer. The SPPPE treated tissue had the greatest expression of Bcl-2 in the stroma, beyond the dark layer and low in both luminal and glandular epithelium. The CCPPPE treatment appeared to restrict the expression of Bcl-2 in the stroma as well as maintaining a high punctuate expression in the luminal epithelium and seems to prevent the change of expression from epithelium to stroma. The effect of CC was similar to that of the controls, in that expression of Bcl-2 was greatest in the uterine luminal epithelium and lowest in the stroma, although CC caused arbitrary expression in some sections of the uterine luminal epithelium and surrounding stroma, and was absent in other sections, suggesting that some cells in the luminal epithelium are sensitive to clomiphene, whilst adjacent cells may not be, and may have a more PPPE-like expression of Bcl-2. The expression of Bcl-2 was at the

base of the luminal epithelial cells, possibly at the basement membrane, in the SPPPE treatment. This might inhibit the attachment of the blastocyst during implantation.

The control tissues and the single CC treated tissues had the greatest expression of Bax in the uterine luminal epithelium, then glandular epithelium and lowest in the stroma. In the control tissues, Bax localisation was confined to the dark layer, whereas the CC treatment had localisation extended to the glandular stroma, suggesting that CC causes a shift in Bax expression to the stroma.

Expression of Bax in P_4 treated tissue was greatest in the glands, followed by the luminal epithelium and least in the stroma. This suggests that progesterone shifts the expression from the luminal epithelium to the glandular epithelium.

Expression of Bax in both CCPPPE and SPPPE tissues was greatest in the stroma followed by the luminal epithelium and least in the glandular epithelium. Expression of Bax in the stroma extended to the glandular epithelium.

The levels of Bcl-2 and Bax are maintained in the uterine compartments of the SPPPE treated animals, with the greatest expression in the stroma, then the luminal epithelium and least expression of both proteins in the glands. In contrast the CCPPPE treated tissue shows the same uterine compartment activity as SPPPE in terms of Bax expression, but the Bcl-2 expression in CCPPPE treated tissue is highest in the luminal epithelium, then the glands and least in the stroma. This suggests that CC affects the Bcl-2/Bax ratios and promotes cell survival in the luminal epithelium, which may account for the hyperplasia seen in this tissue, which has been seen in CC treated tissue (Hosie and Murphy, 1995, Hosie, 1997). Wei *et al.* (2005) have found that the Fas/Fas L system may also affect the apoptotic pathways in the epithelia of cycling endometria in an autocrine or paracrine fashion. Sato and colleagues (2003) found increased levels of TNF-α and Fas and Fas ligand 24 hours after ovariectomy and little change in Bcl-2/Bax levels. This suggests that the extrinsic apoptotic pathways of TNF-α and Fas/FasL

mediate programmed cell death in ovariectomised mouse uteri, whereas the intrinsic Bax/Bcl-2 pathway has little effect (Sato *et al.*, 2003). Theron (2010) found that apoptosis induced by the anti-progestin, RU486, was not mediated by the Bcl-2/Bax pathway, and she suggested that the Fas/FasL system may promote programmed cell death in this treatment. However, Dai *et al*. (2000) found that RU-486 resulted in the upregulation of Bax expression, resulting in an increase in the Bax/Bcl-2 ratio and an increase in apoptotic activity.

Shao and co-workers (2009) showed that E_2 treatment on ovariectomised rats improved recovery from apoptotic damage in the uterine tubes, but did not have a protective effect against apoptosis. They also found that chronic treatment with CC promoted apoptosis to occur in the isthmus, suggesting that CC has an oestrogen antagonistic effect in this tissue. Clomiphene displayed a stronger anti-oestrogenic effect in the presence of an oestrogen primed uterus (Hosie and Stewart, 2006). The single CC treatment may have had insufficient time, or doses, to promote the apoptotic pathway, whereas the CC and the E_2 in the CCPPPE treatment may have promoted the apoptotic pathway.

The expression of Bcl-2 was heavy in the uterine luminal epithelium and diminished in the stroma when treated with CC and P_4, but the opposite result was seen in the PPPE treated tissue. This shift in the Bcl-2 profile suggests that the reduction of Bcl-2 in the epithelium of PPPE treated tissues would allow for apoptosis during adherence and infiltration of the attaching blastocyst, whereas the increased levels of Bcl-2 in the CC treated animals would inhibit the process of apoptosis in this tissue.

The SPPPE treated animals did not express Bax in the apex of the luminal epithelial cells, while the other treatments and the control tissues had expression of Bax at the apical edge of the uterine luminal epithelium.

The single CC treatment had patchy expression of Bax in the luminal epithelium, which indicates that the Bax did not shift away from the apex of the epithelial cells.

Lai and co-workers (2000) treated ovariectomised rats with oestrogen implants and found that oestrogen promoted DNA synthesis and proliferation of the uterine epithelial cells. After removal of the oestrogen implants from the animals, they found a significant increase in apoptosis. The results in the present study indicate a shift to expression of Bcl-2. Bcl-2 promotes cell survival, and as oestrogen promotes proliferation and cell survival, it indicates that the CC essentially acts as a pro-oestrogen in this case.

Tassell and co workers (2000) found apoptotic activity in the uterine luminal epithelium and to a lesser degree in the stromal cells of rats on the day of fertilisation. However, on day of implantation, they found an absence of apoptosis in non-implantation sites and an extremely high apoptotic index in the uterine luminal epithelium as well as the stromal tissue immediately underlying the implantation site. This result was mimicked by the PPPE treatment, as expected. In contrast, the CCPPPE treatment appeared to reflect the activity of the oestrous-like state.

Expression of Bcl-2 in the glandular epithelium was similar amongst the treatment groups and control tissues, except for the SPPPE treated animals, where the expression was very low. This result also suggests that clomiphene prevents the transformation of the uterus into a receptive state. In the rhesus monkey, Wei *et al.* (2005) found that the expression of Bcl-2 was high in the glandular epithelium during the proliferative phase and diminished during the secretory phase, whereas the expression of Bax was high during the secretory phase and was much lower during the proliferative phase.

The single CC treated animals expressed Bax in the outer layer of the myometrium. This was not observed in the other treatments, and the expression of

anti-apoptotic Bcl-2, when treated with a single CC, did not have a high expression in the outer myometrium. Burroughs *et al*. (2000) found that increased levels of oestrogen and progesterone promoted both cell proliferation and apoptosis in myometria, whereas diminished levels of these hormones promoted apoptosis. Since the single CC promotes the intrinsic apoptotic pathway in the myometrium and behaves in the opposite way to the expected action of oestrogen, it in fact shows anti-oestrogenic activities.

Oestrogens have been shown to modulate the growth, differentiation and functions of the myometrium (Clark and Mani, 1994, Benassayag *et al.*, 1999). Benassayag and co-workers (1999) found that in human endometria, the expression of the oestrogen receptors, ERα and ERβ were differentially expressed in pregnant and non-pregnant myometria. Women at the end of their pregnancies showed low expression of ERα, which has a high affinity to E_2 and activates transcription. In contrast, pregnant and non-pregnant women expressed similar concentrations of ERβ, which has a low affinity for E_2, and inhibits transcription (Benassayag *et al*., 1999). Clomiphene may alter the relative expression of the two receptors in the myometrium, thus promoting the intrinsic apoptotic pathway.

Hosie and Stewart (2006) found that CCPPE in ovariectomised rat endometria did not significantly affect the incidence of apoptosis when compared to SPPPE treated animals. The ELISA results in the present study showed no significant differences between Bcl-2 and Bax expression in ovariectomised animals treated with CC, P_4, SPPPE or CCPPPE. The work performed here was of short duration, with either a single treatment, or a PPPE treatment with a single CC treatment. Thus the effects of CC over time, or its cumulative effects have not been investigated in this study. The effects of both dosage and of time may change the concentrations of Bcl-2 and Bax.

However, the immunohistochemical studies showed that CC affected the expression of Bcl-2 and Bax in the various endometrial compartments. It is possible that changes in expression would have been seen in the myometrium,

stroma, glandular epithelium and luminal epithelium had these endometrial compartments been isolated from each other and ELISAs performed separately.

4.2.3. Localisation of PR, Bcl-2 and Bax in the rat endometrium

The progesterone receptor isoforms, PRA and B, were decreased in mouse uteri after progesterone treatment. PR antagonist treatment was shown to increase PR protein isoforms and increase mitochondrial associated apoptosis, particularly in the uterine luminal epithelium of mice (Shao *et al.*, 2006). Early pregnancy is primed to promote cell survival of the decidua, whereas apoptosis is a greater feature later in the pregnancy, (Ogle, 2002). The results of the work done in the current study show that treatment with P_4 causes the greatest expression of PR, Bcl-2 and Bax in the luminal epithelium and least in the stroma. It seems unlikely that the single treatment of P_4 significantly increased apoptosis in the uterine compartments via the Bcl-2/Bax pathway, which was unexpected as progesterone has been shown to diminish PR expression and to increase apoptosis. Interestingly, the single CC treatment and the CCPPPE treatment both had the greatest expression of PR and Bax in the stroma and least in the glandular tissue. By contrast, Bcl-2 expression was greatest in the luminal epithelium and lowest in the stromal tissue. This may indicate that CC strongly promotes cell survival in the endometrial epithelium, and allows for premature apoptosis in the stromal tissue, which may have an impact on the low implantation rates seen in individuals treated with CC for infertility.

CHAPTER 5. CONCLUSION

Childlessness has important social and economic consequences for couples and the burden of blame for infertility is traditionally attributed to women. However, it is estimated that only 40% of infertility cases are attributed to female infertility, 40% are due to male infertility, and 20% of cases have unknown etiology (Bernstein, 1999). Clomiphene citrate is one of the first treatments used for female infertility. However, the success rates with clomiphene citrate are low, with a 1 in 10 probability of getting pregnant compared to normal pregnancy rates (Greenblatt *et al.*, 1961, Gazit *et al.*, 1986).

This study investigated the effects of clomiphene when compared to progesterone, as well as clomiphene in conjunction with hormonal treatments that were reflective of those seen in pregnancy, namely PPPE, in ovariectomised rats. In particular, this study focused on the effects of CC, P_4, CCPPPE and SPPPE on the general microanatomy of the uterine components by viewing haematoxylin and eosin sections. It also focused on the expression of the progesterone receptor, the anti-apoptotic protein, Bcl-2, and the pro-apoptotic protein, Bax, in the various uterine compartments using immunohistochemical and ELISA methods.

The major findings of this study showed:

1. Clomiphene affects the various uterine compartments, including the long and short uterine diameters and particularly affects the overall shape of the lumen and the uterine luminal epithelial height, as seen by previous investigators.

2. The expression of the progesterone receptor was altered by CC treatment and this may affect the spatial expression of the PR's in such a manner as to impair implantation.

3. Bcl-2 expression with clomiphene treatment was extremely patchy around the uterine lumen. This expression may diminish the ability of a viable blastocyst to penetrate the epithelium, and in this manner may interfere with implantation.

4. The expression of Bax in the different uterine compartments shifted when treated with clomiphene, which may also have affected the ability of the blastocyst to infiltrate the endometrium during implantation.

5. Clomiphene appeared to behave in a manner that was both oestrogenic and anti-oestrogenic. Moreover, clomiphene also seemed to behave in a manner unrelated to oestrogen and may affect hormonal pathways that are unrelated to oestrogen.

Future investigations for this study

1. In order to elucidate the oestrogenic or anti-oestrogenic effects of clomiphene more fully, it would have been advantageous to compare the treatments to a single E_2 treatment.

2. The ELISA results did not show any changes in expression of PR, Bcl-2 or Bax, as the entire uterine sections were combined before performing this assay. In future, it would be useful to separate the luminal epithelium, glandular epithelium, stroma and myometrium for analysis by ELISA.

3. Clomiphene citrate has shown to have a cumulative effect, affected by both period of application as well as number of treatments. It would be interesting to increase the number of treatments and duration of this project to investigate the cumulative effects of CC.

4. The progesterone receptor exists in two different isoforms, with different downstream effects. The immunoassays used in this study did not differentiate between PRA and PRB and it may be of use to further distinguish between expressions of these isoforms.

REFERENCES

Abrahamsohn, P. A., and Zorn, T. M. T. (1993). Implantation and decidualization in rodents. *J Experimental Zoology* **266**, 603-628.

Achache, H., and Revel, A. (2006). Endometrial receptivity markers, the journey to successful embryo implantation. *Hum Reprod Update* **12**, 731-746.

Adashi, E. Y. (1986). Clomiphene-initiated ovulation: A clinical update. *Seminars in Reproductive Endocrinology* **4**, 255-276.

Aksel, S., Saracoglu, O. F., Yeoman, R. R., and Wiebe, R. H. (1986). Effects of clomiphene citrate on cytosolic estradiol and progesterone receptor concentrations in secretory endometrium. *Am J Obstet Gynecol* **155**, 1219-1223.

Antonsson, B., Conti, F., Ciavatta, A., Montessuit, S., Lewis, S., Martinou, I., Bernasconi, L., Barnard, A., Mermod, J. J., Mazzei, G., Maundrell, K., Gambale, F., Sadoul, R., and Martinou, J. C. (1997). Inhibition of Bax channel forming activity by Bcl-2. *Science* **277**.

Assuncao Guimaraes, C., and Linden, R. (2004). Programmed cell death: Apoptosis and alternative deathstyles. *Eur J Biochem* **271**, 1638-1650.

Baranda-Avila, N., Mendoza-Rodriguez, C. A., Morimoto, S., Langley, E., and Cerbon, M. (2009). Molecular mechanism of cell proliferation in rodent uterus during the estrous cycle. *J Steroid Biochem Mol Biol* **113**, 259-268.

Benassayag, C., Leroy, M. J., Rigourd, V., Robert, B., Honore, J. C., Mignot, T. M., Vacher-Lavenu, M. C., Chapron, C., and Ferre, F. (1999). Estrogen receptors (ERalpha/ERbeta) in normal and pathological growth of the human myometrium: pregnancy and leiomyoma. *Am J Physiol* **276**, E1112-1118.

Bentin-Ley, U., Pedersen, B., Lindenberg, S., Larsen, J. F., Hamberger, L., and Horn, T. (1994). Isolation and culture of human endometrial cells in a three-dimensional culture system. *J Reprod Fertil* **101**, 327-332.

Bernstein, J. (1999). Infertility: From a personal to a public problem. *Public Health Reports* **114**, 494-504.

Bissonnette, R. P., Exheverri, F., Mahboubi, A., and Green, D. R. (1992). The proto-oncogene Bcl-2 can selectively rescue neurotrophic factor-dependent neurons from apoptosis *Nature* **359**, 552-554.

Boostanfar, R., Jain, J. K., Mishell, D. R., and Paulson, R. J. (2001). A prospective randomized trial comparing clomiphene citrate with tamoxifen citrate for ovulation induction. *Fertil Steril* **75**, 1024-1026.

Bras, M., Queenan, B., and Susin, S. A. (2005). Programmed cell death via mitochondria: different modes of dying. *Biochemistry (Mosc)* **70**, 231-239.

Broker, L. E., Kruyt, F. A., and Giaccone, G. (2005). Cell death independent of caspases: a review. *Clin Cancer Res* **11**, 3155-3162.

Brosens, I., Campo, R., and Gordts, S. (2002). Reproductive disorders affecting fertility in endometriosis. *Reprod Biomed Online* **4 Suppl 3**, 59-63.

Brosens, J. J., and Gellersen, B. (2006). Death or survival--progesterone-dependent cell fate decisions in the human endometrial stroma. *J Mol Endocrinol* **36**, 389-398.

Brown-Grant, K., John, P., and Rogers, A. W. (1972). Analysis of the effects of progesterone on the synthesis of RNA and protein in the uterus of the ovariectomized rat and on the development of an iodide concentrating mechanism. *J Endocrinol* **53**, 363-374.

Brown, J. L., Byrd, S. J., Mitchell, A. S., Nelso, M. F., Young, R. L., and Chakraborty, P. K. (1991). Comparison of the long-term effects of estrogen and clomiphene citrate on pituitary and uterine function in ovariectomised rats. *Gynecol Obstet Invest* **31**, 23-29.

Brown, R. (1996). The Bcl-2 family of proteins. *British Medical Bulletin* **53**, 466-477.

Burroughs, K. D., Fuchs-Young, R., Davis, B., and Walker, C. L. (2000). Altered hormonal responsiveness of proliferation and apoptosis during myometrial maturation and the development of uterine leiomyomas in the rat. *Biol Reprod* **63**, 1322-1330.

Carlson, B. M. (1998). *Human embryology and developmental biology*, 2nd edn St. Louis, Missouri: Mosby.

Castro, A., Johnson, M. C., Anido, M., Cortinez, A., Gabler, F., and Vega, M. (2002). Role of nitric oxide and Bcl-2 family genes in the regulation of human endometrial apoptosis. *Fertil Steril* **78**, 587-595.

Chabbert-Buffet, N., Meduri, G., Bouchard, P., and Spitz, I. M. (2005). Selective progesterone receptor modulators and progesterone antagonists: mechanisms of action and clinical applications. *Hum Reprod Update* **11**, 293-307.

Chen-Leavy, S., and Cleary, M. L. (1990). Membrane topology of the Bcl-2 proto-oncogenic protein demonstrated in vitro. *J Biol Chem* **265**.

Clark, J. H., and Mani, S. K. (1994). Actions of ovarian steroid hormones, In The Physiology of Reproduction, E. Knobil, and J. D. Neill, eds. New York: Raven Press, Ltd.

Clark, J. H., and Markaverich, B. M. (1982). The agonist-antagonist properties of clomiphene: A review. *Pharmoc Theory* **15**.

Collins, J. A., Wrixon, W., James, L. B., and Wilson, E. H. (1983). Treatment-independent pregnancy among infertile couples. *N Engl J Med* **309**, 1201-1206.

Coppens, M. T., De Boever, J. G., Dhont, M. A., Serreyn, R. F., Vandekerckhove, D. A., and Roels, H. J. (1993). Topographical distribution of oestrogen and progesterone receptors in the human endometrium and Fallopian tube: An immunocytochemical study. *Histochem* **99**, 127-131.

Critchley, H. O., and Saunders, P. T. (2009). Hormone receptor dynamics in a receptive human endometrium. *Reprod Sci* **16**, 191-199.

Cummings, A. M., Perreault, S. D., and Harris, S. T. (1991). Validation of protocols for the assessment of maternally mediated toxicity during early pregnancy failure in the rat; Clomiphene Citrate. *Fundamentals in Applied Toxicology* **16**, 506-516.

Curtis, S. W., Clark, J., Myers, P., and Korach, K. S. (1999). Disruption of estrogen signalingdoes not prevent progesterone action in the estrogen receptor α knockout mouse uterus. *PNAS* **96**, 3646-3651.

Dai, D., Moulton, B. C., and Ogle, T. F. (2000). Regression of the decidualized mesometrium and decidual cell apoptosis are associated with a shift in expression of Bcl2 family members. *Biol Reprod* **63**, 188-195.

Daikoku, E., Ito, Y., and Otsuki, Y. (1998). The induction of apoptosis in ovaries and uteri of *bcl-2*-deficient mice. *Med Electron Microsc* **31**, 68-76.

De Falco, M., De Luca, L., Aconfora, F., Cavalloti, I., Cottone, G., Laforgia, V., De Luca, B., Baldi, A., and De Luca, A. (2001). Alteration of the Bcl-2:Bax ratio in the placenta as pregnancy proceeds. *Histochem J* **33**, 421-425.

Derman, S. G., and Adashi, E. Y. (1994). Adverse effects of fertility drugs. *Drug Safety* **11**, 408-421.

Develioglu, O. H., Hsiu, J.-G., Nikas, G., Toner, J. P., Oehninger, S., and Jones, H. W. (1999). Endometrial estrogen and progesterone receptor and pinopode expression in stimulated cycles of oocyte donors. *Fertil Steril* **71**, 1040-1047.

Dey, S. K., Lim, H., Das, S. K., Reese, J., Paria, B. C., Daikoku, T., and Wang, H. (2004). Molecular clues to implantation. *Endocr Rev* **25**, 341-373.

Drugbank (Acessed June 2009). www.drugbank.ca: Departments of Computing Science and Biological Sciences, University of Alberta

Dyer, S. J., Abrahams, N., Hoffman, M., and Van der Spuy, Z. M. (2002a). Infertility in South Africa: women's reproductive health knowledge and treatment-seeking behaviour for involuntary childlessness. *Hum Reprod* **17**, 1657-1662.

Dyer, S. J., Abrahams, N., Hoffman, M., and Van der Spuy, Z. M. (2002b). 'Men leave me as I cannot have children": women's experience with involuntary childlessness. *Hum Reprod* **17**, 1663-1668.

Dyer, S. J., Abrahams, N., Mokoena, N. E., Lombard, C. J., and Van der Spuy, Z. M. (2005). Psychological distress among women suffering from couple infertility in South Africa: a quantitative assessment. *Hum Reprod* **20**, 1938-1943.

Dyer, S. J., Abrahams, N., Mokoena, N. E., and van der Spuy, Z. M. (2004). 'You are a man because you have children': experiences, reproductive health knowledge and treatment-seeking behaviour among men suffering from couple infertility in South Africa. *Hum Reprod* **19**, 960-967.

Edwards, E. G. (1996). Time to revolutionize ovarian stimulation. *Hum Reprod* **11**, 917-919.

Enders, A. C., and Schlafke, S. (1967). A morphological analysis of the early implantation stages in the rat. *Am J Anat* **120**, 185-226.

Farnell, Y. Z., and Ing, N. H. (2003). Myometrial effects of selective estrogen receptor modulators on estradiol-responsive gene expression are gene and cell-specific. *J Steroid Biochem Mol Biol* **84**, 527-536.

Fritz, M. A., Holmes, R. T., and Keenan, E. J. (1991). Effect of clomiphene citrate treatment on endometrial estrogen and progesterone receptor induction in women. *Am J Obstet Gynecol* **165**, 177-185.

Galluzzi, L., Maiuri, M. C., Vitale, I., Zischka, H., Castedo, M., Zitvogel, L., and Kroemer, G. (2007). Cell death modalities: classification and pathophysiological implications. *Cell Death Differ* **14**, 1237-1243.

Garcia, E., Bouchard, P., De Brux, J., Berdah, J., Frydman, R., Schaison, G., Milgrom, E., and Perrot-Applanat, M. (2001). Use of immunocytochemistry of progesterone and estrogen for endometrial dating. *J Clin Endocrin Metab* **67**, 80-87.

Gazit, A., Livshitz, T., and Shani, J. (1986). Flouro-clomiphene and its synthetic precursors: synthesis and receptor binding. *Steroids* **48**, 73-84.

Gellersen, B., Fernandes, M. S., and Brosens, J. J. (2009). Non-genomic progesterone actions in female reproduction. *Hum Reprod Update* **15**, 119-138.

Glasser, S. R., Julian, J., Decker, G. L., Tang, J. P., and Carson, D. D. (1988). Development of morphological and functional polarity in primary cultures of immature rat uterine epithelial cells. *J Cell Biol* **107**, 2409-2423.

Goldman, J. M., Murr, A. S., and Cooper, R. L. (2007). The rodent estrous cycle: characterization of vaginal cytology and its utility in toxicological studies. *Birth Defects Res B Dev Reprod Toxicol* **80**, 84-97.

Graham, J. D., and Clarke, C. L. (1997). Physiological action of progesterone in target tissues. *Endocr Rev* **18**, 502-519.

Greenblatt, R. B., Rov, S., Mahesh, V. B., Barfield, W. E., and Jungck, E. C. (1961). Induction of ovulation. *Am J Obstet Gynecol* **84**, 900-912.

Gregory, C. W., Wilson, E. M., Apparao, K. B. C., Lininger, R. A., Meyer, W. R., Kowalik, A., Fritz, M. A., and Lessey, N. A. (2002). Steroid receptor coactivator expression throughout the menstrual cycle in normal and abnormal endometrium. *J Clin Endocrin Metab* **87**, 2960-2966.

Grese, T. A., Sluka, J. P., Bryant, H. U., Cullinan, G. J., Glasebrook, A. L., Jones, C. D., Matsumoto, K., Palkowits, A. D., Sato, M., Termine, J. D., Winter, M. A., Yang, N. N., and Dodge, J. A. (1997). Molecular determinants of tissue selectivity in estrogen receptor modulators. *PNAS* **94**, 14105-14110.

Harada, T., Kaponis, A., Iwabe, T., Taniguchi, F., Makrydimas, G., Sofikitis, N., Paschopoulos, M., Paraskevaidis, E., and Terakawa, N. (2004). Apoptosis in human endometrium and endometriosis. *Hum Reprod Update* **10**, 29-38.

Haskell, S. G. (2003). Selective estrogen receptor modulators. *Southern Medical Journal* **96**, 469-476.

Havelka, P., Oborna, I., Brezinova, J., and Lichnovsky, V. (2005). Apoptosis and expression of Bcl-2 in human endometrium in natural and artificial cycles. *Biomed Pap Med Fac Univ Palacky Olomouc Czech Repub* **149**, 303-307.

Hecht, B. R., Khan-Dawood, F. S., and Dawood, M. Y. (1989). Peri-implantation phase endometrial estrogen and progesterone receptors: effect of ovulation induction with clomiphene citrate. *Am J Obstet Gynecol* **161**, 1688-1693.

Hockenbery, D., Nuñez, G., Milliman, C., Schreiber, R. D., and Korsmeyer, S. J. (1990). Bcl-2 is an inner mitochondrial membrane protein that blocks programmed cell death. *Nature* **348**, 334-336.

Hollos, M. (2003). Profiles of infertility in Southern Nigeria: women's voices from Amakiri. *African Journal of Reproductive Health* **7**, 46-56.

Homburg, R. (2008). Oral agents for ovulation induction--clomiphene citrate versus aromatase inhibitors. *Hum Fertil (Camb)* **11**, 17-22.

Hosie, M., Terry, V., Shaw, T., Dwarte, D., and Murphy, C. R. (2000). Expression of glucosamine trisaccharides on the rat uterine surface is altered by clomiphene citrate. II. Combination with ovarian hormones. *Acta Histochem* **102**, 309-321.

Hosie, M. J. (1997) *Studies on the effects of clomiphene citrate on the morphology and ultrastructure of the rat uterus*, University of Sydney, Sydney.

Hosie, M. J., and Murphy, C. R. (1992). Clomiphene citrate alters surface ultrastructure of uterine luminal epithelial cells. *Acta Anat (Basel)* **145**, 175-178.

Hosie, M. J., and Murphy, C. R. (1995). A scanning and light microscope study comparing the effects of clomiphene citrate, estradiol 17-beta and progesterone on the structure of uterine luminal epithelial cells. *Eur J Morphol* **33**, 39-50.

Hosie, M. J., Shaw, T. J., Dwarte, D. M., and Murphy, C. R. (1999). Expression of glucosamine trisaccharides on the rat uterine surface is altered by clomiphene citrate. *Acta Histochem* **101**, 383-396.

Hosie, M. J., and Stewart, C. M. (2006). Apoptosis is not altered by clomiphene citrate in pseudopregnant rat uteri. *Acta Histochem* **108**, 105-116.

Hsu, S. Y., and Hsueh, A. J. W. (1998). A splicing variant of the Bcl-2 member bok with a truncated BH3 domain induces apoptosis but does not dimerize with antiapoptotic Bcl-2 proteins in vitro. *J Biol Chem* **273**, 30139-30146.

Hubbard, R. E., Pike, A. C. W., Brzozowski, A. M., Walton, J., Bonn, T., Gustafsson, J.-A., and Carlquist, M. (2000). Structural insight into the mechanisms of agonism and antagonism in oestrogen receptor molecules. *Eur J Cancer* **36**, S13-S23.

Huet, Y. M., and Dey, S. K. (1987). Role of early and late oestrogenic effects on implantation in the mouse. *J Reprod Fert* **81**, 453-458.

Ilesanmi, A. O., Hawkins, D. A., and Lessey, B. A. (1993). Immunohistochemical markers of uterine receptivity in the human endometrium. *Microsc Res Tech* **25**, 208-222.

Inbal, B., Bialik, S., Sabanay, I., Shani, G., and Kimchi, A. (2002). DAP kinase and DRP-1 mediate membrane blebbing and the formation of autophagic vesicles during programmed cell death. *J Cell Biol* **157**, 455-468.

Jin, Z., and El-Deiry, W. S. (2005). Overview of cell death signaling pathways. *Cancer Biol Ther* **4**, 139-163.

Jordan, V. C. (1984). Biochemical pharmacology of antiestrogen action. *Pharmoc Rev* **36**, 245-276.

Jordan, V. C., Gapstur, S., and Morrow, M. (2001). Selective estrogen receptor modulation and reduction in risk of breast cancer, osteoporosis and coronary heart disease. *J Nat Cancer Institute* **93**, 1449-1457.

Juries, B. (2005) *An exploratory study of involuntarily childless women's experience from potential parenthood to the acceptance of their non-parenthood status*, University of the Western Cape, Bellville.

Kaneko, Y., Lecce, L., and Murphy, C. R. (2009). Ovarian hormones regulate expression of the focal adhesion proteins, talin and paxillin, in rat uterine luminal but not glandular epithelial cells. *Histochem Cell Biol* **132**, 613-622.

Kerr, J. F., Wyllie, A. H., and Currie, A. R. (1972). Apoptosis: a basic biological phenomenon with wide-ranging implications in tissue kinetics. *Br J Cancer* **26**, 239-257.

Kierszenbaum, A. L. (2002). *Histology and cell biology: an introduction to pathology*, 1 edn St. Louis, Missouri: Mosby, Inc.

Korsmeyer, S. J., Shutter, J. R., Veis, D. J., Merry, D. E., and Oltvai, Z. N. (1993). Bcl-2/Bax: a rheostat that regulates an anti-oxidant pathway and cell death. *Semin Cancer Biol* **4**, 327-332.

Krzymowski, T., and Stefanczyk-Krzymowska, S. (2004). The oestrous cycle and early pregnancy - a new concept of local endocrine regulation. *Veterinary Journal* **168**, 285-296.

Kurita, T., Lee, K., Saunders, P. T. K., Cooke, P. S., Taylor, J. A., Lubahn, D. B., Zhao, C., Makela, S., Gustafsson, J. A., Dahiya, R., and Cunha, G. R. (2001). Regulation of progesterone receptors and decidualization in uterine stroma of the estrogen receptor-α knockout mouse. *Biol Reprod* **64**, 272-283.

Kurosawa, T., Hiroi, H., Momoeda, M., Inoue, S., and Taketani, Y. (2010). Clomiphene citrate elicits estrogen agonistic/antogonistic effects differentially via estrogen receptors α and β. *Endocrine Journal*.

Lai, M. D., Lee, L. R., Cheng, K. S., and Wing, L. Y. (2000). Expression of proliferating cell nuclear antigen in luminal epithelium during the growth and regression of rat uterus. *J Endocrinol* **166**, 87-93.

Larson, U. (2005). Research on infertility: which definition should we use? *Fertil Steril* **83**, 846-852.

Lee, K. Y., and DeMayo, F. J. (2004). Animal models of implantation (Review). *Reproduction* **128**, 679-695.

Ljungkvist, I. (1971a). Attachment reaction of rat uterine luminal epithelium. I. Gross and fine structure of the endometrium of the spayed, virgin rat. *Acta Soc Med Upsal* **76**, 91-109.

Ljungkvist, I. (1971b). Attachment reaction of the rat uterine luminal epithelium. II. The effect of progesterone on the morpholgy of the uterine glands and the luminal epithelium of the spayed, virgin rat. *Acta Soc Med Upsal* **76**, 110.

Ljungkvist, I. (1971c). Attachment reaction of the rat uterine luminal epithelium. The effect of estradiol, estrone and estriol on the morphology of the luminal epithelium of the spayed, virgin rat. *Acta Soc Med Upsal* **76**, 139-157.

Ljungkvist, I. (1972). Attachment reaction of rat uterine luminal epithelium IV. The cellular changes in the attachment reaction and its hormonal regulation. *Fertil Steril* **23**, 847-863.

Logeat, F., Sartor, P., Hai, M. T. V., and Milgrom, E. (1980). Local effect of the blastocyst on estrogen and progesterone receptors in the rat endometrium. *Science* **207**, 1083-1085.

Loke, Y. W., and King, A. (1995). *Human implantation: Cell biology and immunology*, 1 edn Cambridge: Cambridge University Press.

Long, J. A., and Evans, H. M. (1922). The oestrous cycle in the rat and its associated phenomena. *Mem Univ Calif* **6**.

Lowry, O. H., Roserbrough, N. J., A.L., F., and Randall, R. J. (1951). Protein measurement with the Folin phenol reagent. *Journal of Biological Chemistry* **193**, 265-275.

Lydon, J. P., DeMayo, F. J., Funk, C. R., Mani, S. K., Hughes, A. R., Montgomery, C. A., Jr., Shyamala, G., Conneely, O. M., and O'Malley, B. W. (1995). Mice lacking progesterone receptor exhibit pleiotropic reproductive abnormalities. *Genes Dev* **9**, 2266-2278.

Ma, W. G., Song, H., Das, S. K., Paria, B. C., and Dey, S. K. (2003). Estrogen is a critical determinant that specifies the duration of the window of uterine receptivity for implantation. *Proc Natl Acad Sci U S A* **100**, 2963-2968.

Mahajan, D. K., and London, S. N. (1997). Mifepristone (RU486): a review. *Fertil Steril* **68**, 967-976.

Majno, G., and Joris, I. (1995). Apoptosis, oncosis, and necrosis. An overview of cell death. *Am J Pathol* **146**, 3-15.

Maksem, J. A., Meiers, I., and Robboy, S. J. (2007). A primer of endometrial cytology with histological correlation. *Diagn Cytopathol* **35**, 817-844.

Mandl, A. M. (1951). The phases of the oestrous cycle in the adult white rat. *J Experimental Biology* **28**, 576-584.

Marcondes, F. K., Bianchi, F. J., and Tanno, A. P. (2002). Determination of the estrous cycle phases of rats: some helpful considerations. *Braz J Biol* **62**, 609-614.

McCormack, S. A., and Glasser, S. R. (1980). Differential response of individual uterine cell types from immature rats treated with estradiol. *Endocrinology* **106**, 1634-1649.

Medh, R. D., and Thompson, E. B. (2000). Hormonal regulation of physiological cell turnover and apoptosis. *Cell Tissue Res* **301**, 101-124.

Mereseman, G. F., Augé, L., Barañao, R. I., Lombardi, E., Tesone, M., and Sueldo, C. (2002). Oral contraceptives suppress cell proliferation and enhance apoptosis of eutopic endometrial tissue from patients with endometriosis. *Fertil Steril* **77**, 1141-1147.

Mereseman, G. F., Vighi, S., Buquet, R. A., Contreras-Ortiz, O., Tesone, M., and Rumi, L. S. (2000). Apoptosis and expression of Bcl-2 and Bax in eutopic endometrium from women with endometriosis. *Fertil Steril* **74**, 760-766.

Motseki, L. (2004) *Anthropometric measurements and biochemical parameters in black women in the unit for reproductive care at Universitas Hospital, Bloemfontein*, University of the Free State, Bloemfontein.

Murata, T., and Higuchi, T. (2003). Progesterone receptor mRNA levels during pregnancy, labor, lactation and the estrous cycle in rat uterus. *J Reprod Dev* **49**, 425-432.

Murphy, C. R. (2004). Uterine receptivity and the plasma membrane transformation. *Cell Res* **14**, 259-267.

Murphy, C. R., and Rogers, A. W. (1981). Effects of ovarian hormones on cell membranes in the rat uterus. III. The surface carbohydrates at the apex of the luminal epithelium. *Cell Biophysics* **3**, 305-320.

Murphy, C. R., and Shaw, T. J. (1994). Plasma membrane transformation: a common response of uterine epithelial cells during the peri-implantation period. *Cell Biol Int* **18**, 1115-1128.

Newberne, J. W., Kuhn, W. L., and Elsea, J. R. (1966). Toxicologic studies on clomiphene. *Toxicology and Applied Pharmacology* **9**, 44-56.

Nisolle, M., Casanas-Roux, F., Wyns, C., de Menten, Y., Mathieu, P.-E., and Donnez, J. (1994). Immunohistochemical analysis of estrogen and progesterone receptors in endometrium and peritoneal endometriosis: A new quantitative method. *Fertil Steril* **62**, 751-759.

Obrero, M., Yu, D. V., and Shapiro, D. J. (2002). Estrogen receptor-dependent and estrogen receptor-independent pathways for tamoxifen and 4-hydroxytamoxifen-induced programmed cell death. *J Biol Chem* **277**, 45695-45703.

Ogle, T. F. (2002). Progesterone-action in the decidual mesometrium of pregnancy. *Steroids* **67**, 1-14.

Ohno, Y., and Fujimoto, Y. (1998). Endometrial oestrogen and progesterone receptors and their relationship to sonographic appearance of the endometrium. *Hum Reprod Update* **4**, 560-564.

Ohta, Y., Sato, T., and Iguchi, T. (1993). Immunocytochemical localization of progesterone receptor in the reproductive tract of adult female rats. *Biol Reprod* **48**, 205-213.

Oltvai, Z. N., and Korsmeyer, S. J. (1994). Checkpoints of dueling dimers foil cell death. *Cell* **79**, 189-192.

Oltvai, Z. N., Milliman, C. L., and Korsmeyer, S. J. (1993). Bcl-2 heterodimerises in vivo with a conserved homologue, Bax, that accelerates programmed cell death. *Cell* **74**, 609-619.

Otsuki, Y., Misaki, O., Sugimoto, O., Ito, Y., Tsujimoto, Y., and Akao, Y. (1994). Cyclic Bcl-2 expression in human uterine endometrium during menstrual cycle. *The Lancet* **344**, 28-29.

Palomino, W. A., Fuentes, A., Gonzalez, R. R., Gabler, F., Boric, M. A., Vega, M., and Devoto, L. (2005). Differential expression of endometrial integrins and progesterone receptor during the window of implantation in normo-ovulatory women treated with clomiphene citrate. *Fertil Steril* **83**, 587-593.

Parczyk, K., Madjno, R., Michna, H., Nishino, Y., and Schneider, M. R. (1997). Progesterone receptor repression by estrogens in rat uterine epithelial cells. *J Steroid Biochem Mol Biol* **63**, 309-316.

Paria, B. C., Song, H., and Dey, S. K. (2001). Implantation: molecualr basis of embryo-uterine dialogue. *Int J Dev Biol* **45**, 597-605.

Paria, B. C., Tan, J., Lubahn, D. B., Dey, S. K., and Das, S. K. (1999). Uterine decidual response occurs in estrogen receptor-alpha-deficient mice. *Endocrinology* **140**, 2704-2710.

Pecci, A., Scholz, A., Pelster, D., and Beato, M. (1997). Progestins prevent apoptosis in a rat endometrial cell line and increase the ratio of bcl-X_L to bcl-X_S. *J Biol Chem* **272**, 11791-11798.

Peters, A. J., Wentz, A. C., Kazer, R. R., Jeyendran, R. S., and Chatterton, R. T., Jr. (1995). Estrogenic and antiestrogenic activities of anordiol: a comparison of uterine and vaginal responses with those of clomiphene citrate. *Contraception* **52**, 195-202.

Pike, A. C., Brzozowski, A. M., and Hubbard, R. E. (2000). A structural biologist's view of the oestrogen receptor. *J Steroid Biochem Mol Biol* **74**, 261-268.

Pike, A. C., Brzozowski, A. M., Hubbard, R. E., Bonn, T., Thorsell, A. G., Engstrom, O., Ljunggren, J., Gustafsson, J. A., and Carlquist, M. (1999). Structure of the ligand-binding domain of oestrogen receptor beta in the presence of a partial agonist and a full antagonist. *EMBO J* **18**, 4608-4618.

Pinter, J. H., Deep, C., and Park-Sarge, O.-K. (1996). Progesterone receptors: expression and regulation in the mammalian ovary. *Clin Obstetrics and Gynecology* **39**, 424-435.

Psychoyos, A. (1966). Recent research on egg implantation, In Ciba foundation study group on egg implantation, G. E. Wolstenholm, and O'Connor, eds. 4-28.

Psychoyos, A. (1967). The hormonal interplay controlling egg implantation in the rat, In Avances in Reproductive Physiology, A. McLaren, ed. London: Logos Press, pp. 256.

Psychoyos, A. (1969). Hormonal requirements for egg-implantation, In Advances in the Biosciences, G. Raspe, ed.: Pergamon, pp. 275.

Psychoyos, A. (1973). Hormonal control of ovoimplantation. *Vitams Horm* **31**, 201-256.

Reese, J., Das, S. K., Paria, B. C., Lim, H., Song, H., Matsumoto, H., Knudtson, K. L., DuBois, R. N., and Dey, S. K. (2001). Global gene expression analysis to identify molecular markers of uterine receptivity and embryo implantation. *J Biol Chem* **256**, 44137-44145.

Rider, V., McRae, A., Heap, R. B., and Feinstein, A. (1985). Passive immunization against progesterone inhibits endometrial sensitization in pseudopregnant mice and has antifertility effects in pregnant mice which are reversible by steroid treatment. *J Endocrinol* **104**, 153-158.

Rogers, P. A. W., Polson, D., Murphy, C. R., Hosie, M. J., Susil, B., and Leoni, M. (1991). Correlation of endometrial histology, morphometry and ultrasound appearance following different stimulation protocols for in vitro fertilization. *Fertil Steril* **55**.

Sasson, S., and Notides, A. C. (1982). The inhibition of the estrogen receptor's positive cooperative [^{3}H]estradiol binding by the antogonist, clomiphene. *J Biol Chem* **257**, 11540-11545.

Sato, T., Fukazawa, Y., Kojima, H., Enari, M., Iguchi, T., and Ohta, Y. (1997). Apoptotic cell death during the estrous cycle in the rat uterus and vagina. *Anat Rec* **248**, 76-83.

Sato, T., Fukazawa, Y., Kojima, H., Ohta, Y., and Iguchi, T. (2003). Multiple mechanisms are involved in apoptotic cell death in the mouse uterus and vagina after ovariectomy. *Reprod Toxicology* **17**, 289-297.

Scholtz, K. E., Penny, C. B., and Hosie, M. J. (2008). A high resolution SEM study of the effects of RU486, used as a postcoital contraceptive, on the rat uterus during early pregnancy. *Cell Biol Int* **32**, 436-446.

Sexton, M. J., and Gherman, R. B. (2001). Selective estrogen receptor modulators: the ideal estrogen replacement? *Prim Care Update Ob Gyns* **8**, 25-30.

Shao, R., Nutu, M., Weijdegard, B., Egecioglu, E., Fernandez-Rodriguez, J., Karlsson-Lindahl, L., Gemzell-Danielsson, K., Bergh, C., and Billig, H. (2009). Clomiphene citrate causes aberrant tubal apoptosis and estrogen receptor activation in rat fallopian tube: implications for tubal ectopic pregnancy. *Biol Reprod* **80**, 1262-1271.

Shao, R., Weijdegard, B., Ljungstrom, K., Friberg, A., Zhu, C., Wang, X., Zhu, Y., Fernandez-Rodriguez, J., Egecioglu, E., Rung, E., and Billig, H. (2006). Nuclear progesterone receptor A and B isoforms in mouse fallopian tube and uterus: implications for expression, regulation and cellular function. *Am J Physiol Endocrinol Metab* **291**, 59-72.

Sharara, F. I., and McClamrock, H. D. (2000). Differences in in vitro fertilization (IVF) outcome between white and black women in an inner city, university-based IVF program. *Fertil Steril* **73**, 1170-1173.

Shaw, T. J., and Murphy, C. R. (1996). Leucocyte binding to the uterine epithelial cell surface during lectin-induced decidualization. *Cell Biol Int* **20**, 717-722.

Shelly, W., Draper, M. W., Krishnan, V., Wong, M., and Jaffe, R. B. (2008). Selective estrogen receptor modulators: an update on recent clinical findings. *Obstet Gynecol Surv* **63**, 163-181.

Shi, S.-R., Imam, S. A., Young, L., Cote, R. J., and Taylor, C. R. (1995). Antigen retrieval immunohistochemistry under the influence of pH using monoclonal antibodies. *J Histochem Cytochem* **43**, 193-201.

Smith, M. S., Freeman, M. E., and Neill, J. D. (1974). The Control of Progesterone Secretion During the Estrous Cycle and Early Pseudopregnancy in the Rat: Prolactin, Gonadotropin and Steroid Levels Associated with Rescue of the Corpus Luteum of Pseudopregnancy. *Endocr* **96**, 219-226

Song, H., Han, K., and Lim, H. (2007). Progesterone supplementation extends uterine receptivity for blastocyst implantation in mice. *Reproduction* **133**, 487-493.

Stevens, A., and Louw, J. (1992). *Histology* London: Gower Medical Publishing.

Sun, Y., and Peng, Z. L. (2009). Programmed cell death and cancer. *Postgrad Med J* **85**, 134-140.

Tan, J., Paria, B. C., Dey, S. K., and Das, S. K. (1999). Differential uterine expression of estrogen and progesterone receptors correlates with uterine preparation for implantation and decidualization in the mouse. *Endocrinology* **140**, 5310-5321.

Tao, X.-J., Tilly, J. I., Maravei, D. V., L., S. J., Krajewski, S., Reed, J. C., Tilly, J. L., and Isaacson, K. B. (1997). Diffential expression of members of the Bcl-2 gene family in proliferative and secretory human endometrium: glandular epithelial cell apoptosis is associated with increased expression of Bax *Clinical Endocrinology and Metabolism* **82**, 2738-2746.

Tassell, W., Slater, M., Barden, J. A., and Murphy, C. R. (2000). Endometrial cell death during early pregnancy in the rat. *Histochem J* **32**, 373-379.

Tessier, C., Deb, S., Prigent-Tessier, A., Ferguson-Gottschall, S., Gibori, G. B., Shiu, R. P., and Gibori, G. (2000). Estrogen receptors alpha and beta in rat decidua cells: cell-specific expression and differential regulation by steroid hormones and prolactin. *Endocrinology* **141**, 3842-3851.

Thatte, U., and Dahanukar, S. (1997). Apoptosis – clinical relevance and pharmacological manipulation. *Drugs* **54**, 511-532.

Theron, K. E. (2010) *The effects of RU486, used as a postcoital contraceptive, on the rat uterus during early pregnancy*, University of the Witwatersrand, Johannesburg.

Tibbetts, T. A., Mendoza-Meneses, M., O'Malley, B. W., and Conneely, O. M. (1998). Mutual and intercompartmental regulation of estrogen receptor and progesterone receptor expression in the mouse uterus. *Biol Reprod* **59**, 1143-1152.

Tran, D. Q., Jin, L., Chen, J., McLachlan, J. A., and Arnold, S. F. (1997). Evaluation of clinical and environmental anti-estrogens with human estrogen receptor expressed in *Saccharomyces cerevisiae*: A novel role for ABC-cassette transporters in mediating anti-estrogenic activity. *Biochemical and Biophysical Research Communications* **235**, 669-674.

Van Cruchten, S., and Van Den Broeck, W. (2002). Morphological and biochemical aspects of apoptosis, oncosis and necrosis. *Anat Histol Embryol* **31**, 214-223.

Vaux, D. L., and Strasser, A. (1996). The molecular biology of apoptosis. *PNAS* **93**, 2239-2244.

Viegas, L. R., Hoijman, E., Beato, M., and Pecci, A. (2008). Mechanisms involved in tissue-specific apoptosis regulated by glucocorticoids *J Steroid Biochem Mol Biol* **109**, 273-278.

Vigano, P., Somigliana, E., Mangioni, S., Vignali, M., Vignali, M., and Di Blasio, A. M. (2002). Expression of interleukin-10 and its receptor is up-regulated in early pregnant versus cycling human endometrium. *J Clin Endocrin Metab* **87**, 5730-5736.

Wang, H., and Dey, S. K. (2006). Roadmap to embryo implantation: clues from mouse models. *Nat Rev Genet* **7**, 185-199.

Wei, P., Jin, X., Tao, S. X., Han, C. S., and Liu, Y. X. (2005). Fas, FasL, Bcl-2, and Bax in the endometrium of rhesus monkey during the menstrual cycle. *Mol Reprod Dev* **70**, 478-484.

Westwood, F. R. (2008). The female rat reproductive cycle: a practical histological guide to staging. *Toxicol Pathol* **36**, 375-384.

Wilcox, A. J., Baird, D. D., and Weinberg, C. R. (1999). Time of implantation of the conceptus and loss of pregnancy. *N Engl J Med* **340**, 1796-1799.

Williams, G. T., and Smith, C. A. (1993). Molecular regulation of apoptosis: genetic controls on cell death. *Cell* **74**, 777-779.

Wilson, I., and Gamble, M. (2002). Ch 8. The Hematoxylins and Eosin, In Theory and practice of histological techniques, J. D. Bancroft, and M. Gamble, eds. London: Churchill-Livingstone, pp. 125-138.

Wood, G. A., Fata, J. E., Watson, K. L., and Khokha, R. (2007). Circulating hormones and estrous stage predict cellular and stromal remodeling in murine uterus. *Reproduction* **133**, 1035-1044.

Wright, V. C., Chang, J., Jeng, G., Chen, M., and Macaluso, M. (2007). Assisted reproductive technology surveillance—United States, 2004. *MMWR Surveill Summ* **56**, 1-22.

Wyllie, A. H. (1997). Apoptosis: an overview. *Br Med J* **53**, 451-465.

Yang, E., and Korsmeyer, S. J. (1996). Molecular thanatopsis: A discourse on the Bcl-2 family and cell death. *Blood* **88**, 386-401.

Yang, E., Zha, J., Jockel, J., Boise, L. H., Thompson, C. B., and Korsmeyer, S. J. (1995). Bad, a heterodimeric partner for Bcl-x_L and Bcl-2, displaces Bax and promotes cell death. *Cell* **80**, 285-291.

Yin, X.-M., Oltvai, Z. N., and Korsmeyer, S. J. (1994). BH1 and BH2 domains of Bcl-2 are required for inhibition of apoptosis and heterodimerization with Bax. *Nature* **369**, 321-323.

Young, B., and Heath, J. W. (2002). *Wheater's Functional Histology - A text and colour atlas*, 4th edn Edinburgh: Churchill Livingstone.

Young, R. L., Goldzieher, J. W., Chakraborty, P. K., Panko, W. B., and Bridges, C. N. (1991). Qualitative differences in estrogenic effects of clomiphene and zuclomiphene. *International Journal of Fertility* **36**, 291-295.

Zegers-Hochschild, F., Adamson, G. D., de Mouzon, J., Ishihara, O., Mansour, R., Nygren, K., Sullivan, E., and Vanderpoel, S. (2009). International committee for monitoring assisted reproductive technology (ICMART) and the World Health Organization (WHO) revised glossary of ART termiology, 2009. *Fertil Steril* **92**, 1520-1524.

APPENDIX A: SOLUTIONS

A. 1. General solutions

Paraformaldehyde, 4%

Paraformaldehyde	4 g
PBS Buffer	100 ml

Heat to 60 ºC

Add 4% NaOH drop-wise, until the 4% paraformaldehyde has cleared.

pH the 4% paraformaldehyde to pH 7.4.

Phosphate buffered saline, pH 7.4

NaCl	8.0 g
KCl	0.2 g
Na_2HPO_4	1.44 g
KH_2PO_4	0.24 g
Distilled water	800 ml

Adjust to pH 7.4 with HCl

Make up to 1 litre with distilled water.

0.01 M Phosphate buffered saline, pH 7.1-7.2

NaCl	9.0 g
$Na_2HPO_4.12H_2O$	2.60 g
$NaH_2PO_4.2H_2O$	0.29 g
Distilled water	1 000 ml

pH to between 7.1 and 7.2

Store: maximum 1 week at room temperature.

Saline (0.9% NaCl)

NaCl	9.0 g
Distilled water	1000 ml

Tris buffered saline (TBS), pH 7.6

Tris Base	6.06 g
NaCl	8.77 g
Distilled water	1 000 ml

Use HCl to lower pH to 7.6

Tris buffered saline and 0.05% Tween 20 (TBST)

TBS, pH 7.6	200 ml
Tween 20	100 µl

A.2. Solutions for haematoxylin and eosin staining

Modified Mayer's haematoxylin

Haematoxylin	4.0 g
Distilled water	1 000 ml
Sodium Iodate	0.3 g
Aluminium Potassium sulphate	50.0 g
Citric Acid	1.5 g
Chloral Hydrate	75.0 g

Dissolve alum in water (do not heat). Add, in order, haematoxylin, iodate, citric acid and chloral hydrate. Filter haematoxylin solution through coarse filter paper.

Eosin stock solution

Eosin	8.0 g
Erythrosin	2.0 g
Distilled water	1 000 ml

Eosin working solution

Stock Eosin	250 ml
Distilled water	750 ml
Calcium Chloride	20 g

A.3. Solutions for immunohistochemistry

3,3' Diaminobenzidine tetrahydrochloride (DAB)

Option 1: **0.05% DAB ($^{w}/_{v}$) - BDH Laboratories**

BDH Laboratory supplies, Poole, England, 1330332P

- Weigh 1 mg DAB into a bijou bottle.
- At the start of the day, when one is using the secondary antibody, leave a measuring cylinder with 29 ml distilled water at 4 °C.
- Just before use, add 2 ml Tris-HCl, pH 7.6 to the DAB in the Bijou bottles.
- Then add 1 ml of 30% perhydrol (Merck, Germany) to the cold distilled water to make a 1% solution, mix well.
- Add 20 µl of the 1% perhydrol to the DAB solution
    - Mix on whirlimix
    - Pipette 30 µl into each well
    - Time individually for 5 minutes
- Final concentration: 0.05% ($^{w}/_{v}$) DAB diluted in Tris-HCl with 0.01% Perhydrol

Option 2: **DAB- Dako Kit**

Dako Ark (Animal Research Kit), Peroxidase

Dako Cytomation, CA, USA, # K3955

To mix: 1 ml buffered substrate (bottle 5)
Add 1 drop DAB and chromagen (bottle 6)
Mix well

Option 3: **DAB - Roche Kit**

DAB substrate, Roche, Germany, 1 718 096

Add 1 part DAB/metal concentrate (10x concentration)

To 9 parts Peroxide Buffer

(i.e. 1/10 dilution)

Diluent for anti-sera

Tris-saline	100 ml	
Sodium azide	0.25 g	(Add in fume hood)
Bovine serum albumin	5 mg	
Thyroglobulin	5 mg	
EDTA	40 mg	
Swine serum	1 ml	

Heat induced antigen retrieval (HIAR)

Option 1: **Citrate buffer, pH 6.0**

(10 mM citric acid, 0.05% tween-20)

Citric acid (anhydrous)	1.92 g
(Or citric acid monohydrate	2.10 g)
Distilled Water	1 000 ml

Mix to dissolve.

Adjust to pH 6.0 with 1 M NaOH.

Add 0.5 ml Tween-20 and mix well.

Store: Room temperature for 3 months, or longer in fridge.

Note: This starts with a very low pH

Therefore, add 800 ml water, pH to 6.0 and make up to 1 000 ml.

Then add Tween-20.

Option2: **EDTA buffer, pH 8.0**

(1 mM EDTA, 0.05% tween-20)

EDTA	0.37 g
Distilled Water	1 000 ml

Mix to dissolve.

Adjust to pH 8.0 with 1N NaOH.

Add 0.5 ml Tween-20 and mix well.

Store: Room temperature for 3 months, or longer in fridge.

Note: This buffer often gives high background, so primary antibody can often be highly diluted. Is useful for low affinity antibodies or when tissue antigens are not intense.

Option 3: **Tris buffer, pH 10.0**

(10 mM Tris base, 0.05% tween-20)

Tris Base	1.21 g
Distilled Water	1 000 ml

Mix to dissolve.

Adjust to pH 10.0 with 1 M NaOH.

Add 0.5 ml Tween-20 and mix well.

Store: Room temperature for 3 months, or longer in fridge.

Note: Method sometimes causes tissue damage or sections to detach from slides. This may be due to the high pH.

Option 4: **Tris-EDTA buffer, pH 9.0**

(10 mM Tris base, 1 mM EDTA, 0.05% tween-20)

Tris Base	1.21 g
EDTA	0.37 g
Distilled Water	1 000 ml

Mix to dissolve. pH is usually at 9.0.

Add 0.5 ml Tween-20 and mix well.

Store: Room temperature for 3 months, or longer in fridge.

Note: This buffer often gives high background, so primary antibody can often be highly diluted. It is useful for low affinity antibodies or when tissue antigens are not intense

1% Peroxide in PBS

Perhydrol (30%)	1 ml
PBS	30 ml

Store at 4ºC for up to 3 months.

Serum block - 1.0% goat serum

goat serum	100 µl
PBS	9.9 ml

A.4. Solutions for the Lowry-Folin method of protein determination

2 mg/ml BSA made up in PBS

BSA	0.2 g
PBS	100 ml

1% Copper sulphate

$CuSO_4.5H_2O$	0.1 g
Distilled water	10 ml

Folin-Ciocalteu's phenol reagent (Sigma, F 9252)

Folin-Ciocalteu's reagent diluted 1:4 in dH_2O

dilute just before use

2% Sodium carbonate in 0.1M NaOH

Na_2CO_3	2 g
NaOH (0.1 M)	100 ml

2% Sodium potassium tartrate

$NaKC_4H_4O_6.4H_2O$	0.2 g
Distilled water	10 ml

A.5. Solutions for ELISA

Block (0.1% BSA in PBS)

BSA	0.1 g
PBS	100 ml

0.5 M Sulphuric acid (1 N H_2SO_4)

H_2SO_4	2.7 ml
Distilled water	100 ml

APPENDIX B: RECIPES

B.1. Preparation of 3-aminopropyltriehoxysilane (APES) coated slides

1. Wash slides in detergent overnight.
2. Wash slides in hot running tap water for 30 mins.
3. Wash slides in distilled water, 2 x 5mins.
4. Wash slides in 95% alcohol, 2 x 5 mins.
5. Air dry for 10 mins.
6. Immerse in freshly prepared 2% silane in acetone for 30 mins.
   300 ml silane is sufficient for 200 slides
   add 6 ml of 3-aminopropyltriehoxysilane (Sigma, A-3648) to 294 ml acetone
7. Dip in acetone 1 – 2 times.
8. Wash in distilled water twice.
9. Dry overnight at 42 ºC.
10. Store at room temperature.

B.2. Haematoxylin and eosin staining

Method

1. Dewax sections, 2 x 5 mins, xylene
2. Rehydrate sections, absolute alcohol, 2 x 2 mins
   95% alcohol, 2 mins
3. Rinse in running tap water
4. Stain in Haematoxylin, 5 mins
5. Blue in running tap water
6. Dip 2-3 times in acid alcohol
7. Rinse in tap water
8. Stain in Eosin, 1 min
9. Rinse in tap water
10. Dehydrate and clear sections,
    95% alcohol, 2 mins
    absolute alcohol, 2 x 2 mins
    xylene, 2 x 5 mins
11. Mount in Entellen and view

Results

Nuclei	Blue
Erythrocytes	Orange
Other Tissue	Pink

B.3. Lowry-Folin method for protein determination

Reagent A

50 ml of 2% Sodium Carbonate in 0.1 M NaOH

0.5 ml of 1% Copper Sulphate

0.5 ml of 2% Sodium Potassium Tartrate

Make up just before use

Reagent B

Folin-Ciocalteu's phenol Reagent (Sigma, F 9252) diluted 1:4 in dH_2O

dilute just before use

Standard stock solution

2 mg/ml BSA stock made up in PBS.

Table B.3.1. Dilutions of BSA to make up a protein concentration gradient

[BSA] (µg/ml)	Vol (BSA)	Vol (PBS)
2 000	50 µl stock	0
1 000	50 µl (2 000)	50 µl
500	50 µl (1 000)	50 µl
250	50 µl (500)	50 µl
125	50 µl (250)	50 µl
62.5	50 µl (125)	50 µl
31.25	5 0µl (62.5)	50 µl
0	0	50 µl

Method

Using the ELISA plates, each well contained, in order:

1. 50 µl of sample
2. 200 µl Reagent A → leave for 10 mins (shake)
3. 50 µl Reagent B → leave for 30 mins (shake)
4. Read absorbance at 690 nm.

APPENDIX C– OPTIMISATION OF METHODS:

IMMUNOHISTOCHEMISTRY (IHC);

ENZYME LINKED IMMUNOSORBENT ASSAY (ELISA)

C.1. Optimisation of IHC against PR, Bcl-2 and Bax

Figure C.1.1. Flow diagram showing optimisation of primary antibody using Santa Cruz and Dako antibodies

Sections (4 μm) on APES slides
pregnant uterus (for PR) or colon (for Bcl-2 and Bax)
Dewax and rehydrate
Aspirate excess liquid

↓

Mark with Dako pen

↓

PBS wash, 3 x 2 mins

↓

Quench endogenous peroxidase activity
1% H_20_2 in PBS, 10 mins

↓

PBS wash, 2 x 5mins

↓

Serum block, 20 mins

The serum for blocking was made up as follows:

Primary antibody	**Manufacturer of primary**	**Serum used**
Anti-PR and anti-Bax	Santa Cruz	1% horse serum in PBS
Anti-Bcl-2	Santa Cruz	1% goat serum in PBS
Anti-PR, anti-Bcl-2 and anti-Bax	Dako	1% goat serum in PBS

The serum used was based upon the animal in which the secondary antibody was raised. Therefore, since the Santa Cruz secondary for Bax and PR were raised in donkey, horse serum was used to block the sections at this step. Similarly, since the secondary for the Dako antibodies and the Bcl-2 from Santa Cruz were raised in goat, goat serum was used to block at this step.

↓

Aspirate excess liquid

↓

Primary antibody made up in diluent (see appendix A)
4 °C, overnight, humidified chamber

↓

↓

Primary antibodies were used as follows:

Primary antibody	Manufacturer	Dilutions
Anti-PR (rabbit polyclonal, C19)	Santa Cruz, sc-538	1/100; 1/200; 1/400; 1/800; 1/1600; diluent only
Anti-PR (rabbit polyclonal)	Dako, A-0098	1/50; 1/100; 1/200; diluent only
Anti-Bcl-2 (mouse monoclonal, C2)	Santa Cruz, sc-7382	1/100; 1/250; 1/500; 1/800; 1/1000, diluent only
Anti-Bcl-2 (mouse monoclonal)	Dako, M-0887	1/25; 1/50; 1/100; diluent only
Anti-Bax (rabbit polyclonal, P19)	Santa Cruz, sc-526	1/100; 1/200; 1/400; 1/800; 1/1600; diluent only
Anti-Bax (rabbit polyclonal)	Dako, A-3533	1/50; 1/100; 1/200; diluent only

↓

Rinse with PBS
Wash PBS, 2 x 2mins

↓

Secondary antibody

↓

The sections were then incubated with secondary antibody as follows:

Primary antibody	From	Secondary antibody used	From	Dilute	Diluent used	Time
Anti-PR, Anti-Bax	Santa Cruz	Anti-rabbit (donkey)	Santa Cruz, sc-2313	1/500	1% horse serum in PBS	30 mins
Anti-PR, Anti-Bax	Dako	Anti-rabbit (goat)	Dako, P-0448	1/500	PBS	1 hour
Anti-Bcl-2	Santa Cruz	Anti-mouse (goat)	Santa Cruz, sc-2005	1/500	1% goat serum in PBS	30 mins
Anti-Bcl-2	Dako	Anti-mouse (goat)	Dako, P-0447	1/500	PBS	1 hour

The above table shows the combination of primary and secondary antibodies. It also indicates the diluent for the secondary antibodies, and incubation times for the secondary antibodies. All of the secondary antibodies were conjugated with horse radish peroxidase (HRP). All incubations were done at room temperature.

↓

Rinse with PBS
Wash PBS, 2 x 2mins

↓

DAB, 5 mins

↓

Rinse with dH_20
Wash with dH_20, 1 x 2 mins

↓

Dehydrate, clear and mount

Figure C.1.2. Flow diagram showing optimisation of different DABs

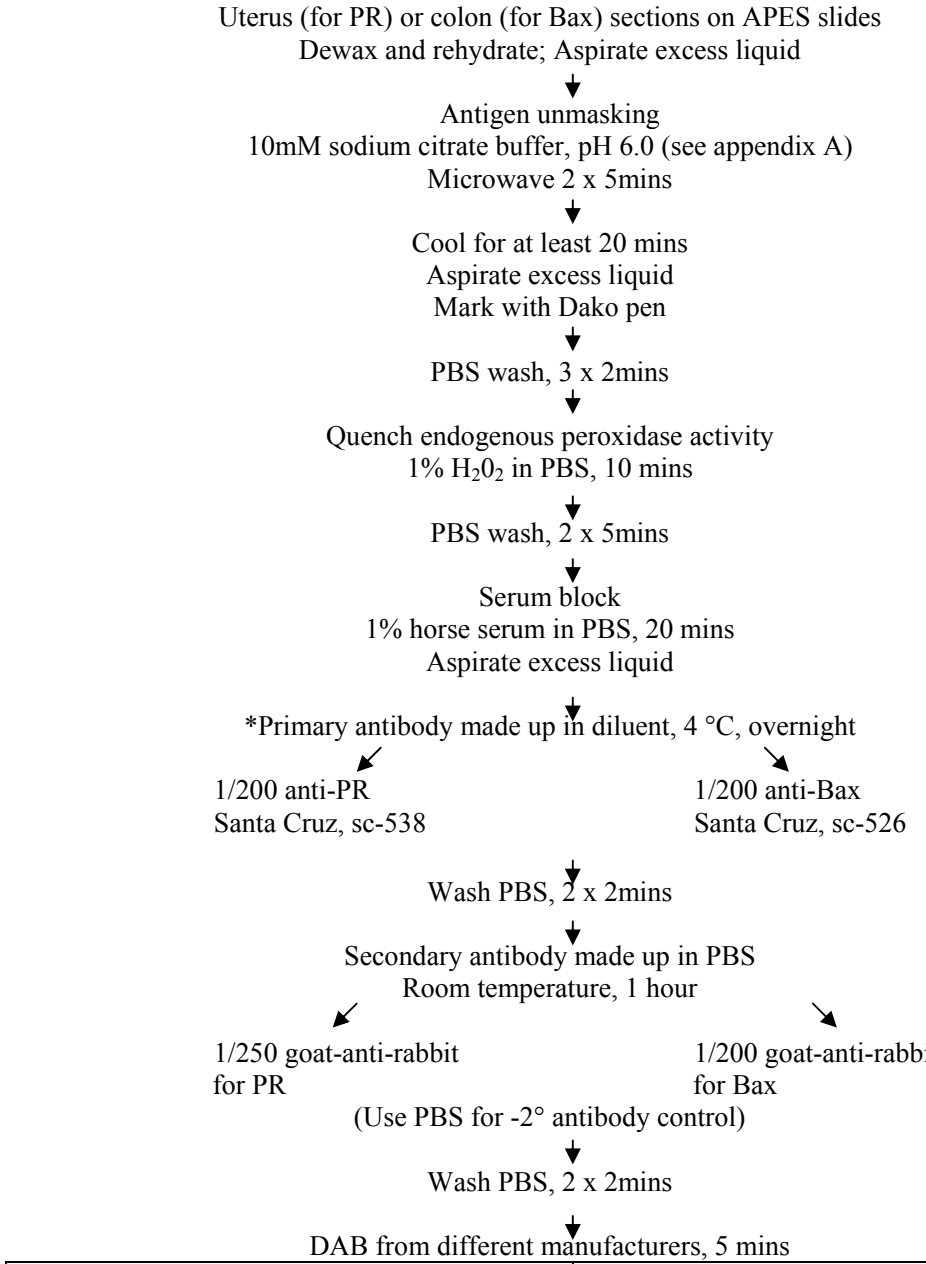

Manufacturer	**Method to make up DAB**
0.05% DAB ($^{w}/_{v}$) , BDH Laboratory supplies, Poole, England, 1330332P	0.05% ($^{w}/_{v}$) DAB diluted in Tris-HCl, pH 7.6 with 0.01% Perhydrol (see appendix)
Dako Ark (Animal Research Kit), Peroxidase, Dako Cytomation, CA, USA, # K3955	1 ml buffered substrate (bottle 5), add 1 drop DAB and chromagen (bottle 6). Mix well
Roche Kit, DAB substrate, Roche, Germany, 1 718 096	Add 1 part DAB/metal concentrate (10x concentration) to 9 parts Peroxide Buffer (i.e. 1/10 dilution)

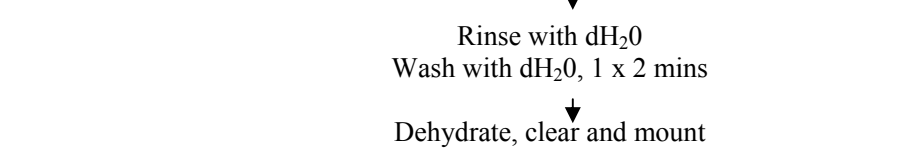

Figure C.1.3. Flow diagram showing IHC using different antigen retrieval buffers, and Dako antibodies against Bax, Bcl-2 and PR

Uterus sections (4 μm) on APES slides
Dewax and rehydrate; Aspirate excess liquid

↓

Antigen unmasking

Antigen retrieval buffer	Composition of buffer
Citrate buffer, pH 6.0	10 mM Citric acid, 0.05% Tween-20
EDTA buffer, pH 8.0	1 mM EDTA, 0.05% Tween-20
Tris-EDTA buffer, pH 9.0	10 mM Tris base, 1 mM EDTA, 0.05% Tween-20
Tris buffer, pH 10.0	10 mM Tris base, 0.05%Tween-20

Slides placed in container with unmasking buffer,
Microwaved at 720 W, 2 x 10 mins
Left to cool for 20 mins

↓

Aspirate excess liquid
Mark with Dako pen

↓

PBS wash, 3 x 2 mins

↓

Quench endogenous peroxidase activity
1% H_20_2 in PBS, 10 mins

↓

PBS wash, 2 x 5 mins

↓

Serum block
1% goat serum in PBS, 20 mins
Aspirate excess liquid

↓

Primary antibody made up in diluent, 4°C, overnight

Primary antibody	Manufacturer	Dilution
Anti-PR	Dako, A-0098	1/25, 1/50
Anti-Bcl-2	Dako, M-0887	1/50, 1/100
Anti-Bax	Dako, A-3533)	1/50, 1/100

↓

Wash PBS, 2 x 2mins

↓

Secondary antibody made up in PBS
Room temperature, 1 hour

↙ ↘

1/250 goat-anti-rabbit
For PR and Bax

1/250 goat-anti-mouse
for Bcl-2

(Use PBS for -2° antibody control)

↓

Rinse with PBS
Wash PBS, 2 x 2mins

↓

DAB (Roche, 130332P), 5 mins

↓

Rinse with dH_20
Wash with dH_20, 1 x 2 mins

↓

Dehydrate, clear and mount

Figure C.1.4. Flow diagram showing IHC with different concentrations of Primary antibodies against Bax, Bcl-2 and PR

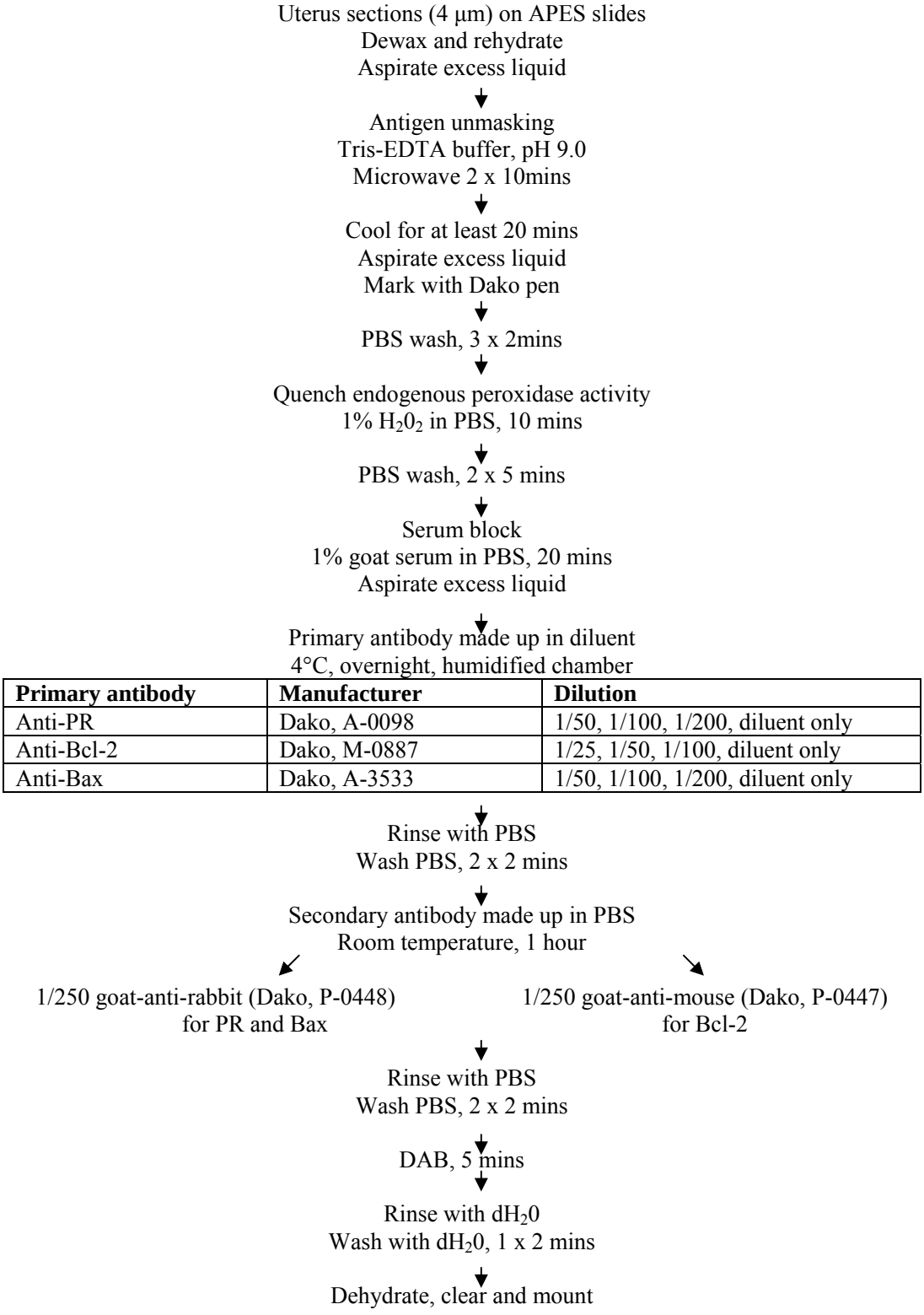

Primary antibody	Manufacturer	Dilution
Anti-PR	Dako, A-0098	1/50, 1/100, 1/200, diluent only
Anti-Bcl-2	Dako, M-0887	1/25, 1/50, 1/100, diluent only
Anti-Bax	Dako, A-3533	1/50, 1/100, 1/200, diluent only

C.1.5. Results from optimisations of IHC

It was found that the most optimal primary and secondary antibodies for IHC were supplied by Dako.
The optimal concentrations for the primary antibodies were 1/50 anti-Bax, 1/50 anti-Bcl-2 and 1/50 anti-PR.
The optimal concentrations for the secondary antibodies were 1/200goat-anti-rabbit IgG/HRP for Bax, 1/200 goat anti-mouse IgG/HRP for Bcl-2 and 1/250 goat-anti-rabbit IgG/HRP for PR
It was found that the optimal primary antibody concentrations were: 1/50 anti-Bax (Dako), 1/50 anti-Bcl-2 (Dako) and 1/50 anti-PR (Dako).
The best secondary antibodies to use were supplied by Dako, and were incubated for 1 hour in PBS.
The best heat induced antigen retrieval method used, was microwaving the sections twice in Tris-EDTA buffer pH9.0.
The best chromagen to use was the diaminobenzidine supplied by Roche.

C.2. Optimisation of ELISA against Bcl-2, Bax and PR

Figure C.2.1. Optimisation of primary and secondary antibodies for ELISA against Bcl-2, Bax and PR

100 µl of 1/100 uterus protein sample in PBS
incubated in a well of a 96 well Nunc maxisorb plate
2 hours at room temperature in a humidified chamber

↓

Aspirate plate

↓

Wash 0.9% saline, 3 x

↓

Block (200 µl of 0.1% BSA in PBS)
on a shaker, 1 hour

↓

Aspirate

↓

Wash 0.9% saline, 4 x

↓

100 µl primary antibody made up in block (0.1% BSA in PBS)
incubated, 2 hours on a shaker
The primary antibodies were applied at decreasing concentrations along the rows:

Primary Antibody	**Dilution**
Anti-PR (Santa Cruz, sc-538)	1/100; 1/200; 1/400; 1/800; 1/1600; 1/3200; 1/6400; 1/12800; 1/25600
Anti-Bcl-2 (Santa Cruz, sc-7382)	1/100; 1/200; 1/400; 1/800; 1/1600; 1/3200; 1/6400; 1/12800; 1/25600
Anti-Bax (Santa Cruz, sc-526)	1/100; 1/200; 1/400; 1/800; 1/1600; 1/3200; 1/6400; 1/12800; 1/25600

↓

Aspirate

↓

Wash 0.9% saline, 4 x

↓

100 µl secondary antibody made up in block (0.1% BSA in PBS)
Incubate for 1½ hours at room temperature on a shaker
The secondary antibodies were applied at decreasing concentrations along the columns

Primary (diluted along rows)	**Secondary (diluted along columns)**	**Secondary dilutions**
Anti-PR	Donkey-anti-rabbit (Santa Cruz, sc-2313)	1/100; 1/200; 1/500, 1/1 000; 1/2 000; 1/4 000; 1/8 000; 1/10 000
Anti-Bcl-2	Goat-anti-mouse (Santa Cruz, sc-2005)	1/100; 1/200; 1/500, 1/1 000; 1/2 000; 1/4 000; 1/8 000; 1/10 000
Anti-Bax	Donkey-anti-rabbit (Santa Cruz, sc-2313)	1/100; 1/200; 1/500, 1/1 000; 1/2 000; 1/4 000; 1/8 000; 1/10 000

↓

Aspirate

↓

Wash with 0.9% saline, 4 x

↓

Add 70 µl soluble BM Blue POD substrate
Leave to incubate in the dark

↓

Stop reaction with 50 µl 0.5 M sulphuric acid

↓

Read A_{450}

Figure C.2.2. Optimise protein concentration, incubation of protein samples and incubation of primary antibodies for ELISA against Bcl-2, Bax and PR

Two 96 well Nunc maxisorb plates were used
100 µl of 10 µg/ml uterus protein sample
Plate 1 was incubated overnight at 4 ºC in a humidified chamber and plate 2 was incubated at room temperature for 2 hours on a shaker

Protein Sample	Protein dilution	Incubation of protein
Sample 1 = 1156µg/ml	1/50 = 23.12 µg/ml; 1/100 = 11.56 µg/ml; 1/200 = 5.78 µg/ml; 1/400 = 2.89 µg/ml; 1/800 = 1.45 µg/ml; 1/1600 = 0.73 µg/ml; PBS alone	Overnight at 4 ˚C (plate 1)
Sample 2 = 4892µg/ml	1/50 = 97.84 µg/ml; 1/100 = 48.92 µg/ml; 1/200 = 24.46 µg/ml; 1/400 = 12.23µg/ml; 1/800 = 6.12 µg/ml; 1/1600 = 3.06 µg/ml; PBS alone	Overnight at 4 ˚C (plate 1)
Sample 1 = 1156µg/ml	1/50 = 23.12 µg/ml; 1/100 = 11.56 µg/ml; 1/200 = 5.78 µg/ml; 1/400 = 2.89 µg/ml; 1/800 = 1.45 µg/ml; 1/1600 = 0.73 µg/ml; PBS alone	Room temperature, 2 hours, shaker (plate 2)
Sample 2 = 4892µg/ml	1/50 = 97.84 µg/ml; 1/100 = 48.92 µg/ml; 1/200 = 24.46 µg/ml; 1/400 = 12.23µg/ml; 1/800 = 6.12 µg/ml; 1/1600 = 3.06 µg/ml; PBS alone	Room temperature, 2 hours, shaker (plate 2)

The protein samples were duplicated at 100 µl/well for incubation with anti-PR, anti-Bax and anti-Bcl-2.

↓

Aspirate plate

↓

Block (200 µl of 0.1% BSA in PBS)
on a shaker, 1 hour

↓

Aspirate

↓

Wash 0.9% saline, 3 x

↓

100 µl primary antibody made up in block (0.1% BSA in PBS)
incubate room temperature, 2 hours, shaking (plate 1)or
overnight, 4 °C, humidified chamber (plate 2)

Sample	Primary antibody	Manufacturer	Incubation of Primary antibody
Samples 1 and 2	1/500 anti-Bcl-2	Santa Cruz, sc-7382	Room temperature, 2 hours, shaking (plate 1)
Samples 1 and 2	1/100 anti-Bax	Santa Cruz, sc-526	Room temperature, 2 hours, shaking (plate 1)
Samples 1 and 2	1/100 anti-PR	Santa Cruz, sc-538	Room temperature, 2 hours, shaking (plate 1)
Samples 1 and 2	1/500 anti-Bcl-2	Santa Cruz, sc-7382	Overnight at 4 ˚C (plate 2)
Samples 1 and 2	1/100 anti-Bax	Santa Cruz, sc-526	Overnight at 4 ˚C (plate 2)
Samples 1 and 2	1/100 anti-PR	Santa Cruz, sc-538	Overnight at 4 ˚C (plate 2)

↓

Aspirate

↓

Wash 0.9% saline, 4 x

↓

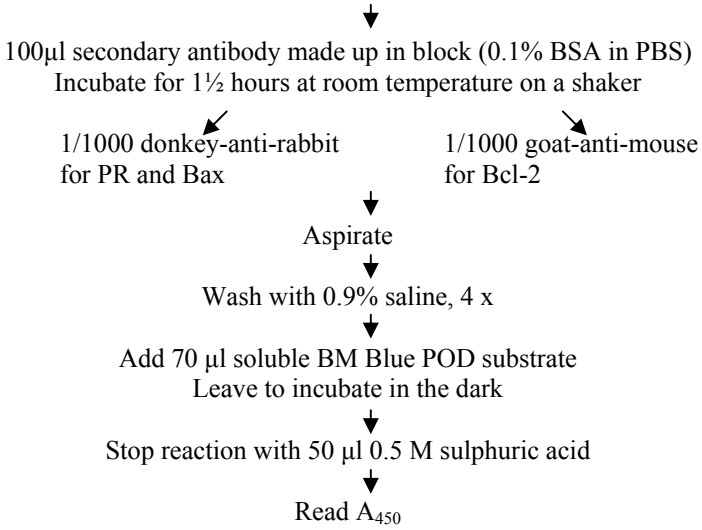

C.2.3. Results of Optimisation of ELISA

It was found that the optimal concentration of protein to use was 100 µl of 10 µg/ml protein and that it was best to leave the protein to incubate overnight at 4 °C in a humidified chamber.

The optimal concentrations of primary antibodies were 1/100 anti-Bax, 1/500 anti-Bcl-2 and 1/100 anti-PR

APPENDIX D: EXAMPLE OF STATISTICAL ANALYSIS

An example of statistical analysis used to analyse the data in this work. The example used shows the analysis of the height of the luminal epithelium.

Oneway Analysis of EPI AVE By Treatment

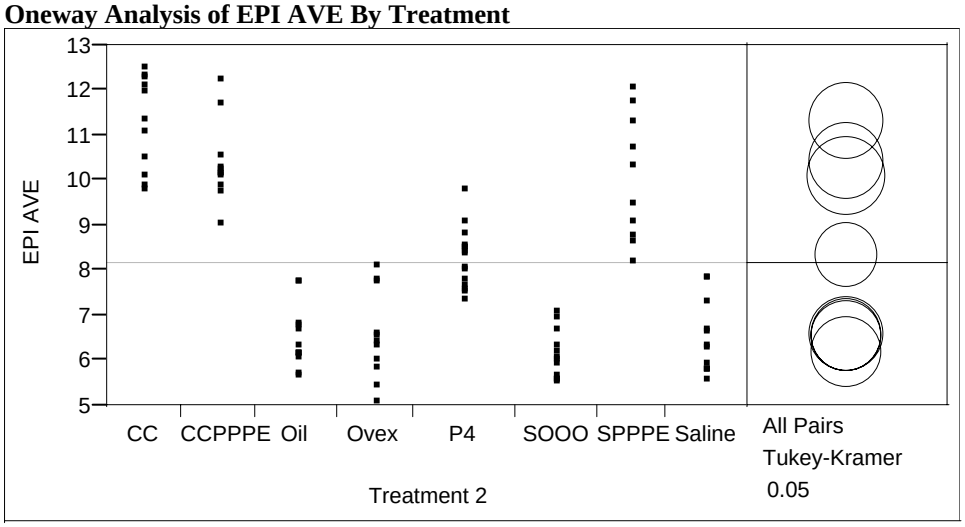

Wilcoxon / Kruskal-Wallis Tests (Rank Sums)

Level	Count	Score Sum	Score Mean	(Mean-Mean0)/Std0
CC	11	919.5	83.5909	4.664
CCPPPE	11	841	76.4545	3.741
Oil	12	323.5	26.9583	-2.788
Ovex	11	297.5	27.0455	-2.641
P4	15	811.5	54.1000	1.017
SOOO	12	230.5	19.2083	-3.841
SPPPE	10	731.5	73.1500	3.140
Saline	12	310	25.8333	-2.941

1-way Test, ChiSquare Approximation

ChiSquare	DF	Prob>ChiSq
74.8539	7	<.0001

Means Comparisons

Dif=Mean[i]-Mean[j]	CC	CCPPPE	SPPPE	P4	Ovex	Oil	Saline	SOOO
CC	0.0000	0.8963	1.2337	3.0016	4.7329	4.7686	4.7867	5.1343
CCPPPE	-0.8963	0.0000	0.3374	2.1053	3.8366	3.8723	3.8903	4.2380
SPPPE	-1.2337	-0.3374	0.0000	1.7679	3.4992	3.5349	3.5530	3.9006
P4	-3.0016	-2.1053	-1.7679	0.0000	1.7313	1.7670	1.7851	2.1327
Ovex	-4.7329	-3.8366	-3.4992	-1.7313	0.0000	0.0357	0.0538	0.4014
Oil	-4.7686	-3.8723	-3.5349	-1.7670	-0.0357	0.0000	0.0181	0.3657
Saline	-4.7867	-3.8903	-3.5530	-1.7851	-0.0538	-0.0181	0.0000	0.3476
SOOO	-5.1343	-4.2380	-3.9006	-2.1327	-0.4014	-0.3657	-0.3476	0.0000

Alpha= 0.05

Comparisons for all pairs using Tukey-Kramer HSD

q*	Alpha
3.10683	0.05

Abs(Dif)-LSD	CC	CCPPPE	SPPPE	P4	Ovex	Oil	Saline	SOOO
CC	-1.1706	-0.2743	0.0342	1.9118	3.5623	3.6227	3.6407	3.9884
CCPPPE	-0.2743	-1.1706	-0.8622	1.0155	2.6660	2.7263	2.7444	3.0920
SPPPE	0.0342	-0.8622	-1.2277	0.6471	2.2997	2.3594	2.3775	2.7251
P4	1.9118	1.0155	0.6471	-1.0024	0.6415	0.7038	0.7218	1.0694
Ovex	3.5623	2.6660	2.2997	0.6415	-1.1706	-1.1103	-1.0922	-0.7446
Oil	3.6227	2.7263	2.3594	0.7038	-1.1103	-1.1208	-1.1027	-0.7551
Saline	3.6407	2.7444	2.3775	0.7218	-1.0922	-1.1027	-1.1208	-0.7731
SOOO	3.9884	3.0920	2.7251	1.0694	-0.7446	-0.7551	-0.7731	-1.1208

Positive values show pairs of means that are significantly different.

Level						Mean
CC	A					11.337350
CCPPPE	A	B				10.441000
SPPPE		B				10.103638
P4			C			8.335727
Ovex				D		6.604425
Oil				D		6.568719
Saline				D		6.550660
SOOO				D		6.203038

Levels not connected by same letter are significantly different